

**Simultaneous Structural/Acoustical Design of Composite Panels**

by

**Christopher E. Ruckman**

**Thesis submitted to the Faculty of the**

**Virginia Polytechnic Institute and State University**

**in partial fulfillment of the requirements for the degree of**

**Master of Science**

in

**Aerospace Engineering**

**APPROVED:**

**Dr. Karl E. Sundkvist, Chairman**

**Dr. Raphael T. Haftka**

**Dr. Rakesh K. Kapania**

**August, 1986**

**Blacksburg, Virginia**

# **Simultaneous Structural/Acoustical Design of Composite Panels**

by

**Christopher E. Ruckman**

**Dr. Karl E. Sundkvist, Chairman**

**Aerospace Engineering**

**(ABSTRACT)**

Since advanced composite materials generally experience coincidence at lower frequencies than metals when used in aircraft fuselage sidewalls, they may allow more transmission of airborne noise thereby requiring heavier acoustical treatments. A sequential design approach of addressing first structural and then acoustical design does not take advantage of structural/acoustical coupling. A simultaneous approach is expected to help minimize the total sidewall mass. This thesis uses numerical optimization to examine structural/acoustical interactions and compare the sequential and simultaneous design approaches.

Acoustical performance is defined in terms of the infinite panel transmission loss at frequencies surrounding the coincidence region (1600 Hz - 12800 Hz for the panels studied.) Impedance transfer theory is used to predict the acoustical properties of a flat, unstiffened anisotropic panel treated with a fibrous acoustic blanket, airgap, and limp-mass septum. Structural analysis is based on a fatigue damage resistance criterion.

Sequentially designed treated composite panels exhibit transmission losses 15 dB - 45 dB higher (transmitted pressure is 6 - 180 times smaller) than a structurally equivalent, equal-mass aluminum panel. Depending on the type of acoustic excitation (specific incidence direction or diffuse source) and the acoustic frequency considered, the simultaneous approach alters the sequential minimum-mass panel in order to 1) improve low frequency performance by raising coincidence frequencies, 2) improve high frequency performance by lowering coincidence frequencies, or 3) make the coincidence region as narrow as possible. Since these structural alterations require that more mass be allotted to the panel and less to the treatment, they only occur for strong structural/acoustical interactions (i.e. near coincidence.) The si-

multaneous design approach can achieve a moderate improvement (TL increased up to 10 dB, transmitted pressure decreased by a factor of 3) over a sequential design for a particular acoustic performance index, although computation time is increased and acoustic performance may be sacrificed in other regions.

# Acknowledgements

I am deeply indebted to Dr. Karl Sundkvist for his guidance, insight, and patience during this research effort and in particular during the writing of this thesis. He always took writing which could probably have passed as thesis-quality and taught me how to make it even better. Thanks are due to Dr. Raphael Haftka for giving direction to the early phases of the research, to Dr. Rajiv Thareja for showing me how not to be overwhelmed by NEWSUMTA, and to Diane for encouragement during those trying moments (of which there were many.) I also acknowledge the support of the Computing Center staff in helping solve the many programming difficulties which have arisen during the past year.

Finally, I would like to thank the ADM5 terminals in Femoyer Lounge for helping me learn about FORTRAN, about SCRIPT, and about the virtues of showing patience and restraint when I felt like smashing a video screen.

# Table of Contents

<b>1.0</b>	<b>Introduction</b>	<b>1</b>
<b>1.1</b>	<b>Background</b>	<b>2</b>
1.1.1	Aircraft Noise Sources, Transmission Paths, and Treatment Concepts	2
1.1.2	Characteristics of Airborne Acoustic Transmission	4
<b>1.2</b>	<b>Scope Of The Present Research</b>	<b>10</b>
<b>2.0</b>	<b>Transmission Through Treated Infinite Panels</b>	<b>12</b>
<b>2.1</b>	<b>Infinite Panel Theory</b>	<b>12</b>
<b>2.2</b>	<b>Transmission Through Multilayered Systems</b>	<b>15</b>
<b>2.3</b>	<b>Frequency Averaging and Spatial Averaging of Transmission Loss</b>	<b>21</b>
<b>3.0</b>	<b>Implementing The Design Procedure</b>	<b>25</b>
<b>3.1</b>	<b>Structural Analysis</b>	<b>25</b>
<b>3.2</b>	<b>Design Formulation</b>	<b>27</b>
<b>3.3</b>	<b>Programming Considerations</b>	<b>29</b>
<b>4.0</b>	<b>Results and Discussion</b>	<b>33</b>

4.1 Preliminary Study .....	34
4.2 Design Study .....	40
4.2.1 Specific Incidence .....	45
4.2.2 Grazing Incidence .....	49
4.2.3 Field Incidence .....	53
4.3 Conclusions .....	55
 References .....	 61
 Appendix A. Optimization Program TLROP .....	 63
 Appendix B. Shear Buckling Strength of Finite Panels and Infinite Strips .....	 92
 Appendix C. Acoustic Properties of Fibrous Blankets .....	 97
 Appendix D. Figures .....	 99
 Vita .....	 138

# List of Illustrations

Figure 1. Basic Elements of NASA Research Program	101
Figure 2. Cabin Noise Levels With And Without Propulsor-Generated Noise	102
Figure 3. Airborne vs. Structureborne Transmission Paths	103
Figure 4. Typical Treatment Configurations	104
Figure 5. Typical Specific Incidence Transmission Loss vs. Frequency	105
Figure 6. Transmission Loss vs. Incidence Direction (Aluminum Panel)	106
Figure 7. Transmission Loss vs. Incidence Direction (Graphite/Epoxy Panel)	107
Figure 8. Geometry of Infinite Panel Transmission	108
Figure 9. Blocked Pressures For Multi-Layered System	109
Figure 10. Plane Interface Between Two Semi-Infinite Media	110
Figure 11. Comparison of Transmission Loss TL and Transmission Difference TD	111
Figure 12. Eigenvalue Shear Buckling Strength of Shear-Critical Panels	112
Figure 13. Flowchart of Program TLROP	113
Figure 14. Mass Required By Shear-Critical Panels	114
Figure 15. Variation of Rigidity Parameter With Azimuth	115
Figure 16. Variation of Coincidence Frequency With Azimuth	116
Figure 17. Specific Incidence Transmission Loss of Shear-Critical Panels	117
Figure 18. Specific Incidence Transmission Loss of Mass-Critical Panels	118
Figure 19. Grazing Incidence Transmission Loss of Shear-Critical Panels	119
Figure 20. Grazing Incidence Transmission Loss of Mass-Critical Panels	120
Figure 21. Field Incidence Transmission Loss of Shear-Critical Panels	121

Figure 22. Field Incidence Transmission Loss of Mass-Critical Panels .....	122
Figure 23. TL of Typical Mid and Low Frequency Treatments .....	123
Figure 24. TL of Untreated Aluminum Panel .....	124
Figure 25. TL of Optimal Designs: Specific Incidence / 1600 Hz .....	125
Figure 26. TL of Optimal Designs: Specific Incidence / 6400 Hz .....	126
Figure 27. TL of Optimal Designs: Specific Incidence / 8063 Hz .....	127
Figure 28. TL of Optimal Designs: Specific Incidence / 12800 Hz .....	128
Figure 29. TL of Optimal Designs: Specific Incidence / TLL .....	129
Figure 30. TL of Optimal Designs: Specific Incidence / TDL .....	130
Figure 31. TL of Optimal Designs: Grazing Incidence / 1600 Hz .....	131
Figure 32. TL of Optimal Designs: Grazing Incidence / 6400 Hz .....	132
Figure 33. TL of Optimal Designs: Grazing Incidence / 8063 Hz .....	133
Figure 34. TL of Optimal Designs: Grazing Incidence / 12800 Hz .....	134
Figure 35. TL of Optimal Designs: Grazing Incidence / TLL .....	135
Figure 36. TL of Optimal Designs: Field Incidence / 1600 Hz .....	136
Figure 37. TL of Optimal Designs: Field Incidence / 12800 Hz .....	137



## List of Tables

Table 1. Coincidence Bandwidths of Mass-Critical and Shear-Critical Panels . . . . .	35
Table 2. Properties of Panel And Treatment Materials . . . . .	37
Table 3. Specific Incidence Optimization Results . . . . .	41
Table 4. Grazing Incidence Optimization Results . . . . .	42
Table 5. Field Incidence Optimization Results . . . . .	43
Table 6. Infinite Strip Shear Buckling Coefficients . . . . .	95

## List of Symbols

$a$	Panel dimension parallel to x-axis
$b$	Panel dimension parallel to y-axis
$b_b$	Complex blanket propagation constant
$c_a$	Air acoustic velocity (= 343 m/s <sup>2</sup> )
$D_{ij}$	Panel directional rigidities
$D_{\phi\phi}$	Panel rigidity in $\phi$ -direction
$E_1$	Modulus of elasticity in x-direction
$E_2$	Modulus of elasticity in y-direction
$f$	Acoustic frequency
$f_c$	Coincidence frequency
$f_{c_{\max}}$	Maximum grazing coincidence frequency
$f_{crit}$	Critical frequency
$f_{target}$	Target frequency
$f_1$	1600 Hz target frequency
$f_2$	6400 Hz target frequency
$f_3$	8063 Hz target frequency
$f_4$	12800 Hz target frequency

$G_{12}$	Panel torsional rigidity
$j$	$\sqrt{-1}$
$k$	Acoustic wavenumber ( $= \omega/c_s$ )
$N_{xy}$	Eigenvalue shear buckling load
$NB$	Number of 1/3-octave bands over which $TLL$ is averaged
$NSB$	Number of sub-bands over which a 1/3-octave band transmission loss is averaged
$NT$	Number of treatments in a multilayered system
$P_i$	Acoustic pressure amplitude of incident wave
$P_j$	Blocked (total) acoustic pressure at $j^{\text{th}}$ interface of a multilayered system
$P_{NT+1}$	Blocked (total) acoustic pressure on inner face of a multilayered system
$P_r$	Acoustic pressure amplitude of reflected wave
$P_t$	Acoustic pressure amplitude of transmitted wave
$R_1$	Blanket flow resistivity
$S(f_i)$	Acoustic power spectral density at frequency $f_i$
$t_j$	Thickness of $j^{\text{th}}$ layer of a multilayered system
$TD_j$	Transmission difference at center frequency of $j^{\text{th}}$ 1/3-octave band
$TDL$	Transmission difference level
$TDL_{\text{max}}$	Maximum allowable transmission difference level
$TL$	Transmission loss
$TL_j$	Transmission loss at center frequency of $j^{\text{th}}$ 1/3-octave band
$TL_{\text{min}}$	Minimum allowable transmission loss
$TL_{\text{ref}}$	Reference transmission loss
$TLL$	Transmission loss level
$TLL_{\text{min}}$	Minimum allowable transmission loss level
$\bar{X}$	Vector of design variables
$w$	Panel deflection parallel to z-axis
$Z_{\text{ent}}$	Entry impedance
$Z_{\text{exit}}$	Exit impedance

$Z_j$	Entry impedance of $j^{\text{th}}$ layer of a multilayered system
$Z_0$	Characteristic impedance
$\alpha$	Panel layup angle
$\gamma$	Dimensionless frequency parameter ( $= f/f_c$ )
$\Delta f_{\text{coin}}$	Grazing coincidence bandwidth
$\Delta f_i$	Narrow frequency bandwidth used with 1/3-octave band averaging
$\eta$	Panel damping coefficient
$\theta_i$	Inclination angle (measured from the normal)
$\theta_{\text{lim}}$	Limiting (grazing) inclination angle ( $= 78^\circ$ )
$\nu_{12}$	Poisson's ratio
$\xi$	Dummy variable used to make objective function in NEWSUMTA linear
$\rho_a$	Air density ( $= 1.21 \text{ kg/m}^3$ )
$\sigma_j$	Surface mass of $j^{\text{th}}$ layer of a multilayered system
$\sigma_{\text{max}}$	Maximum allowable total surface mass
$\sigma_{\text{tot}}$	Total surface mass (panel + treatment)
$\tau$	Specific incidence, discrete frequency transmission coefficient
$\bar{\tau}$	Field incidence transmission coefficient
$\bar{\tau}_{ml}$	Field incidence mass law transmission coefficient
$\bar{\tau}_\theta$	Azimuthal incidence transmission coefficient
$\tau_{cr}$	Critical shear stress
$\tilde{\tau}$	Approximate critical shear stress
$\tilde{\tau}_{\text{min}}$	Minimum allowable approximate critical shear stress
$\varphi_i$	Azimuthal angle (measured in plane of panel)
$\psi_j$	Complex amplitude and phase difference of $j^{\text{th}}$ layer of a multilayered system
$\omega$	Acoustic circular frequency

# 1.0 Introduction

In applications where high aircraft cabin noise levels are undesirable, add-on acoustic treatments can present a substantial weight penalty<sup>[1]</sup>. Although advanced composite materials can reduce structural weight in the fuselage, they may have detrimental effects on cabin noise. Composite panels tend to be more rigid than metal panels, which reduces the coincidence frequency and allows more noise transmission. Weight savings may be compromised by the need for heavier add-on acoustic treatments.

The acoustic transmission of a bare panel is determined by its mass and rigidity (the same properties that influence structural behavior) resulting in a complex coupling between structural and acoustical design. The traditional sequential design approach does not take advantage of structural/acoustical coupling. First, the panel is designed for minimum weight subject to structural criteria; then, acoustic fixes or treatments are applied to the finished structure to remedy any excessive noise problems. The tailoring possible with composite materials should enhance the feasibility of a simultaneous structural/acoustical approach in which the panel and treatment are symbiotically designed to satisfy structural and acoustical criteria. Finding the optimal balance of coupled and counteracting mass and rigidity effects on structural and acoustic performance is a challenging design problem. This thesis uses

numerical optimization to study the feasibility of simultaneous structural/acoustical design in terms of additional effort and design advantages over the sequential approach.

## **1.1 Background**

The Structural Acoustics Branch at the NASA Langley Research Center is conducting a research program to investigate the acoustical performance of composite structures<sup>[7]</sup>. The basic elements of this program are outlined in Figure 1 on page 101. Initially, the emphasis was on predicting the noise characteristics of simple structural panels. This included developing analytical models for both infinite and finite panels, and generating experimental data with which to verify the analytical results. The later emphasis is on representing more complicated structural elements including panel curvature, stiffeners, add-on acoustic treatments, and other configurations. Also being developed is a finite element representation of the structures and acoustical processes.

### **1.1.1 Aircraft Noise Sources, Transmission Paths, and Treatment Concepts**

The two most important sources of aircraft cabin noise are 1) boundary layer flow noise (broadband-type noise; affects wide range of frequencies), and 2) propulsor-generated noise (tonal noise; concentrated at specific frequencies). For example, tonal noise can be generated by propellers, by piston and exhaust firing in reciprocating-piston engines, or by turbines in jet engines. Figure 2 on page 102 compares cabin noise levels of a twin-engine aircraft in cruise and engines-off dive flight conditions by showing cabin noise level as a function of fre-

quency. Note the differences in the shape of the curve at low and high frequencies, illustrating both tonal and broadband noise. At high frequencies, where boundary layer flow noise dominates, the curves are relatively smooth because boundary layer flow creates broadband-type noise which affects all frequencies to some extent. Due to propeller wash, the flow velocity on the outer skin is higher in the cruise flight condition than in the dive flight condition; therefore, the amount of flow noise is higher. At low frequencies, the high-intensity spikes indicate the presence of propulsor-generated tonals. For example, the spike at 80 Hz is due to the passage of propeller blade tips past the cabin wall.

Noise paths are usually classified as either airborne or structureborne; this study considers only the airborne path. An example of airborne transmission is an acoustic wave generated by propeller motion passing directly through the fuselage wall into the cabin (see Figure 3 on page 103.) On the other hand, engine vibrations can excite wing structures and in turn fuselage structural members which then radiate noise into the cabin. This is classified as structureborne noise.

Conventional noise reduction concepts address both structureborne and airborne transmission<sup>[9]</sup>. Structureborne noise can be isolated by improving engine mounts, by stiffening engine mounting points, and by damping the engine suspension system. To reduce airborne transmission (the subject of this study) fuselage panels are usually treated with various combinations of the following:

- Porous acoustic blankets, typically fiberglass or other lightweight materials.
- Limp mass septa – impervious layers which have mass but do not contribute to the panel strength. These may include interior trim panels and/or layers of plastic for containing the fibers of porous blankets.
- Airgaps between other layers. An airgap can reduce sidewall transmission by preventing direct physical contact between material layers or by modifying acoustic interactions between layers.
- Damping tape to help control panel resonances.

Figure 4 on page 104 shows several typical treatment configurations. Figure 4d represents the configuration used in this design study: an airgap followed by a fibrous acoustic blanket and a limp-mass septum representing a trim panel. This treatment is applied to a structurally designed composite panel as the second phase of a sequential design process. In the simultaneous design process the panel and this treatment are designed in unison.

Structural flanking occurs when trim panel mounts transmit vibrations from the outer skin directly to the inner trim panel. While structural flanking can adversely affect cabin noise, it is not considered in this simplified analysis.

Cabin noise levels depend upon the (external) noise sources, transmission into the cabin, and interior cavity modes and resonances. Other considerations include absorption coefficients of interior surfaces and placement of facilities such as galleys and latrines<sup>[9]</sup>. The present study considers noise transmission through the fuselage wall rather than addressing the entire source/transmission path/cavity problem.

### 1.1.2 Characteristics of Airborne Acoustic Transmission

Several characteristics of acoustic transmission via the airborne path may be illustrated by considering transmission through an untreated panel. Airborne transmission is commonly defined in terms of a *transmission loss*,  $TL$  (in decibels):

$$TL \equiv 10 \log(1/\tau) \quad [1.1]$$

where  $\tau$  is the fraction of incident acoustic intensity which is transmitted into the cabin. The transmission loss depends on the incidence direction, the acoustic frequency  $f$ , the panel flexural rigidities  $D_{ij}$ , the panel mass per unit area  $\sigma_p$ , and the panel damping factor  $\eta$ . The direction of incidence is defined by the two spherical angles: an azimuthal angle  $\phi_i$ , measured in the plane of the panel, and an angle of inclination  $\theta_i$ , measured from the normal. (Figure 8 on page 108 shows the incidence geometry.)



Specific incidence approximates the case of a given external source location, while field incidence approximates a diffuse noise source such as boundary layer noise. Specific incidence refers to a plane wave incident from a given direction  $(\varphi_i, \theta_i)$ . Field incidence may be considered as plane waves incident from all directions up to the grazing angle of  $\theta_{lim} = 78^\circ$ . (The limiting inclination angle  $\theta_{lim}$  is chosen to agree with experiments<sup>[6]</sup>; the assumption is that for inclinations greater than  $\theta_i = \theta_{lim}$  the incident acoustic wave is absorbed or completely reflected.) The transmission loss is a function of the angles  $\varphi_i$  and  $\theta_i$ ; thus for diffuse acoustic waves, the field incidence transmission coefficient  $\bar{\tau}$  must be integrated over  $\varphi_i$  and  $\theta_i$  (up to  $\theta_{lim}$ .)

The designer must also consider both tonal noise sources (noise concentrated in a narrow frequency band) and broadband noise sources (noise distributed over a wide range of frequencies). Since  $TL$  depends on frequency, it is often useful to average the transmission losses in the range of frequencies considered as a *transmission loss level*  $TLL$ . Both spatial and frequency averaging are discussed further in Section 3.1.

The transmission loss of an untreated panel can be approximated by two types of models. At very low frequencies where the acoustic wavelength is on the order of the panel dimensions, panel resonances play an important part in determining acoustic properties, and a finite panel theory (not considered here) must be used to account for panel edge conditions. As in Ref. [7], the panel may be modelled as a rectangular plate in an infinite rigid baffle. The incident acoustic wave is assumed to be a plane wave, but the directivity of the transmitted wave must be accounted for by integrating over the panel's inner surface.  $TL$  is strongly affected by panel resonances. The material damping and the global panel stiffness, i.e. panel stiffness with respect to boundary conditions, control the response amplitude and therefore control  $TL$ . One expected benefit of using composite materials is that, since a composite panel is usually more rigid than a comparable aluminum panel, the composite panel may transmit less noise at very low frequencies<sup>[7]</sup>.

Boundary conditions are significant only within a few wavelengths of the panel edges. Thus, at higher frequencies when the acoustic wavelength is small compared to panel dimensions, the conditions at the panel boundaries are irrelevant over most of the panel area (except at the fringes). Infinite panel theory approximates this situation by considering the panel as a thin plate of infinite area<sup>[9]</sup>. The incident, transmitted, and reflected acoustic waves are assumed to be plane waves. Infinite panel theory is used in this study; for the panels considered, the model applies for frequencies above approximately 300 Hz - 400 Hz.

Coincidence is the most important structural/acoustical interaction modelled by infinite panel theory. The coincidence frequency,  $f_c$ , is the frequency for which the projection of the acoustic wavelength in the plane of the panel coincides with the flexural wavelength in the direction of incidence. Thus, coincidence is influenced by local, rather than global, stiffness characteristics. Figure 5 on page 105 represents a typical frequency plot of untreated infinite panel transmission loss for a given incidence direction. Different effects govern  $TL$  in three frequency regions defined with respect to the coincidence frequency:

**Mass Law Region ( $f \ll f_c$ ):** At frequencies far below the coincidence region (approximately 400 - 6000 Hz for most panels in this study), inertial effects govern  $TL$ . The mass law transmission loss describes transmission 1) at frequencies in the mass law region, 2) at any frequency if panel rigidities are small enough to be ignored, as is the case with a limp-mass septum, and 3) for normal incidence at any frequency. In the mass law region, a composite panel generally has lower  $TL$  than a comparable aluminum panel because of its lower mass.

**Coincidence Region ( $f \cong f_c$ ):** For the panels in this study, coincidence can occur at frequencies as low as 4000 Hz or as high as 20000 Hz, although a more common range is 6000 - 13000 Hz. In the coincidence region,  $TL$  drops below the values predicted by mass law, with significant degradation (from mass law predictions) beginning at approximately  $\frac{1}{2}f_c$ , and ending at approximately  $\sqrt{2}f_c$ . For specific incidence, the coincidence frequency depends on the panel flexural rigidities  $D_{ij}$  and the azimuthal and incidence angles  $\phi_i$  and  $\theta_i$ . The coincidence fre-

quency of an isotropic panel (e.g. aluminum) is independent of the azimuthal angle  $\phi_i$ . For an anisotropic panel (e.g. composite) the flexural rigidities  $D_{ij}$  vary with azimuth, so that the frequency affected by coincidence depends on  $\phi_i$  as well as  $\theta_i$ .

The *critical frequency*,  $f_{crit}$ , is the lowest possible coincidence frequency, which occurs at grazing incidence ( $\theta_{lim} = 78^\circ$ ) and in the most rigid azimuthal direction. The *maximum grazing coincidence frequency*,  $f_{c_{max}}$ , is the highest frequency for which coincidence occurs at grazing incidence. For field incidence, although all frequencies above  $f_{crit}$  are degraded by coincidence, the frequencies between  $f_{crit}$  and  $f_{c_{max}}$  are affected most severely. Therefore, an important parameter to consider is the coincidence bandwidth  $\Delta f_{coin} = f_{c_{max}} - f_{crit}$ . Note that for an isotropic panel  $\Delta f_{coin} = 0$ ; thus the field incidence transmission loss for an isotropic panel is only severely affected over a relatively narrow band of frequencies. For composite panels,  $\Delta f_{coin}$  can be more than 10000 Hz (see Table 1 on page 35) so that a wide band of frequencies is affected by coincidence; this is one aspect in which composite materials compare poorly with aluminum.

Composite panels are usually more rigid than aluminum panels, which may adversely affect cabin noise in the coincidence region. A very rigid panel has a long flexural wavelength, and therefore experiences coincidence at relatively low frequencies. Aluminum panels usually experience coincidence at high frequencies where 1) add-on treatments are very effective and 2) the amount of noise encountered is not large. However, add-on treatments are less effective at lower frequencies. Also, as in Figure 2 on page 102, the amount of noise due to boundary layer flow increases as frequency decreases (above approximately 500 Hz.) Moving coincidence to lower frequencies can combine a region of poor panel/treatment performance with a region where more noise is encountered, thus allowing higher cabin noise levels (or requiring heavier acoustic treatments.)

**Rigidity Region (  $f \gg f_c$  ):** At frequencies far above  $f_c$  (above approximately 13000 Hz for most panels in this study), rigidity terms govern the transmission loss. In this post-coincidence region,  $TL$  increases with frequency as the panel recovers from coincidence. For

specific incidence,  $TL$  eventually exceeds the transmission loss predicted by mass law, although this may not occur until frequencies above the range of interest. (For field incidence, the recovery is slower.) A composite panel may have higher or lower transmission loss than an aluminum panel, depending on how the coincidence frequencies compare. For specific incidence the panel with the lower coincidence frequency begins its rigidity recovery sooner, so that high frequency transmission loss is higher.

In order to visualize the dependence on  $TL$  on frequency and incidence direction, it is helpful to examine the surfaces obtained when  $TL$  is plotted as distance from the origin against the spherical incidence angles  $\phi_i$  and  $\theta_i$ . Figure 6 on page 106 shows  $TL$  for an aluminum panel at frequencies surrounding the coincidence region. At 1600 Hz (Figure 6a) the panel exhibits mass law behavior, characterized by the “bulb” shape that extends out from the plane of the panel along the z-axis. Since the material is isotropic,  $TL$  is independent of  $\phi_i$  and the bulb is symmetric about the z-axis. The thick curve on the edge of the surface denotes the grazing incidence where  $\theta_i = 78^\circ$ . At 8063 Hz (Figure 6b), mass law behavior still dominates;  $TL$  has increased, and the “bulb” is larger. At 12800 Hz (Figure 6c), notice that the thick curve denoting  $\theta_i = 78^\circ$  is smaller in radius than at 6400 Hz. This indicates coincidence degradation;  $TL$  is first affected at grazing incidence. The radius of the grazing incidence circle approaches zero at the coincidence frequency of 12481 Hz. At 17000 Hz (Figure 6d), above the frequencies considered in this study, the panel still exhibits mass law behavior for inclination angles less than approximately  $40^\circ$  (near normal incidence.) However, coincidence decreases  $TL$  for angles between approximately  $50^\circ$  and  $65^\circ$ . The region of higher  $TL$  between  $\theta_i = 65^\circ$  and grazing incidence ( $\theta_{lim} = 78^\circ$ ) represents rigidity-controlled transmission loss. The transmission loss at grazing incidence is first to be degraded by coincidence, but also recovers from coincidence the earliest.

Figure 7 represents a  $\pm 33^\circ$  graphite/epoxy panel – the “structural panel” defined in Section 4.2. The  $TL$  surface is not symmetric about the z-axis because the panel is not isotropic. At 1600 Hz (Figure 7a), the mass law “bulb” is smaller than that of the aluminum

panel, i.e.  $TL$  is smaller because the composite panel has less mass. At 6400 Hz (Figure 7b), the panel already experiences coincidence at grazing incidence (represented by the thick line at the edge of the surface) and in the most rigid azimuthal directions. Recall that the aluminum panel did not experience grazing coincidence until its critical frequency of 12481 Hz. At 8063 Hz (Figure 7c) and grazing incidence, the panel experiences rigidity-controlled transmission in the most rigid azimuthal directions and coincidence in the softest azimuthal directions. The lobes on either side of the mass bulb represent rigidity-controlled transmission. Finally, at 12800 Hz (Figure 7d) the transmission at grazing incidence is governed by rigidity while other inclinations still experience coincidence or mass law behavior.

The main point here is that the composite panel experiences coincidence in some directions long before the aluminum panel experiences coincidence, although other directions are not affected until higher frequencies. Grazing incidence ( $\theta_i = \theta_{lim}$ ) is affected earliest, and is of particular interest in terms of structural/acoustical interactions. Also, the composite panel's lower mass gives it lower  $TL$  in some directions, although its rigidity properties can give it higher  $TL$  in other directions (compare the  $TL$  surfaces at 12800 Hz.) Two additional points are illustrated by the  $TL$  surfaces. First, for a symmetric angle-ply layup, there exists an axis in the plane of the panel about which  $TL$  is symmetric. Therefore, rigidity effects for all azimuthal directions are accounted for by considering the half-space from  $\varphi_i = 0$  to  $\varphi_i = \pi$ . (Recall that for the isotropic aluminum panel  $TL$  is symmetric about the  $z$ -axis.) Second, the transmission loss near normal incidence is always mass-controlled and is generally much larger than away from normal incidence. Values of field incidence transmission loss are higher than values of specific incidence transmission loss because of the influence of near-normal inclinations.

## 1.2 Scope Of The Present Research

This thesis considers sequential and simultaneous design of treated infinite composite panels subject to mass, structural, and acoustical criteria.

The primary research objectives are to

1. Combine optimization software with existing experimentally verified analytical models for acoustic transmission to produce an automated panel design procedure.
2. Investigate the feasibility of the simultaneous vs. sequential approach by studying the effects of structural/acoustical interactions (particularly coincidence) on optimal panel design.
3. Identify theoretical and practical issues which merit further study.

The first section of Chapter 4 is a preliminary study of untreated 8-ply graphite/epoxy laminates. Only mid-plane symmetric angle-ply layups are considered. With this simplification, the panel is defined by only two variables – the thickness  $t_p$  and the layup angle  $\alpha$ . Results of this preliminary study help identify candidate design trends which are likely to compete with the treatment for a portion of the allotted mass.

The design study in Section 4.2 replaces a typical flat aluminum panel with a structurally equivalent treated composite panel. In order to facilitate acoustic comparisons, the total mass of the treated composite panel equals the mass of the aluminum panel. The treatment consists of an airgap, an acoustic blanket, and a limp-mass septum representing a trim panel. The structural/acoustical performance of this baseline configuration is optimized using both sequential and simultaneous approaches.

The first step of the sequential approach minimizes the mass of an untreated panel subject to structural criteria; this is the “structural panel” defined in Sec. 4.1. The second step incorporates acoustic criteria but designs only the treatment, i.e. the panel design does not

change during optimization. With the simultaneous approach, the panel and treatment are designed concurrently to reflect the optimal balance between structural and acoustical effects.

Structural comparisons are based on a fatigue damage resistance criterion, which is essentially a lower bound on the shear buckling capacity. (See Section 3.1.) Acoustic performance is defined in terms of the infinite panel transmission loss across a treated panel for frequencies surrounding panel coincidence – between 1600 Hz and 12800 Hz for the panels studied. This eliminates the need for a noise spectrum and focuses on the treated panel rather than on stiffeners, engine mounts, other structural elements, and the interior cavity.

A variety of acoustic performance indices are useful to address the coincidence effect. The specific, azimuthal, and field incidence transmission losses are defined in Section 2.3. Transmission loss for these types of incidence are considered at four discrete target frequencies:  $f_1 = 1600$  Hz (in the mass law region),  $f_2 = 6400$  Hz (sub-coincident; in the low frequency region of coincidence degradation),  $f_3 = 8063$  Hz (sub-coincident; just below the structural panel coincidence frequency), and  $f_4 = 12800$  Hz (super-coincident; in the structural panel rigidity region.) In addition, two frequency-averaged transmission loss levels are considered.

## 2.0 Transmission Through Treated Infinite Panels

This chapter summarizes the theory required for analysis of acoustic transmission through treated infinite composite panels. Section 2.1 outlines theory for plane wave, specific incidence, specific frequency transmission through an infinite panel; equations are presented for the transmission loss and characteristic impedance of an untreated anisotropic panel. Section 2.2 gives the equations necessary to find the transmission loss across the panel/airgap/blanket/septum configuration. Finally, Section 2.3 explains the different schemes of spatial averaging (for diffuse noise) and frequency averaging (for broadband noise) of plane wave transmission loss.

### 2.1 *Infinite Panel Theory*

The infinite panel analysis of Roussos and Powell (Ref. [6]) is used to calculate panel acoustical properties at frequencies where edge conditions can be ignored. According to studies carried out at the NASA Langley Research Center, bare panel transmission losses



predicted using this theory were usually within  $\pm 0.5$  dB of experimentally measured values<sup>[6]</sup>.

Figure 8 on page 108 shows the geometry of infinite panel transmission. For a harmonic plane acoustic wave of a particular frequency  $f$ , the incidence direction is defined by an azimuthal angle  $\phi_i$  in the plane of the panel and an angle of inclination  $\theta_i$  measured from the normal. The medium on both sides of the panel is air of density  $\rho_a$  and acoustic velocity  $c_a$ .

The composite panel has surface mass  $\sigma_p$  (mass per unit area.) The flexural rigidities  $D_{ij}$  are derived using classical laminated plate theory as presented by Jones in Ref. [8]. Only 8-ply mid-plane symmetric, alternating angle-ply laminates are considered; therefore, the panel is described completely by the thickness  $t_p$  and the layup angle  $\alpha$ . A small damping factor of  $\eta = 0.01$  is assumed (Ref. [9] uses  $\eta = 0.05$  for a undamped panel.)

A common measure of acoustic performance is the *transmission loss*,  $TL$ :

$$TL \equiv 10 \log(1/\tau) \quad [2.1]$$

where the transmission coefficient  $\tau$  is defined as the fraction of incident acoustic intensity which is transmitted. (The reader should bear in mind that the transmission loss is large when the transmitted acoustic intensity is small; in other words, the goal is to *maximize*  $TL$ .)

The acoustic field is assumed to be composed of an incident wave (pressure amplitude  $P_i$ ) generated by an external source, a reflected wave (pressure amplitude  $P_r$ ) which is reflected away from the panel, and a transmitted wave (pressure amplitude  $P_t$ ) which passes through to the inner side. The (high frequency) incident, reflected, and transmitted waves are assumed to be plane waves, so that  $\tau$  reduces to the ratio of transmitted to incident mean square pressures:

$$\tau = \frac{|P_t|^2}{|P_i|^2} \quad [2.2]$$

The pressure ratio across a flat, unstiffened, untreated, infinite panel is, from Ref. [6],

$$\frac{P_i}{P_t} = 1 + \frac{\cos \theta_i}{j(2\pi f)\rho_a c_a}(1 + j\eta) \left[ \frac{-2(2\pi f)^2}{1 + j\eta} \sigma_p + \frac{(2\pi f)^4 \sin^4 \theta_i}{c_a^4} D_{\phi\phi} \right] \quad [2.3]$$

where the panel rigidity in the azimuthal direction is defined as

$$D_{\phi\phi} = D_{11} \cos^4 \phi_i + 4D_{16} \cos^3 \phi_i \sin \phi_i + 2(D_{12} + 2D_{66}) \cos^2 \phi_i \sin^2 \phi_i + 4D_{26} \cos \phi_i \sin^3 \phi_i + D_{22} \sin^4 \phi_i \quad [2.4]$$

Note that in general a composite panel possesses twisting-bending coupling and the rigidities  $D_{16}$  and  $D_{26}$  are not necessarily zero as they are for an isotropic aluminum panel.

The first term within brackets in Eqtn. 2.3 governs  $TL$  for mass law transmission (low frequencies), while the second term within brackets governs  $TL$  in the high frequency rigidity region. Note that these mass and rigidity terms are of opposite sign. In the absence of damping, the cancellation of these two terms gives  $P_i/P_t = 1$  and  $TL = 0$ , and the incident wave is completely transmitted. The frequency for which this occurs is the coincidence frequency, given by

$$f_c = \frac{1}{2\pi} \frac{c_a^2}{\sin^2 \theta_i} \sqrt{\sigma_p / D_{\phi\phi}} \quad [2.5]$$

The *critical frequency*  $f_{crit}$  is the lowest possible coincidence frequency. Since  $\sin \theta_i$  and  $D_{\phi\phi}$  appear in the denominator in Eqtn. 2.5, the critical frequency occurs at grazing ( $\theta_i = 78^\circ$ ) and in the direction of maximum panel rigidity.

For an undamped panel ( $\eta = 0$ ) Eqtn. 2.3 may be rewritten in terms of the nondimensional frequency parameter  $\gamma \equiv \frac{f}{f_c}$ :

$$1/\tau = 1 + \left[ \frac{(2\pi f)\sigma_p \cos \theta_i}{2\rho_a c_a} \right]^2 (1 - \gamma^2) \quad [2.6]$$

At low frequencies (small  $\gamma$ ) the transmission coefficient becomes asymptotic to the mass law transmission coefficient given by

$$1/\tau_{ml} = 1 + \left[ \frac{(2\pi f)\sigma_p \cos \theta_i}{2\rho_a c_a} \right]^2 \quad [2.7]$$

Note that in Eqtn. 2.7  $\sigma_p$  and  $f$  appear in the numerator; panel mass is beneficial to transmission loss, and increasingly beneficial at increasing frequencies. Near the coincidence frequency  $\gamma \cong 1$  the transmission loss is degraded due to counteracting mass and rigidity terms. At sub-coincident frequencies ( $\gamma < 1$ ) the panel rigidity is detrimental as it reduces TL below the mass law value. At super-coincident frequencies ( $\gamma > 1$ ) increases in rigidity increase the transmission loss. At frequencies above  $\sqrt{2}f_c$  ( $\gamma > \sqrt{2}$ ), the rigidity dominates the mass and transmission loss surpasses mass law values.

The transmission loss across a treated panel requires an expression for the characteristic impedance of the untreated panel:

$$Z_{0p} = \frac{\eta D_{\phi\phi}(2\pi f)^3 \sin^4 \theta_i}{c_a^4} + j2\pi f \sigma_p - \frac{jD_{\phi\phi}(2\pi f)^3 \sin^4 \theta_i}{c_a^4} \quad [2.8]$$

where  $\omega$  is the acoustic circular frequency expressed in radians per second.

## 2.2 Transmission Through Multilayered Systems

The “impedance transfer” theory used to estimate acoustic transmission across treated panels is due to Beranek and Work (Ref. [10]) as presented more recently by Rennison and Wilby in Ref. [11]. Reflection and refraction between the layers are accounted for in terms of the blocked (total) pressure at each interface. Propagation is considered in airgaps and fibrous acoustic blankets; since panel and septa thicknesses are small compared to the acoustic wavelength, these are modeled as impedance layers. The assumptions made for the present research include all those stated in Ref. [11] as quoted below:

1. Even though there are abrupt changes in material properties at a boundary, the pressure, [normal] velocity, condensation, and particle displacement must be continuous across the boundary.
2. The acoustic excitation consists of plane acoustic waves. These are incident on boundaries between two media and are transmitted and reflected as plane waves.
3. The transmitted wave has the same frequency as the incident wave.
4. Pressure at a boundary adds as a scalar, while particle velocity adds as a vector.
5. The acoustic impedance of a medium relates the acoustic pressure to the [normal] particle velocity. For plane progressive waves, the acoustic impedance equals the characteristic impedance of the medium.
6. The entry impedance of a medium is defined as the ratio of acoustic pressure to acoustic particle velocity normal to the boundary of the medium.
7. The angle of incidence of an incident acoustic wave is equal to the angle of reflection of the reflected component.

Since  $TL$  is considered across an isolated panel without considering cabin effects, the same air density and acoustic velocity are always used wherever the air occurs. The infinite panel characteristic impedance described in Section 2.1 accounts for rigidity as well as mass effects. The characteristic impedances and propagation constants of acoustic blankets are modeled using Beranek's <sup>[12,13]</sup> model of complex gas compressibility and density as described in Appendix C.

In order to find the transmission loss across a treated panel one must find the ratio of incident to transmitted pressure, which may be expressed in terms of the blocked pressure ratios of each of the layers. The blocked pressure at a surface or interface (denoted by a numeral subscript, see Figure 9 on page 109) is the resultant of all incident and reflected waves. The treated panel model considered is bounded on both sides by semi-infinite air media. This neglects interior cavity reflections, hence the blocked pressure at the inner surface is simply the transmitted pressure ( $P_{NT} = P_t$ ). At the outer surface the incident pressure is separated from the reflected pressure contributions to the blocked pressure by the ratio  $P_i/P_1$ :

$$\frac{P_i}{P_t} = \frac{P_i}{P_1} \frac{P_1}{P_2} \frac{P_2}{P_3} \dots \frac{P_{NT-1}}{P_{NT}} \frac{P_{NT}}{P_{NT+1}} = \frac{P_i}{P_1} \frac{P_1}{P_{NT+1}} \quad [2.9]$$

where

$P_i$  = incident pressure  
 $P_t$  = transmitted pressure  
 $P_1$  = blocked pressure on outer face of panel  
 $P_2$  = blocked pressure at interface 2  
 $P_{NT}$  = blocked pressure at interface NT  
 $P_{NT+1}$  = blocked pressure on inner face of treatment ( =  $P_t$  )

and  $NT$  is the total number of layers including the panel. The blocked pressure ratio across the treated panel is the product of the pressure ratios across each of the individual layers:

$$\frac{P_1}{P_{NT+1}} = \prod_{j=1}^{NT} RP_j \quad [2.10]$$

where  $RP_j = P_j/P_{j+1}$  is the blocked pressure ratio for the  $j^{\text{th}}$  layer.

The entry or exit impedance of a layer or multilayered system is the ratio of acoustic pressure to normal acoustic velocity at the entrance or exit boundary of the layer or system. (At an interface, the entry impedance is the impedance seen "looking inwards," and the exit impedance is the impedance seen "looking outwards.") The characteristic impedance  $Z_0$  of a medium is an acoustical property which relates acoustic pressure to normal acoustic velocity at any point within the medium. For a semi-infinite medium, the entry or exit impedance is equal to the characteristic impedance. For a layered system the entry impedance depends on all backing layers.

Figure 10 on page 110 shows a plane wave incident on a plane boundary between a semi-infinite air medium and a semi-infinite medium of unknown entry impedance  $Z_{em}$ . The exit impedance of the first medium  $Z_{exit-air}$  is the characteristic impedance of air:

$$Z_{exit-air} = Z_{0_a} = \frac{\rho_a c_a}{\cos \theta_i} \quad [2.11]$$

The unknown entry impedance of the second medium  $Z_{em}$  represents the entry impedance of the treated panel  $Z_p$ , which may be built up as described below. As in Ref. [11], the ratio of incident to blocked pressure at the outer surface is

$$\frac{P_i}{P_1} = \frac{Z_{\text{exit-air}} + Z_{\text{ent}}}{2Z_{\text{ent}}} = \frac{Z_{0_s} + Z_p}{2Z_p} \quad [2.12]$$

For each treatment,  $RP_i$  depends on the entry impedance of the next medium the acoustic wave will encounter, i.e. the medium which is closer to the cabin interior. This in turn depends on the impedance of the following medium. Therefore, each  $RP_i$  must be computed successively beginning with the innermost layer and working outward towards the panel.

The following development is for a panel insulated with an airgap, a fibrous blanket, and a limp-mass septum representing an inner trim panel (see Figure 4 on page 104.) Letting subscripts  $p$ ,  $g$ ,  $b$ , and  $s$  denote the panel, airgap, blanket, and septum respectively, the pressure ratio reduces to

$$\frac{P_i}{P_t} = \frac{P_i}{P_1} (RP_s)(RP_b)(RP_g)(RP_p) \quad [2.13]$$

The innermost treatment, the limp-mass septum, has a characteristic impedance of

$$Z_{0_s} = j\omega\sigma_s \quad [2.14]$$

The next medium into which the acoustic wave will pass is the cabin interior, modeled as a semi-infinite layer of air (characteristic impedance  $Z_{0_a}$ ) since the interior cavity is not considered. The septum is seen as a mass reactance in series with  $Z_{0_a}$ , so that its entry impedance is

$$Z_s = Z_{0_a} + Z_{0_s} \quad [2.15]$$

and the pressure ratio across the septum is then

$$\begin{aligned} RP_s &= \frac{Z_{\text{exit}_s} + Z_{\text{ent-cabin}}}{Z_{\text{ent-cabin}}} \\ &= \frac{Z_{0_s} + Z_{0_a}}{Z_{0_a}} \end{aligned} \quad [2.16]$$

Notice that, if the septum is considered alone without the panel and other treatments, the pressure ratio is

$$\begin{aligned}
 \frac{P_i}{P_t} &= \frac{P_i}{P_1} RP_s \\
 &= \frac{Z_{0_s} + (Z_{0_s} + Z_{0_s})}{2(Z_{0_s} + Z_{0_s})} \frac{Z_{0_s} + Z_{0_s}}{Z_{0_s}} \\
 &= 1 + \frac{j\omega\sigma_p \cos \theta_i}{\rho_a c_a}
 \end{aligned} \tag{2.17}$$

which is the familiar mass law expression.

The treatment adjacent to the septum is the blanket, which has characteristic impedance  $Z_{0_b}$  and propagation constant  $b_b$  as developed in Appendix C. The pressure ratio across the blanket is

$$RP_b = \frac{\cosh(b_b t_b \cos \theta_b + \psi_b)}{\cosh \psi_b} \tag{2.18}$$

where  $t_b$  is the blanket thickness and  $\theta_b$  is the angle of refraction in the blanket (found using Snell's Law). The complex amplitude and phase difference  $\psi_b$  resulting from interaction between the incident and reflected waves is given by

$$\psi_b = \coth^{-1} \left[ Z_{ent_s} \frac{\cos \theta_b}{Z_{0_b}} \right] \tag{2.19}$$

As before,  $Z_s = Z_{0_s} + Z_{0_s}$ . The impedance of the blanket is

$$Z_b = \frac{Z_{0_b}}{\cos \theta_b} \coth(b_b t_b \cos \theta_b + \psi_b) \tag{2.20}$$

Once the impedance of the blanket is known, the pressure ratio across the airgap of gap thickness  $t_g$  is

$$RP_g = \frac{\cosh(jkt_g \cos \theta_i + \psi_g)}{\cosh \psi_g} \quad [2.21]$$

where the wavenumber is

$$k = \frac{\omega}{c_a} \quad [2.22]$$

$$\psi_g = \coth^{-1} \left[ \frac{Z_b}{Z_{0_s}} \right] \quad [2.23]$$

and the entry impedance of the airgap is

$$Z_g = Z_{0_s} \coth(jk t_g \cos \theta_i + \psi_g) \quad [2.24]$$

The pressure ratio across the panel is similar to that of the septum, except that the panel rigidity effects are included as well as inertial effects and the panel is backed by the treatment layers as well as the semi-infinite air medium. Therefore,

$$RP_p = \frac{(Z_{0_p} + Z_g)}{Z_g} \quad [2.25]$$

$$Z_p = Z_{0_p} + Z_g \quad [2.26]$$

The characteristic impedance of the panel,  $Z_{0_p}$ , includes the effects of rigidity and thus coincidence. (See Section 2.1.)

At this point, the pressure ratios  $RP_i$  and the panel entry impedance  $Z_p$  are known, so that the transmission coefficient for a plane wave of a particular frequency incident from a given direction ( $\phi_i, \theta_i$ ). may be found from

$$\frac{1}{\tau} = \left| \frac{(Z_{0_s} + Z_p)}{2Z_p} (RP_s)(RP_b)(RP_g)(RP_p) \right|^2 \quad [2.27]$$



## 2.3 Frequency Averaging and Spatial Averaging of Transmission Loss

The previous sections have described how to calculate the specific incidence transmission loss at a given frequency, i.e.  $TL$  for a specified combination of  $\phi_i$ ,  $\theta_i$ , and  $f$ . *Specific incidence* approximates a discrete tone from a given external source location, e.g. a propeller; it also has the advantage of requiring very little computation time. For diffuse noise all directions must be accounted for by spatial averaging of both  $\phi_i$  and  $\theta_i$  (*field incidence*.) Because of the relatively large amount of computation time needed for field incidence transmission loss, it is also useful to define an *azimuthal incidence* transmission loss which considers all azimuthal directions at a constant value of  $\theta_i$ . To consider transmission over a narrow band of frequencies rather than at one discrete frequency, the transmission loss at several discrete frequencies may be averaged over a *1/3 octave band*. (An octave is a doubling in frequency.) For broadband noise such as flow noise, 1/3 octave band transmission losses may be averaged over a wide range of frequencies to form a *transmission loss level*.

The designer must carefully consider which type of acoustic function to choose. Some measures of acoustic performance do not reflect certain types of behavior; some are expensive to use. A panel which performs well according to one criterion may be unacceptable according to others. Usually plots of  $TL$  vs. frequency for both specific and spatially averaged incidences are necessary to get an accurate representation of overall performance.

**Spatial Averaging:** In some cases noise from one direction dominates transmission and noise from other directions may be ignored. This situation may be modeled by the specific incidence transmission loss developed in the previous sections. (See Eqtns. 2.1 - 2.7.) The simultaneous design approach can take advantage of panel anisotropy to optimize acoustic properties in the incidence direction. However, the resulting design may perform poorly in

other directions if the panel is highly anisotropic; this tradeoff may be taken into consideration by spatial averaging in the azimuthal direction as with azimuthal incidence or field incidence.

For a diffuse source, a more appropriate measure is the field incidence transmission loss which is spatially averaged in both the  $\varphi_i$  and  $\theta_i$  directions. The field incidence transmission coefficient is

$$\bar{\tau} = \frac{\int_{\varphi_i=0}^{2\pi} \int_{\theta_i=0}^{\theta_{lim}} \tau(\theta_i, \varphi_i, f) \cos \theta_i \sin \theta_i d\theta_i d\varphi_i}{\int_{\varphi_i=0}^{2\pi} \int_{\theta_i=0}^{\theta_{lim}} \cos \theta_i \sin \theta_i d\theta_i d\varphi_i} \quad [2.28]$$

The grazing limit of the inclination angle,  $\theta_{lim}$ , is commonly set to  $78^\circ$  to agree with experiments. The field incidence mass law transmission coefficient follows from performing the field incidence integration on the specific incidence mass law transmission coefficient in Eqn. 2.7:

$$\bar{\tau}_{ml} = \ln \frac{\left[ \frac{1 + \left[ \frac{\sigma_p \pi f}{\rho_a c_a} \right]^2}{1 + \left[ \frac{\sigma_p \pi f}{\rho_a c_a} \cos \theta_{lim} \right]^2} \right]}{\left[ \frac{\sigma_p \pi f}{\rho_a c_a} \sin \theta_{lim} \right]^2} \quad [2.29]$$

An azimuthal incidence transmission loss is defined from averaging the transmission coefficient over all azimuthal directions for a specific value of the inclination angle  $\theta_i$ . The computation time spent integrating the field incidence transmission coefficient over both spatial variables can become large if the design process calls for many evaluations of  $TL$ . Integrating over only  $\varphi_i$  reduces computation time but still retains averaging of panel anisotropy effects. The azimuthal incidence transmission coefficient is

$$\bar{\tau}_\theta = \frac{\int_{\varphi_i=0}^{2\pi} \tau(\theta_i, \varphi_i, f) \cos \theta_i \sin \theta_i d\varphi_i}{\int_{\varphi_i=0}^{2\pi} \cos \theta_i \sin \theta_i d\varphi_i} \quad [2.30]$$

Since mass law behavior is independent of azimuth, the mass law transmission coefficient for azimuthal incidence is identical to that for specific incidence.

Note that the rigidity term in Eqtn. 2.3 is proportional to  $\sin^4\theta_i$ . Therefore, rigidity effects are most pronounced when  $\sin \theta_i$  is maximum, at the grazing angle of  $78^\circ$ . Coincidence occurs at the lowest frequencies for transmission from  $\theta_i = 78^\circ$ ; therefore,  $\theta_i = 78^\circ$  is of particular interest. Also, axis orientation is arbitrary with respect to acoustics, since the the acoustical analysis does not consider panel boundaries. Hence, the azimuthal angle used with specific incidence is somewhat arbitrary as well. *The remainder of this thesis adopts the following definitions:* Specific incidence refers to excitation from  $(\varphi_i, \theta_i) = (0^\circ, 78^\circ)$  to emphasize rigidity effects. Grazing incidence refers to  $\varphi_i$ -averaged excitation from an inclination angle of  $\theta_i = 78^\circ$  because coincidence occurs first at this inclination. Finally, field incidence refers to excitation from all angles to  $\theta_i = \theta_{lim}$ .

**Frequency Averaging:** For a given incidence type (specific, grazing, or field), the acoustic performance index may be defined as the transmission loss at a discrete frequency (the *target frequency*). However, even tonal noise has a finite bandwidth. Commonly a 1/3 octave band average of several discrete sub-band frequencies is used as a performance index in the vicinity of a specific (center) frequency. In regions where  $\tau$  changes rapidly with respect to frequency, many such sub-bands may be needed to give an accurate center-frequency  $TL$ . The sub-band averaged transmission coefficient for a 1/3 octave band is given by

$$\tau = \frac{\sum_{i=1}^{NSB} S(f_i) \Delta f_i \tau_i}{\sum_{i=1}^{NSB} S(f_i) \Delta f_i} \quad [2.31]$$

where  $S(f_i)$  is the power spectral density of the incident pressure at frequency  $f_i$  with narrow frequency bandwidth  $\Delta f_i$ , and NSB is the number of sub-bands. The power spectral density  $S(f_i)$  is taken as unity since the frequency characteristics of the noise are not specifically considered.

For broadband noise excitation and to quantify panel behavior over a wider response region a number of 1/3-octave band transmission losses are appropriate and may be combined into a single wide range frequency averaged index, the *transmission loss level*,  $TLL$ :

$$TLL = 10 \log \left[ \sum_{i=1}^{NB} 10^{(TL_i/10)} \right] \quad [2.32]$$

where  $NB$  is the number of one-third octave bands over which  $TLL$  has been averaged, and  $TL_i$  is the transmission loss at the center frequency of the  $i^{\text{th}}$  one-third octave band. The transmission loss level is dominated by the largest values of  $TL$ , which usually occur at high frequencies (instead of near coincidence.) Thus, if the design process maximizes  $TLL$ , the result is often biased so strongly towards improving  $TL$  at high frequencies that it essentially ignores the coincidence region. To address the coincidence region, one may consider a transmission difference level defined as

$$TDL = 10 \log \left[ \sum_{i=1}^{NB} 10^{(TD_i/10)} \right] \quad [2.33]$$

$$TD_i = TL_{ref} - TL_i \quad [2.34]$$

where  $TL_{ref}$  is a reference transmission loss, usually taken to be 100 dB. Figure 11 on page 111 shows a typical comparison between  $TL$  and  $TD$ . Notice that the largest values of  $TD$  occur not at high frequencies as with  $TL$ , but in the coincidence region. Thus, the maximum value of  $TDL$  is obtained by improving performance near coincidence rather than wasting effort in regions of good acoustic performance.

## 3.0 Implementing The Design Procedure

This chapter describes how transmission loss theory is applied to the problem of optimal structural/acoustical panel design. Recall that the design problem is to replace an aluminum panel with a sequentially or simultaneously designed composite panel and compare acoustic performance. The first section discusses the types of structural analysis used. Section 3.2 outlines the different design strategies and describes the optimization routine. Finally, Section 3.3 addresses some of the programming considerations involved.

### 3.1 *Structural Analysis*

Among the factors considered in the structural design of a fuselage skin panel are its impact tolerance, fatigue damage resistance, and ability to maintain flight safety in the event of structural damage<sup>[6]</sup>. A fatigue damage constraint is essentially a lower bound on the shear buckling strength  $N_{xy}$  of the panel. Therefore, as in Ref. [6], the structural analysis used here compares the shear buckling strength of the design panel to that of a representative aluminum panel with thickness  $t_p = 1.01\text{mm}$  and dimensions  $(a,b) = (0.241\text{m}, 0.406\text{m})$ .

Program TLTROP in Appendix A can use either of two methods to calculate the shear buckling strength. (Equations for these methods are given in Appendix B.) The more accurate of the two methods is an eigenvalue solution derived from the panel equation of motion <sup>[14]</sup>. Since this solution requires relatively large amounts of computation time, an approximate solution based on "infinite strip" theory <sup>[14]</sup> is used during optimization in order to reduce costs. Using the approximate solution reduces structural analysis time by three to four orders of magnitude as compared to the eigenvalue solution.

An infinite strip is a thin panel of finite width but infinite length. The approximate function used during optimization is the sum of the infinite strip critical shear stresses obtained by letting first the  $x$ -dimension,  $a$ , and then the  $y$ -dimension,  $b$ , become infinite:

$$\tilde{\tau} = \tau_{cr} \Big|_{a \rightarrow \infty} + \tau_{cr} \Big|_{b \rightarrow \infty} \quad [3.1]$$

Here, two panels are considered structurally equivalent if their approximate shear stresses are equal. A shear-critical panel is defined as a panel which has *the same approximate critical shear stress  $\tilde{\tau}$  as the aluminum panel.*

For a composite panel with a given thickness, the layup angle which yields the highest shear buckling capacity depends on the panel aspect ratio. For a panel which is infinite in the  $x$ -direction ( $a \rightarrow \infty$ ), the structurally optimal layup is  $\pm 30^\circ$ , while  $\pm 60^\circ$  is the best layup for the case of  $b \rightarrow \infty$ . (For a square panel, a  $\pm 45^\circ$  layup is best.) Thus, regardless of aspect ratio one would expect the structurally optimal layup angle to lie between  $30^\circ$  and  $60^\circ$ . The  $0.241\text{m} \times 0.406\text{m}$  panel used in this thesis has an aspect ratio of 1.7, and the structurally optimal layup angle is shown in Sec. 4.1 to be  $33.3^\circ$ .

Figure 12 on page 112 shows  $N_{xy}/N_{xy_{alum}}$  (the ratio of composite panel eigenvalue shear buckling load to aluminum panel eigenvalue shear buckling load) as a function of layup angle. The curve shown is for shear-critical panels, i.e. each point on the curve represents a shear-critical panel. By definition all shear-critical panels have the same approximate critical shear stress  $\tilde{\tau} = \tilde{\tau}_{alum}$ . Therefore, if  $\tilde{\tau}$  accurately approximated shear strength, then all shear-critical

panels would also have  $N_{xy} = N_{xy,alum}$  and the curve in Figure 12 would be a horizontal line. Actually, the values vary by as much as 35% for some layups. The 33° layup has the same  $N_{xy}$  as the aluminum panel; all other shear-critical panels have higher  $N_{xy}$  than the aluminum panel.

The effect of this approximation is that large changes in layup angle away from the structurally optimum angle of 33° are probably slightly suppressed. For example, the 90° layup needs a mass increase of approximately 14% over the 33° layup in order to satisfy the (approximate) shear constraint. This mass increase gives an eigenvalue shear buckling load almost 25% greater than that of the aluminum panel. In other words, the mass penalty needed to satisfy the lower bound on  $\tilde{\tau}$  is larger than that which is needed to give the same  $N_{xy}$  as the aluminum panel.

The approximate solution is designed to influence optimizations in the same manner as the eigenvalue solution. The approximation is fairly accurate in the immediate region of the structurally optimal layup angle, which is used in sequential design approach (see Sec. 4.1.) Accuracy decreases away from that angle, with the largest error occurring for layup angles near 90°. None of the optimization results in Sec. 4 utilize panels in the region of maximum error near 90°; however it is not clear whether this is because changes toward this layup were suppressed by the approximation error. For the present research the accuracy of the structural analysis is a secondary issue and the approximation is appropriate.

## 3.2 *Design Formulation*

A practical design approach would be to analyze the acoustic performance of a treated aluminum panel, and then either 1) find the lightest possible treated composite panel which is equivalent both structurally and acoustically, or 2) specify a desired weight savings, then optimize the acoustic performance of a structurally equivalent treated composite panel.

However, such an approach requires designing the aluminum panel treatment or selecting an appropriate weight savings. Instead, the design approach taken here is to replace an untreated aluminum panel with an equal mass, structurally equivalent treated composite panel. It is easier to compare designs based on different acoustic criteria if their masses are the same. Then superior acoustic performance in one design implies that mass may be reduced without allowing excessive noise levels.

The most straightforward design formulation is the acoustic objective (loss-objective) formulation, which optimizes the acoustic performance index subject to mass and structural constraints. With this formulation, the mass constraint is usually active so that the surface masses are equal and the results may be compared without ambiguity.

A dual problem to the loss-objective formulation is the mass-objective formulation: the total (panel + treatment) surface mass is minimized subject to both structural and acoustical constraints. performance index meet or exceed some specified values. To produce comparable designs, the design must be iterated with adjustments of the acoustic constraint until the resulting mass equals that of the aluminum panel.

By the definition in the previous section, two panels are structurally equivalent if their approximate critical shear stresses  $\tilde{\tau}$  are equal. In order for a composite panel to qualify as a suitable replacement for a 1.01mm-thick aluminum panel, it must satisfy the constraint

$$\tilde{\tau}_{\min} = \tilde{\tau} \Big|_{aluminum} = 0.831 \times 10^7 \text{ N/m}^2 \quad [3.2]$$

If the mass is constrained (loss-objective formulation), the total mass  $\sigma_{tot}$  of the panel and treatment must not exceed the mass of the aluminum panel:

$$\sigma_{tot} \leq \sigma_{aluminum} = 2.828 \text{ kg/m}^2 \quad [3.3]$$

If the acoustic performance is constrained (mass-objective formulation) the acoustic performance index must satisfy one of the following constraints:



$$\begin{aligned}
TL &\geq TL_{\min} \\
TLL &\geq TLL_{\min} \\
TDL &\leq TDL_{\max}
\end{aligned}
\tag{3.4}$$

where  $TL_{\min}$ ,  $TLL_{\min}$ , or  $TDL_{\max}$  is determined iteratively to yield the desired mass minimum.

### 3.3 Programming Considerations

NEWSUMTA is a computer program written in subroutine form for solving linear and nonlinear constrained or unconstrained function minimization problems [15,16]. The basic algorithm is the sequence of unconstrained minimizations (using Newton's method with approximate derivatives) of a total function formulated from the objective function, penalty multiplier, and constraint functions. Problems must be formulated as follows:

$$\begin{aligned}
&\text{Minimize} && f(x_1, x_2, \dots, x_n) \\
&\text{subject to} && g_q(x_1, x_2, \dots, x_n) \geq 0, \quad q = 1, 2, \dots, n_{ineq} \\
&\text{and/or} && h_q(x_1, x_2, \dots, x_n) = 0, \quad q = 1, 2, \dots, n_{eq}
\end{aligned}
\tag{3.5}$$

The operation of NEWSUMTA is such that nonlinear functions are more efficiently handled as nonlinear constraints with a linear objective function. Since the acoustic functions are highly nonlinear, a dummy linear objective function is substituted in the following manner:

Let  $\vec{X}$  be the vector of design variables needed to fully describe the configuration. Consider the loss-objective formulation of minimizing the *nonlinear* objective function

$$obj(\vec{X}) = -TL \tag{3.6}$$

subject to the constraints

$$g_1(\vec{X}) = \tilde{\tau} - \tilde{\tau}_{\min} \geq 0 \quad [3.7]$$

$$g_2(\vec{X}) = \sigma_{\max} - \sigma_{\text{tot}} \geq 0 \quad [3.8]$$

where  $\tilde{\tau}$  is the approximate critical shear stress,  $\tilde{\tau}_{\min}$  is the minimum allowable approximate critical shear stress,  $\sigma_{\text{tot}}$  is the total surface mass, and  $\sigma_{\max}$  is the maximum allowable total surface mass. An equivalent problem statement would be to minimize the *linear* objective function

$$\text{obj}(\vec{X}) = -\xi \quad [3.9]$$

subject to the constraints

$$g_1(\vec{X}) = \tilde{\tau} - \tilde{\tau}_{\min} \geq 0 \quad [3.10]$$

$$g_2(\vec{X}) = \sigma_{\max} - \sigma_{\text{tot}} \geq 0 \quad [3.11]$$

$$g_3(\vec{X}) = TL - \xi \geq 0 \quad [3.12]$$

where  $\xi$  is a dummy variable. Here,  $\xi$  is included in the design vector  $\vec{X}$ , so that the objective function is linear in  $\xi$  and independent of the other design variables.

The surface mass is a linear function, so that no advantage is gained by treating the mass objective formulation in this manner. Nevertheless, the dummy variable  $\xi$  is used with the mass objective for ease of programming: the problem is to minimize the linear objective function

$$\text{obj}(\vec{X}) = -\xi \quad [3.13]$$

subject to the constraints

$$g_1(\vec{X}) = \tilde{\tau} - \tilde{\tau}_{\min} \geq 0 \quad [3.14]$$

$$g_2(\vec{X}) = \xi - \sigma_{\text{tot}} \geq 0 \quad [3.15]$$

$$g_3(\vec{X}) = TL - TL_{\text{min}} \geq 0 \quad [3.16]$$

In practice, both the constraint functions and the design variables are scaled to prevent numerical instabilities in NEWSUMTA. The design variable scale factors are assigned values such that, for most configurations, the values of the design variables remain between 0.1 and unity. The values used to compute the constraints are normalized by the values calculated for the initial design, so that the constraints usually remain between zero and unity. (The practical lower limit for constraint values is approximately  $10^{-4}$  where they begin to affect the total function being minimized.) Both formulations include side bounds which restrict the layup angle to the first quadrant and prevent the treatment thicknesses from becoming negative.

To use NEWSUMTA, the user must supply a main program to call the optimization subroutine and an analysis subroutine to evaluate the objective function, constraint functions, and derivatives. A flowchart is shown in Figure 13 on page 113. TLTROP is the main program which reads input data, performs pre- and post-processing operations, calls the NEWSUMTA subroutine, and prints output data. The analysis subroutine, TLTRAN, is called by NEWSUMTA to evaluate the objective function and the constraint functions. TLTRAN calls only those subroutines needed to compute the constraints; a full structural/acoustical analysis is performed by the pre- and post-processor units in TLTROP.

For field and azimuthal incidence, integration of the transmission coefficient is performed by one of the following subroutines:

- DCADRE: Adaptive IMSL integration subroutine for functions of one variable.
- DBLIN: Adaptive IMSL integration subroutine for functions of several variables.
- DMLIN: Non-adaptive IMSL integration subroutine for functions of several variables.
- SIMP: Subroutine for Simpson's Rule integration.

The integrand  $\tau$  is smooth except near coincidence, where the derivative with respect to incidence direction can be large. (See Figure 7 on page 107.) This seems to suggest that an adaptive integration subroutine be used, i.e. one which would maintain accuracy in regions of rapid variation by using smaller step sizes. However,  $\tau$  is several orders of magnitude larger in directions affected by coincidence than in other directions. Hence,  $TL$  is small there and inaccuracies do not have a large effect on the result. Integration errors are made even less critical by the logarithmic nature of  $TL$ . Some operations require many evaluations of  $TL$ ; particularly, optimizations using field incidence and/or frequency-averaged acoustic criteria. Therefore, in such cases a non-adaptive integration routine should be used to reduce the cost of acoustical analysis.

The optimization results presented in Chapter 4 were performed using both adaptive and non-adaptive integration subroutines. For field incidence, optimizations could not be completed using the IMSL integration subroutines because the repeated evaluations of  $TL$  required too much computation time. Instead, the Simpson's Rule subroutine was used with  $5^\circ$  increments in the  $\phi$ -direction and  $4.33^\circ$  increments in the  $\theta$ -direction.

## 4.0 Results and Discussion

Section 4.1 is a preliminary study of untreated composite panels. Its purpose is to 1) define the admissible range of replacements for the aluminum panel, 2) develop the concept of structurally optimized panel, and 3) illustrate the acoustic properties of admissible panels. The design study in Section 4.2 examines the results of simultaneous and sequential optimizations performed with a variety of acoustic functions, and compares the simultaneous and sequential design approaches. Finally, Section 4.3 summarizes the results of this study and proposes topics for future work.

For convenience in discussing the position of a particular frequency with respect to the coincidence region, the following terminology is adopted in this section:

<b>Mass Law Region</b>	Low frequency region far enough below coincidence that negligible degradation occurs.
<b>Sub-coincidence Region</b>	Frequencies where significant degradation occurs. For specific incidence, beginning with the upper limit of the mass law region and ending with $f_c$ . For grazing incidence and field incidence, beginning with the upper limit of the mass law region and ending with $f_{crit}$ .

**Trans-coincidence Region** Defined only for grazing incidence or field incidence. Includes frequencies between  $f_{c/n}$  and  $f_{c_{max}}$  where coincidence occurs at grazing ( $\theta_i = 78^\circ$ ) in some azimuthal direction.

**Super-coincidence Region** High frequencies at which the post-coincidence rigidity recovery occurs. For specific incidence, frequencies above  $f_c$ . For grazing incidence and field incidence, frequencies above  $f_{c_{max}}$ .

The target frequencies  $f_1$ ,  $f_2$ ,  $f_3$ , and  $f_4$  are related to the structural panel as follows:  $f_1$  is in the mass law region;  $f_2$  is sub-coincident;  $f_3$  is sub-coincident for specific incidence from  $(\phi_i, \theta_i) = (0^\circ, 78^\circ)$ , or trans-coincident for grazing and field incidence;  $f_4$  is super-coincident.

## 4.1 Preliminary Study

As outlined in Section 3.3, the design objective is to replace an untreated aluminum panel with a treated composite panel of 1) lower or equal total mass, and 2) greater or equal shear buckling capacity. Therefore, the range of admissible replacement panels is bounded by the shear-critical case (lower mass than aluminum panel; treatments may be applied to improve acoustic performance), and the mass-critical case (same mass as aluminum panel; no treatment mass may be applied). The masses, shear buckling capacities, and coincidence frequencies of shear-critical and mass-critical panels are summarized in Table 1 on page 35. (Panel and treatment material properties are listed in Table 2 on page 37.) In order to better understand structural/acoustical interactions, it is helpful to examine these limiting cases in the context of maximizing acoustic performance.

A special case of the shear-critical panel is the structurally optimized (minimum mass) panel, which is the first step in the sequential design approach. (The second step is to design the acoustic treatment for this structurally designed panel.) Figure 14 on page 114 shows the

fraction of allowable mass needed to satisfy the shear constraint for panels with layup angles between  $\alpha = 0^\circ$  and  $\alpha = 90^\circ$ . Since the panel mass cannot exceed that of the aluminum panel, the maximum total surface mass is  $\sigma_{\max} = 2.828 \text{ kg/m}^2$ . The  $90^\circ$  layup is the least efficient in resisting shear, requiring a mass of  $0.99\sigma_{\max}$  to satisfy the shear constraint; the  $0^\circ$  layup requires a mass fraction of only 0.75. For layup angles between these two limits, the mass fraction falls to its minimum of 0.61 for  $\alpha = 33.3^\circ$ . This is the "structural panel," defined as the lightest panel capable of satisfying the shear constraint. For the 8-ply graphite/epoxy laminates in this report the thickness of the structural panel is 1.1083mm.

Figure 15 on page 115 and Figure 16 on page 116 show the variations of the stiffness parameter  $D_{\theta\theta}$  and coincidence frequency  $f_c$  with azimuth for the aluminum panel and several shear-critical composite panels. For the isotropic aluminum panel,  $D_{\theta\theta}$  and  $f_c$  are independent of azimuth, and the coincidence frequency remains constant at 12481 Hz. For composite panels, the coincidence frequency can vary by almost 16000 Hz and, more importantly, can

**Table 1. Coincidence Bandwidths of Mass-Critical and Shear-Critical Panels**

Description	$\sigma_p/\sigma_{\max}$	$\bar{\tau}/\tau_{\min}$	$f_{\text{crit}}$ (Hz)	$f_{\text{cmax}}$ (Hz)	$\Delta f_{\text{coin}}$ (Hz)
Mass-Critical $0^\circ$	1.000	1.788	3940	14845	10905
Mass-Critical $33^\circ$	1.000	2.707	4641	10147	5506
Mass-Critical $45^\circ$	1.000	2.527	4677	7461	2784
Mass-Critical $90^\circ$	1.000	1.010	3940	14845	10905
Shear-Critical $0^\circ$	0.750	1.000	5266	19842	14576
Shear-Critical $33^\circ$	0.607	1.000	7640	16704	9064
Shear-Critical $45^\circ$	0.629	1.000	7427	11847	4420
Shear-Critical $90^\circ$	0.997	1.000	3950	14881	10931
Aluminum	1.000	1.000	12481	12481	0

be either higher or lower than the coincidence frequency of the aluminum panel. The greatest amount of variation occurs for the 90° panel (all fibers aligned with the long side of the panel), while the most isotropic composite panel is the 45° panel. Therefore, the 90° panel can have a large azimuthal variation in acoustic performance, with some directions being very near coincidence while other directions are mass-controlled or rigidity-controlled. The acoustic properties of the 45° panel vary less drastically with azimuth, resulting in a trans-coincidence region which is relatively small although it occurs at lower frequencies than with the aluminum panel.

The specific, grazing, and field incidence transmission loss of shear- and mass-critical panels is shown in Figure 17 - Figure 22. At mass law frequencies the composite panels have smaller transmission loss than the aluminum panel because of their lower mass. (As a limiting case, the mass-critical panels have the same  $TL$  as the aluminum panel.) However, at higher frequencies the comparison depends on the stiffness properties; the panel which gives the highest transmission loss depends on incidence type and frequency range, as outlined below.

**Specific Incidence:** Figure 17 on page 117 and Figure 18 on page 118 show the specific incidence  $(\phi_i, \theta_i) = (0^\circ, 78^\circ)$  transmission loss for untreated shear-critical and mass-critical panels. The panels with the highest  $TL$  at a particular target frequency are those with high mass and coincidence frequencies far from the target frequency. In the sub-coincident region, panels that are flexible in the direction and have high coincidence frequencies perform best. In the super-coincident region, the opposite is true: the best panels are those which are rigid in the incidence direction and have low coincidence frequencies.

The mass-critical 90° panel has a higher coincidence frequency than the aluminum panel; its sub-coincidence region extends to higher frequencies giving better  $TL$  up to approximately 14000 Hz. On the other hand, the mass-critical 0° panel recovers from coincidence at relatively low frequencies. These cases suggest two design trends: for low frequencies increase the layup angle to raise  $f_c$ , or for high frequencies decrease the layup angle to lower  $f_c$ . By



**Table 2. Properties of Panel And Treatment Materials**

	Density kg/m <sup>3</sup>	$E_1$ $\times 10^9$ N/m <sup>2</sup>	$E_2$ $\times 10^9$ N/m <sup>2</sup>	$G_{12}$ $\times 10^9$ N/m <sup>2</sup>	$\nu_{12}$	$R_1$ Rayls/m	$c_s$ m/s <sup>2</sup>
Aluminum	2800.	72.0	72.0	27.0	0.333	-	-
Graphite/Epoxy	1550.	137.	9.65	4.80	0.30	-	-
Air	1.21	-	-	-	-	-	343.
Blanket	9.60	-	-	-	-	43000.	-
Septum	1000.	-	-	-	-	-	-

these trends, the mass-critical 90° panel is best for low frequencies, while the mass-critical 0° panel is best for high frequencies. However, three other factors must be considered. First, a mass-critical panel allows no treatment to be added. Add-on treatments are very mass-efficient in this frequency range; during optimization the incentive to raise or lower  $f_c$  by using a mass-critical panel is to be balanced against the incentive to allow mass for add-on treatments. Second, in some instances it may not be acceptable to increase high frequency  $TL$  by lowering  $f_c$ , since more noise may be encountered at lower frequencies. (Note that the 33° and 45° panels also have higher transmission loss than the aluminum panel at high frequencies, although their coincidence frequencies are not as low as the mass-critical 0° panel.) Third, a highly anisotropic panel which has a high coincidence frequency in one direction has a low coincidence frequency in other directions. If noise is incident from these other directions it could require that extra treatment mass be added to keep cabin noise levels low. This directional tradeoff is considered by azimuthal averaging as with grazing incidence or field incidence transmission loss.

**Grazing Incidence:** Grazing incidence transmission loss (azimuthally averaged at  $\theta_i = 78^\circ$ ) of bare panels is presented in Figure 19 on page 119 and Figure 20 on page 120. The trans-

coincidence region begins at  $f_{crit}$  as coincidence occurs in the panel's most rigid azimuthal direction, and continues throughout the coincidence band until  $f_{cmax}$  where coincidence at  $\theta_i = 78^\circ$  ends and the super-coincidence region begins. (This contrast with specific incidence, where  $TL$  is degraded only in a relatively narrow region.) Thus, the important parameters are  $f_{crit}$ ,  $f_{cmax}$ , and the grazing coincidence bandwidth  $\Delta f_{coin} \equiv f_{cmax} - f_{crit}$ , as shown in Table 1 on page 35. The upper and lower limits of the trans-coincidence region can be shifted up or down in frequency as with specific incidence, but its width  $\Delta f_{coin}$  must be considered as well giving three design trends. First, at low frequencies  $TL$  may be raised by delaying trans-coincidence, i.e. choosing a panel with a high critical frequency. Second, at high frequencies the best panel is one with a low value of  $f_{cmax}$  which enters super-coincidence early. Third, for broadband noise the best panel is one with a narrow trans-coincidence region.

For sub-coincident frequencies, coincidence can be delayed to 7640 Hz (the highest critical frequency of any layup) by selecting the structural panel; this design also allows the largest treatment mass. However, the coincidence bandwidth is more than 9000 Hz and  $f_{cmax} = 16704$  Hz; the trans-coincidence region is large and high frequency performance is poor. At high frequencies,  $TL$  may be raised by choosing a panel with a low  $f_{cmax}$ . The panel with the lowest critical frequency is the mass-critical  $0^\circ$  panel, but this panel has a coincidence bandwidth of over 14800 Hz so that trans-coincidence extends to  $f_{cmax} = 14845$  Hz. The mass-critical  $45^\circ$  panel has a slightly higher critical frequency (4677 Hz), but has a lower  $f_{cmax}$  (7461 Hz) because its coincidence bandwidth is only 2784 Hz. Therefore it has a small trans-coincidence region; also, its early recovery from coincidence allows it to exceed the aluminum panel  $TL$  at high frequencies.

Note that for the aluminum panel  $\Delta f_{coin} = 0$ ; the large trans-coincidence region associated with anisotropy may be a major fault of composite panels in field incidence. The  $45^\circ$  panel is the most isotropic, and therefore has the smallest trans-coincidence region.

The mass-critical designs allow no treatment mass; thus, other designs of interest for high frequencies are the shear-critical panels (although the balance between treatment mass and panel mass is not discussed until the Design Study.) The shear-critical  $45^\circ$  panel provides

a good compromise between low  $f_{c_{max}}$  and low panel mass. The maximum grazing coincidence frequency is less than 4000 Hz higher compared to the mass-critical 45° panel, so that the rigidity recovery starts later and high frequency performance is not quite as good. However, the mass is over 27% lower so that treatment mass may be added.

**Field Incidence:** Figure 21 on page 121 and Figure 22 on page 122 present the field incidence transmission loss of bare panels. The upper and lower limits of the trans-coincidence region ( $f_{crit}$  and  $f_{c_{max}}$ ) have a similar effect on field incidence as on grazing incidence. The mass law region can be extended by choosing the structural panel with its high critical frequency; the 45° layup is attractive for its small trans-coincidence region and/or early super-coincidence region. However, for field incidence the rigidity recovery is not as strong. Coincidence occurs in some range of inclinations for all frequencies above  $f_{crit}$ ; therefore, all those frequencies are affected to some extent. In super-coincidence,  $TL$  slowly recovers as the range of inclinations dominated by rigidity terms gradually increases. Instead of the moderate recovery seen with grazing incidence, the post-coincidence recovery is slower and less pronounced. The incentive to choose a 45° panel still has some observed effect, although it is weaker because there is less gain from entering super-coincidence.

In summary, the amount by which  $TL$  is influenced by changes in panel design depends on the type of incidence considered. With specific incidence, large changes are achieved by stiffening or softening the panel in the azimuthal direction, thereby shifting coincidence to different frequencies. (Highly anisotropic panels may exhibit poor performance in directions other than the direction being considered.) With both azimuthal and field incidence, the sub-coincident  $TL$  is highest when  $f_{crit}$  is high, while at super-coincident  $TL$  is highest when  $f_{c_{max}}$  is small. The field incidence transmission loss is most weakly affected by changes in the panel.

## 4.2 Design Study

This section presents optimal designs for the panel/airgap/blanket/septum configuration and compares the sequential and simultaneous design approaches. The sequential approach designs a treatment for the previously designed structural panel, whereas the simultaneous approach designs the panel and treatment concurrently and requires more computation time than the sequential approach. The configurations examined were optimized using the specific, grazing, and field incidence  $TL$  acoustic criteria at target frequencies of 1600 Hz, 6400 Hz, 8063 Hz, and 12800 Hz, as well as the  $TLL$  and  $TDL$  acoustic criteria. Results obtained with the loss-objective formulation are presented for all cases; mass-objective results are presented for cases in which they differ from the loss-objective results (due to multiple local optima.) The specific incidence, grazing incidence, and field incidence designs are summarized in Table 3, Table 4, and Table 5 respectively.

In comparing the acoustic performance of the untreated aluminum panel and the treated composite panels, the first point to be made is that the composite panels achieve large increases in transmission loss over the aluminum panels. (See Figure 24 on page 124 for transmission loss of the aluminum panel.) The treatments are so effective that the sequential designs exceed the aluminum panel  $TL$  by 15 - 45 dB throughout the entire frequency range, including the composite panel coincidence regions. Secondly, the simultaneous designs achieve moderate gains over the sequential designs for specific performance indices, but performance is generally sacrificed in other regions and the increase in computation time ranges from about 15% for specific incidence to over 60% for field incidence.

The sequential approach gives a range of treatment designs depending on the acoustic criterion, but the amount of variation is limited because the sum of the blanket and septum masses always equals 39.3% of the total mass (since the structural panel mass is  $\sigma_p/\sigma_{tot} = 60.7\%$ , and the total mass is constant.) The largest possible blanket mass is 39.3%, but

**Table 3. Specific Incidence Optimization Results**

Design Data			Panel				Treatment			Acoustic Performance					
Approach Type/ Objective Type	Acoustic Criterion	CPU Time (sec)	Panel $\alpha$ (deg)	Mass (%)	$f_{crit}$ (Hz)	$f_c$ (Hz)	$t_g$ (mm)	Bla. Mass (%)	Sep. Mass (%)	TL in dB @					
										1600 Hz	6400 Hz	8063 Hz	12800 Hz	TLL (dB)	TDL (dB)
Sequential/Loss	TL@1600 Hz	0.8	33.3	60.7	7645	8887	49.0	39.2	0.0	43.5	56.5	45.4	68.5	69.3	59.1
Simultaneous/Loss	TL@1600 Hz	0.9	33.9	60.9	7654	8990	49.3	39.3	0.0	43.5	56.6	45.8	68.2	69.2	59.1
Sequential/Loss	TL@6400 Hz	0.9	33.3	60.7	7645	8887	6.1	29.7	9.6	39.5	66.3	61.4	82.7	82.1	48.5
Simultaneous/Loss	TL@6400 Hz	1.2	40.9	61.7	7584	10314	5.6	28.2	10.1	39.0	67.7	67.4	76.2	76.2	47.5
Sequential/Loss	TL@8063 Hz	0.9	33.3	60.7	7645	8887	6.3	29.1	10.1	39.4	66.3	61.4	82.7	82.1	48.5
Simultaneous/Loss	TL@8063 Hz	1.8	62.6	74.8	6067	15274	44.3	20.4	4.8	33.1	58.9	61.2	60.6	67.2	56.5
Simultaneous/Mass	TL@8063 Hz	0.5	44.5	62.9	5904	11172	3.1	27.6	9.5	38.4	67.4	68.0	71.4	73.2	48.7
Sequential/Loss	TL@12800 Hz	0.9	33.3	60.7	7645	8887	0.4	13.4	25.6	35.8	59.8	55.7	79.4	78.5	54.5
Sequential/Mass	TL@12800 Hz	0.6	33.3	60.7	7645	8887	6.6	31.1	8.0	39.9	54.2	51.5	82.5	81.5	53.4
Simultaneous/Loss	TL@12800 Hz	1.2	8.4	71.3	5622	5639	0.7	12.7	16.0	33.0	51.9	67.4	88.0	87.9	63.1
Simultaneous/Mass	TL@12800 Hz	0.4	18.1	65.3	6487	6605	1.2	24.5	10.2	36.6	46.5	66.8	88.2	88.2	54.0
Sequential/Loss	TLL	36.4	33.3	60.7	7645	8887	67.3	28.5	1.8	39.5	53.8	52.7	83.0	82.0	53.1
Simultaneous/Loss	TLL	48.5	1.2	74.7	5278	5278	67.4	13.0	12.3	31.8	42.3	60.9	87.7	87.3	69.5
Simultaneous/Mass	TLL	14.0	15.5	67.1	6204	6278	0.3	21.2	11.6	34.9	43.0	67.5	88.4	88.3	56.1
Sequential/Loss	TDL	14.4	33.3	60.8	7645	8887	81.9	88.0	9.2	39.7	57.2	58.2	79.9	79.2	52.4
Simultaneous/Loss	TDL	19.7	38.9	61.2	9911	9813	4.7	85.5	9.7	39.3	67.6	66.5	78.4	78.0	47.2
For Comparison:															
Aluminum Panel	-	-	-	-	-	-	-	-	-	17.0	26.5	26.4	10.5	33.4	88.7
Mass Law	-	-	-	-	-	-	-	-	-	17.1	29.1	31.1	35.1	39.4	45.4

Note: CPU time for IBM 3084. Mass-objective computation times are per iteration.

Table 4. Grazing Incidence Optimization Results

Design Data			Panel				Treatment			Acoustic Performance					
Approach Type/ Objective Type	Acoustic Criterion	CPU Time (sec)	$\alpha$ (deg)	Mass (%)	$f_{crn}$ (Hz)	$f_{cmax}$ (Hz)	$t_g$ (mm)	Bla. Mass	Sep. Mass	TL in dB @					
										1600 Hz	6400 Hz	8063 Hz	12800 Hz	TLL (dB)	TDL (dB)
Sequential/Loss	TL@1600 Hz	10.7	33.3	60.7	7645	16572	48.9	39.2	0.0	43.5	56.9	44.3	52.0	66.0	58.7
Simultaneous/Loss	TL@1600 Hz	15.3	33.3	60.8	7644	16571	49.7	39.2	0.0	43.5	56.7	44.3	52.2	65.9	58.7
Sequential/Loss	TL@6400 Hz	31.9	33.3	60.7	7645	16572	6.5	29.7	9.5	39.6	66.6	57.6	65.9	71.9	47.4
Simultaneous/Loss	TL@6400 Hz	39.0	34.6	60.8	7655	16004	6.6	38.6	0.7	42.8	61.9	50.7	54.9	67.9	53.6
Simultaneous/Mass	TL@6400 Hz	15.0	34.2	61.0	7655	16174	5.3	39.2	0.0	43.3	62.2	50.9	54.3	68.4	53.8
Sequential/Loss	TL@8063 Hz	84.9	33.3	60.7	7645	16572	103.8	29.1	10.1	39.3	63.9	57.7	59.5	67.1	53.0
Simultaneous/Loss	TL@8063 Hz	142.0	32.3	60.8	7618	16992	3.8	28.3	10.8	39.3	66.4	57.6	66.3	71.9	47.5
Simultaneous/Mass	TL@8063 Hz	44.1	35.1	60.9	7664	15788	1.5	29.6	9.4	39.4	66.5	57.6	65.9	71.8	47.5
Sequential/Loss	TL@12800 Hz	131.0	33.3	60.7	7645	16572	65.6	28.3	10.9	39.5	54.8	52.5	66.3	68.6	52.0
Simultaneous/Loss	TL@12800 Hz	62.7	45.0	74.5	6277	10012	0.7	12.4	13.1	32.4	41.9	48.5	74.2	72.7	60.5
Simultaneous/Mass	TL@12800 Hz	31.3	45.1	70.4	6581	10521	11.7	29.4	0.2	38.3	47.0	45.8	61.5	62.7	61.3
Sequential/Loss	TLL	57.2	33.3	60.7	7645	16572	50.1	39.2	0.0	43.5	56.6	44.2	52.3	65.9	58.6
Simultaneous/Loss	TLL	2924.	45.0	75.6	6151	9812	133.3	12.6	11.9	30.5	41.9	45.4	73.9	72.0	67.1

For Comparison:

Aluminum Panel	-	-	-	-	-	-	-	-	-	17.0	26.5	26.4	10.5	33.4	88.7
Mass Law	-	-	-	-	-	-	-	-	-	17.1	29.1	31.1	35.1	39.4	45.4

Note: CPU time for IBM 3084. Mass-objective computation times are per iteration.

**Table 5. Field Incidence Optimization Results**

Design Data			Panel				Treatment			Acoustic Performance					
Approach Type/ Objective Type	Acoustic Criterion	CPU Time (sec)	Panel $\alpha$ (deg)	Mass (%)	$f_{crit}$ (Hz)	$f_{cmax}$ (Hz)	Bla. Sep. $t_g$ (mm)	Mass (%)	Mass (%)	TL in dB @					
										1600 Hz	6400 Hz	8063 Hz	12800 Hz	TLL (dB)	TDL (dB)
Sequential/Loss	TL@1600 Hz	175.0	33.3	60.7	7645	16572	49.4	39.2	0.0	50.1	66.0	57.7	60.6	73.2	*
Simultaneous/Loss	TL@1600 Hz	288.0	33.3	60.8	7644	16571	50.8	39.2	0.0	50.2	65.9	57.9	60.6	73.1	*
Sequential/Loss	TL@12800 Hz	175.0	33.3	60.7	7645	16572	106.3	29.2	10.0	46.4	76.9	67.7	74.3	80.2	*
Simultaneous/Loss	TL@12800 Hz	193.0	36.7	66.8	7671	15118	193.3	26.5	7.7	41.7	66.1	62.7	73.6	96.7	*
Simultaneous/Mass	TL@12800 Hz	187.0	36.7	62.8	7411	14606	85.1	27.3	9.7	46.3	72.5	67.8	71.5	76.9	*
For Comparison:															
(Aluminum Panel)	-	-	-	-	-	-	-	-	-	25.4	35.9	36.6	20.9	43.1	*
Mass Law	-	-	-	-	-	-	-	-	-	25.6	37.6	39.6	43.6	47.9	*

Note: CPU time for IBM 3084. Mass-objective computation times are per iteration.

\*Not available.

blanket masses as low as 12.6% are obtained. The septum mass ranges from less than 0.1% to 25.6%. In most cases, the sequential approach chooses treatments similar to one of the following two configurations, which for convenience are referred to as the *low frequency treatment* and the *mid frequency treatment*. The low frequency treatment consists of a massive blanket (approximately 39% of the total mass) with almost no septum; it usually occurs with target frequencies well below coincidence. The mid frequency treatment usually occurs with target frequencies in the sub- or trans-coincidence regions, and is characterized by a moderate septum mass of approximately 10% and a blanket mass of approximately 29%. Figure 23 on page 123 shows the specific incidence transmission loss of the structural panel treated with typical low and mid frequency treatments. In general, there is a trend as frequency increases to increase the mass of the septum and decrease the mass of the blanket. However, at high frequencies two optimal treatments were obtained. One followed the trend of a lighter blanket and heavier septum, whereas the other reversed it and chose a heavy blanket and light septum.

The simultaneous designs are more varied because the panel mass is not fixed. All changes from the structural panel require that mass be shifted from the treatment to the panel for structural reasons. While such changes are not prohibited, they only occur when the structural/acoustical interaction is strong enough to shift mass away from the treatment. For the designs obtained, panel masses range from the structural panel's minimum of 60.7% to over 75%. The layup angle varies from 1.2° to 62.6°. The blanket mass ranges from 12.4% to the maximum of 39.3%, and the septum mass is as large as 25.6%.

Acoustic treatments are very effective at high frequencies, although they are slightly less effective at lower frequencies. In the frequency range considered the treatments are usually more mass-efficient for increasing  $TL$  than additional panel mass. Unless large changes in acoustic performance are obtained from altering panel rigidities, the highest  $TL$  is obtained by using the lightest acceptable panel (the structural panel) and putting as much mass into the treatment as possible. In almost every case, the optimal design includes a shear-critical panel (to allow addition of treatment mass) rather than a mass-critical design (which would



not allow treatment mass.) In the mass law region, panel rigidities do not affect  $TL$  and the minimum-mass panel is always best. Thus, for a low target frequency ( $f_t$ ) both the sequential and simultaneous approaches choose the structural panel regardless of the type of incidence. For target frequencies above the mass law region or for frequency-averaged acoustic criteria, the results depend on incidence type as outlined below.

### 4.2.1 Specific Incidence

The following results were obtained for specific incidence ( $\varphi_i = 0^\circ$ ,  $\theta_i = 78^\circ$ ) acoustic criteria, as presented in Table 3 on page 41 and Figure 25 - Figure 30. As indicated in the Preliminary Study, transmission loss at sub-coincident frequencies (e.g. for target frequencies  $f_2$  or  $f_3$ ) can be increased by softening the panel in the direction of incidence, thereby increasing the coincidence frequency. To improve performance in the structural panel super-coincidence region (e.g. for  $f_4$  or  $TLL$ ), the strategy is to make the panel rigid in the incidence direction, lowering  $f_c$ . The closer the target frequency is to the coincidence region, the stronger the structural/acoustical interaction. However, shifting  $f_c$  means that performance must be sacrificed in other directions and frequencies. In some physical situations it may not be acceptable to lower the coincidence region, since more noise may be encountered at lower frequencies.

The computation time required for discrete frequency specific incidence optimizations is relatively small. Most sequential designs require less than one second on an IBM 3084, although that does not include the cost of designing the structural panel. The simultaneous approach increases computation time by about 15% for the loss-objective formulation and 100% - 200% for the mass-objective formulation. Note that the computation times listed for mass-objective designs in Table 3 - Table 5 are actually per iteration; three to five iterations are usually needed in order to converge the mass. (If the design goal were different, e.g. design a minimum-mass treated panel subject to an acoustic constraint, then the loss-

objective formulation would require iteration instead.) Frequency averaging increases computation time by at least an order of magnitude, since the transmission loss is computed at many discrete frequencies throughout all regions. Transmission loss level optimization requires 36 sec. for the sequential approach and over 50 - 100 sec. for the simultaneous approaches. Transmission difference optimizations require 15 - 20 sec.

Descriptions of results for the various acoustical criteria follow:

**TL @ 1600 Hz, Figure 25:** Both the sequential and simultaneous designs utilize the structural panel/mass law treatment and provide a  $TL$  increase of over 26 dB compared to the aluminum panel. Although the coincidence frequency of the structural panel (8887 Hz) is below that of the aluminum panel, the treatment is effective enough to provide superior performance even in the coincidence region.

**TL @ 6400 Hz, Figure 26:** The sequential approach chooses a mid frequency treatment, i.e. some blanket mass is sacrificed to the septum and yields a 40 dB increase over the aluminum panel transmission loss at 6400 Hz. Since the target frequency is in the structural panel sub-coincidence region, the simultaneous design can justify shifting some mass from the treatment to the panel in order to increase the layup angle by  $7.6^\circ$  and raise  $f_c$  to 10314 Hz. At the target frequency the simultaneous design has the higher transmission loss improvement over the sequential design because the mass law region has been extended. However, the rigidity recovery is also delayed so that the simultaneous design has lower  $TL$  at high frequencies. Thus, an extended mass law region and a slight increase over the sequential design of 1.4 dB at the target frequency is obtained at the price of slightly reduced high frequency performance and additional computation time.

**TL @ 8063 Hz, Figure 27:** The influence of panel rigidities is strong since the target frequency is close to the structural panel coincidence frequency. The sequential design chooses the mid frequency treatment and obtains a 35 dB improvement over the aluminum panel at  $f_j$ . The

simultaneous designs sacrifice treatment mass in order to extend the mass law region by delaying coincidence.

For this target frequency, multiple local optima exist for the simultaneous designs, which are defined as simultaneous/loss or simultaneous/mass depending on whether the loss-objective or mass-objective formulation was used. The simultaneous/loss design increases the panel mass by 14.1% in changing the layup angle to  $\alpha = 62.6^\circ$  and raising  $f_c$  to 15274 Hz (from the structural panel's 8887 Hz.) This yields a 0.2 dB decrease in target frequency  $TL$  compared to the sequential design. The simultaneous/loss design obtains better results from a similar but less drastic strategy: a smaller decrease in treatment mass increases  $f_c$  to only 11172 Hz, but at the target frequency  $TL$  surpasses the sequential design by 6.6 dB.

The  $TL$  for the simultaneous/loss design at low frequencies is 4-8 dB lower than for the other designs because of its relatively thin blanket; there is no improvement over the sequential design at the target frequency, even though performance is severely compromised throughout almost the entire frequency range in order to raise  $f_c$ . On the other hand, the simultaneous/mass design gives a 6.6 dB improvement at the target frequency with only slight decrease in  $TL$  in the region above coincidence and almost no decrease in the mass law region. The simultaneous/mass design is the better local optimum, effectively extending the mass law region to higher frequencies.

**TL @ 12800 Hz,** Figure 28: Multiple optima are found with the sequential approach (two treatments occur) as well as with the simultaneous approach. Following the observed frequency trend for treatments of increasing septum mass and decreasing blanket mass at higher frequencies, the sequential/loss design chooses a 25.6% septum and a 13.4% blanket for a 68.9 dB improvement over the aluminum panel (which is near coincidence) and good performance throughout the high frequency range. The sequential/mass design chooses an 8% septum with a 31% blanket and performs well at almost all frequencies; the improvement over the aluminum panel is 72.0 dB.

Since the target frequency is in the super-coincidence region of the structural panel, the simultaneous designs shift mass to the panel to lower  $f_c$  by decreasing the layup angle. The simultaneous/loss design lowers  $\alpha$  to  $8.4^\circ$  in reducing  $f_c$  to 5639 Hz. The simultaneous/mass design only decreases  $f_c$  to 6605 Hz, but this performs better since it leaves more mass for the treatment. These alterations increase  $TL$  by, respectively, 8.6 and 8.8 dB over the sequential/loss design at the target frequency. However, the price is that coincidence is moved to lower frequencies; the performance of the simultaneous/loss design is poor between  $f_1$  and  $f_2$ , although the simultaneous/mass design is slightly better. Note that in the super-coincidence region the simultaneous/mass design quickly rises to the same transmission loss as the simultaneous/loss design, even though it enters that region at a higher frequency. Also, at low frequencies, the thick blanket of sequential/mass design gives it higher  $TL$  than the simultaneous designs.

**TLL, Figure 29:** Although this acoustic criterion averages  $TL$  over all the frequency regions, it is most sensitive to the high transmission loss in the super-coincidence region. The sequential design gains 48.6 dB over the transmission loss level of the aluminum panel by choosing the mid frequency treatment. The two simultaneous designs are similar to the designs obtained for the 12800 Hz target frequency, with decreased layup angles. The simultaneous/loss design lowers  $\alpha$  to  $1.2^\circ$  and  $f_c$  to 5278 Hz, requiring an decrease in treatment mass of 14% and improving the sequential design  $TLL$  by 5.3 dB. The simultaneous/mass design calls for a similar but less drastic reduction in  $f_c$  to 6278 Hz which allow more treatment mass and yields a 6.3 dB improvement over the sequential design. Thus, slight increases in  $TLL$  are obtained at the cost of reduced  $TL$  at low frequencies (2 - 25 dB lower than the sequential design) and an increase in computation time from less than one second to almost 50 seconds. Also, the coincidence region is moved to lower frequencies. The designs obtained using the 12800 Hz target frequency are comparable in terms of performance, yet are much less expensive.

**TDL**, Figure 30: Rather than improving regions of high  $TL$ , this criterion concentrates on regions of low  $TL$  in the coincidence region. This gives incentive to increase  $f_c$  so that the region which dominates  $TDL$  is moved toward higher frequencies where the treatment is more effective.

The sequential approach cannot shift  $f_c$  but acts to narrow the region of degradation in the immediate vicinity of  $f_c$ . The mid frequency treatment chosen improves  $TDL$  by 36.4 dB over the aluminum panel. (Since  $TD \equiv 100 \text{ dB} - TL$ , the goal is to *lower*  $TDL$ .) The simultaneous design increases  $f_c$  slightly to take advantage of increased treatment efficiency at higher frequencies; also, near coincidence the panel damping is increasingly effective at higher frequencies. The result is that  $TL$  is increased by 5-7 dB in the coincidence region for a 5.1 dB improvement in  $TDL$ .

Frequency averaging increases computation time by an order of magnitude as compared to discrete-frequency optimizations. Similar transmission difference levels were obtained by sequential optimizations with target frequencies near the structural panel coincidence frequency ( $f_2$  and  $f_3$ ) at a much lower cost. However, to obtain such results without frequency-averaging requires previous knowledge of the structural panel coincidence frequencies. The utility of the  $TDL$  acoustic criterion may lie in that it is a mechanical, albeit expensive, procedure which requires no a priori information.

## 4.2.2 Grazing Incidence

See Table 4 on page 42 and Figure 31 - Figure 35 for grazing incidence optimization results. When azimuthal averaging is considered, all azimuthal directions are accounted for; the acoustic performance index cannot ignore some incidence directions as with specific incidence. The upper and lower bounds of the trans-coincidence region  $f_{c_{rn}}$  and  $f_{c_{max}}$  are the primary influences rather than  $f_c$  for a particular incidence direction. For low frequencies, the

goal is to maximize  $f_{crit}$ . For high frequencies, lowering  $f_{c,max}$  gives an low super-coincidence region.

The Preliminary Study pointed out three panel designs as possible candidates. The first is the structural panel which has the highest critical frequency (7640 Hz). For target frequencies below 7640 Hz ( $f_1$  and  $f_2$ ), choosing the structural panel not only maximizes the treatment mass, but also extends the mass law region by increasing  $f_{crit}$ . There is no incentive to shift treatment mass and change the panel since coincidence cannot be raised any higher. The second is the mass-critical 45° panel which has the lowest maximum grazing coincidence frequency ( $f_{c,max} = 7461$  Hz). This design does not occur in the optimization results. The treatments are so effective that better high frequency (e.g.  $f_4$ ) performance is obtained with the third design: the shear-critical 45° panel, which has a slightly higher critical frequency (11847 Hz) but allows for treatment mass.

There is no panel for which frequencies above 7640 Hz are in the sub-coincident region. Similarly, there is no panel for which frequencies below 11847 Hz are super-coincident. Target frequencies between these two limits (e.g.  $f_3$ ) are in the trans-coincidence region of all admissible composite panels; there is no strong incentive for changing the panel design. Secondary effects alter the layup angle by a few degrees.

Spatial averaging increases computation time by one to two orders of magnitude. Sequential designs require 10 - 130 sec., while simultaneous designs require 40 - 200 sec. for discrete frequencies. Frequency averaging further increases computation time to 57 sec. for the sequential *TLL* design and to almost 3000 sec. for the simultaneous *TLL* design.

**TL @ 1600 Hz, Figure 31:** The target frequency is in the mass law region so that acoustic response is insensitive to panel rigidities. As with specific incidence, the sequential and simultaneous designs are nearly identical since there is insufficient incentive to alter the panel. The structural panel/mass law treatment chosen surpasses the aluminum panel transmission loss by 26.5 dB at the target frequency.

**TL @ 6400 Hz, Figure 32:** The target frequency is in the structural panel sub-coincidence region. The optimal sequential design is the mid frequency treatment, which provides an improvement over the aluminum panel of 40.1 dB @ 6400 Hz. The simultaneous designs raise  $f_c$  only slightly from that of the structural panel, while the treatments are quite different from the sequential treatment. Almost all the septum mass is shifted into the blanket, resulting in designs for which  $TL$  is 2 - 3 dB higher at sub-coincidence frequencies, but 4 - 11 dB lower at super-coincidence frequencies, than the sequential design. The transmission loss at the target frequency is actually 4-5 dB lower for the simultaneous designs, suggesting that either the designs are not well converged or other local optima exist and were not found.

**TL @ 8063 Hz, Figure 33:** Since the target frequency is trans-coincident for all admissible panels, there is no strong incentive towards a particular design other than to maximize the treatment mass. The mass distributions of the sequential, simultaneous/loss, and simultaneous/mass designs are each within a few percent of the structural panel/mid frequency treatment configuration. The only significant difference is that the sequential design chooses an airgap thickness of over 100mm, while the simultaneous designs choose airgap thicknesses on the order of 1mm. This gives the simultaneous designs better performance in the mass law and sub-coincident regions. (The transmission losses at the target frequency are nearly identical, surpassing the aluminum panel by over 31 dB.)

The transmission losses of the simultaneous designs are within a few dB of each other throughout the entire frequency range, and are equal to or higher than that of the sequential design at almost all frequencies. The transmission loss rises slightly just above the structural panel coincidence frequency of 7645 Hz, creating a cusp. To avoid this cusp, one simultaneous design lowers  $f_{crit}$  to 7618 Hz, while the other raises  $f_{crit}$  to 7664 Hz.

**TL @ 12800 Hz, Figure 34:** The mid frequency treatment of the sequential design gives it a 55.5 dB increase @ 12800 Hz over the nearly coincident aluminum panel. The target frequency is just above  $f_{c_{max}}$  of the structural panel, so that there is a strong incentive for the simultaneous

designs to choose panels with lower trans-coincidence regions. This is an extreme case in which the structural/acoustic interaction is so strong that additional panel mass (above that needed to satisfy the shear requirement) is more efficient than additional treatment mass. Choosing the shear-critical 45° panel would give a panel mass of 63% and  $f_{c_{max}} = 11847$  Hz (just below the target frequency.) Instead, the simultaneous/loss design chooses a 45° panel with a 74.5% mass and  $f_{c_{max}} = 10012$  Hz for an improvement over the sequential design of 7.9 dB @ 12800 Hz. (The mid frequency treatment chosen gives relatively poor performance at low frequencies.) The simultaneous/mass design chooses a 74.5% mass ( $f_{c_{max}} = 10012$  Hz) but chooses a low frequency treatment type;  $TL$  at the target frequency is 4.8 dB lower than for the sequential design.

**TLL**, Figure 35: As with the 12800 Hz target frequency, the simultaneous design chooses a non-shear-critical 45° panel for its low  $f_{c_{max}}$  and early rigidity recovery. This yields large transmission losses just below the cutoff frequency of 12800 Hz, and  $TLL$  is high, although low frequency performance is greatly reduced since mass was transferred out of the blanket. The treatment designs are somewhat anomalous. The sequential design chooses the low frequency treatment (the mid frequency treatment selected for the 6400 Hz target frequency gives a higher  $TLL$  by 6 dB.) The simultaneous design chooses a septum mass of 11.9%, when a higher  $TLL$  was obtained for the 12800 Hz target frequency by using a slightly heavier septum. There may be other local optima which produce better designs.

As with the specific incidence case, frequency averaging substantially increases computation time. Here the increase is from approximately 100 sec. to almost 3000 sec., and the results are worse than those obtained without frequency averaging. Since  $TLL$  is dominated by transmission losses at high frequencies, better results were obtained using the 12800 Hz target frequency at a fraction of the cost.



### 4.2.3 Field Incidence

Field incidence optimization results are presented in Table 5 on page 43 and Figure 36 - Figure 35. For field incidence, as with grazing incidence, the upper and lower bounds of the coincidence region are important. However, not only does azimuthal averaging decrease the influence of panel rigidities, but as shown in the Preliminary Study the post-coincidence recovery is less pronounced so that the incentive to make the target frequency super-coincident is weaker. (All frequencies above  $f_{crn}$  are coincident at some angle of inclination.) Therefore the field incidence criterion has the weakest effect on optimization of the three incidence types. Even for the 12800 Hz target frequency, where the grazing incidence criterion drives the layup angle to 45°, the field incidence criterion is only strong enough to increase the layup angle by a few degrees. This indicates that the simultaneous approach may be ineffective in designing for field incidence transmission.

Even with the Simpson's Rule approximate integration used for field incidence, optimizations required 175 - 500 sec. of computation time (fifteen times more at  $f_1$  and 1.5 to six times longer at  $f_4$  than the grazing incidence optimizations.) Frequency-averaged field incidence optimizations were not performed as they would probably require 5000-10000 sec. The sequential designs still have much higher  $TL$  than the bare aluminum panel, but the simultaneous designs do not show significant improvements over the sequential designs. (For the 12800 Hz target frequency, the simultaneous designs are actually 1 - 3 dB poorer than the sequential design.)

**1600 Hz, Figure 36:**For this mass law region target frequency, both design approaches choose the structural panel/low frequency treatment configuration, indicating that for field incidence the treatment is more mass-efficient than additional panel mass. The improvement over the aluminum panel is 24.7 dB @ 1600 Hz.

12800 Hz, Figure 37: All three designs are close to the structural panel/mid frequency treatment configuration. The sequential design's mid frequency treatment exceeds the aluminum panel transmission loss by 53.4 dB at the target frequency. Since the target frequency is super-coincident, there is incentive to choose a 45° layup for its early super-coincidence region. The two simultaneous designs shift a small amount of mass from the septum and blanket to panel to increase the layup angle by about 3°, lowering  $f_{c_{max}}$  by 1400 - 2000 Hz (a weak attempt to increase  $\alpha$  to 45°.) The simultaneous/loss design loses some low frequency performance due to its thinner blanket.

The transmission loss at the target frequency is highest for the sequential panel; there may be other local optima which produce higher  $TL$ .

To summarize, the sequential designs give large increases in  $TL$  over the untreated aluminum panel. The simultaneous approach usually yields moderate additional gains at specific performance indices, although transmission loss is usually sacrificed in other regions. The treatments are very efficient so that only very pronounced structural/acoustical interactions are able to steal treatment mass to alter the panel away from the sequential approach's structural panel. For specific incidence, coincidence may be shifted to higher or lower frequencies by altering panel rigidities (provided that the target frequency is sufficiently close to the structural panel coincidence frequency to allow large increases in  $TL$ .) For grazing and field incidence, the onset of coincidence may be delayed to increase low frequency  $TL$  by choosing the structural panel, or the 45° panel may be chosen for its early post-coincidence recovery. With field incidence the recovery is weaker than with grazing incidence, so the incentive to choose the 45° panel is not as strong.

### 4.3 Conclusions

An automated procedure for simultaneous structural/acoustical design of treated composite panels has been developed using existing experimentally verified analytical models for acoustic transmission. A simplified design study was conducted to investigate the effects of structural/acoustical interactions, particularly coincidence, on optimal panel design and to compare the sequential and simultaneous design approaches. The study replaces a  $0.241\text{m} \times 0.406\text{m} \times 1.01\text{mm}$  aluminum panel with a structurally equivalent equal-mass treated composite panel (designed either sequentially or simultaneously) and compares acoustic performance. Two panel types are considered: a typical untreated aluminum panel and an 8-ply, mid-plane symmetric angle-ply graphite/epoxy panel treated with an airgap, fibrous acoustic blanket, and limp-mass septum. The structural analysis is based on a fatigue damage resistance constraint as presented in Ref. [14]. The acoustical analysis is based on infinite panel transmission loss (Ref. [6]) through a multilayered sidewall using the "impedance transfer" theory of Ref's [12] and [13].

The sequential approach first designs a minimum-mass panel subject only to structural criteria, then designs a treatment subject to only acoustical criteria. This fails to take advantage of the coupling between structural and acoustical properties. In the simultaneous approach, both the panel and treatment are designed at once subject to mass, structural, and acoustical criteria, thereby fully utilizing the structural/acoustical interactions.

The treated composite panels yield substantially higher transmission losses than the equal-mass aluminum panel. Typical improvements of 15 - 45 dB are found throughout the frequency range, even in the coincidence regions of the composite panels. (The transmitted acoustic pressure is reduced by a factor of 6 - 180.) This implies that using composite materials can achieve weight savings without sacrificing acoustic performance. In general, the composite panels exhibit coincidence at lower frequencies than the aluminum panel, although for a specific azimuthal direction  $f_c$  can be either lower or higher. Although this analysis does

not specifically address the frequency characteristics of typical external noise sources, more noise may be encountered at mid frequencies than at high frequencies. Since treatments are less effective at mid frequencies than at high frequencies, lowering the coincidence region can combine a region of poor panel/treatment performance with a region of higher noise generation and possibly require a heavier treatment.

In comparison to the 15 - 45 dB improvements over the aluminum panel obtained with the sequential approach, the simultaneous designs yielded moderate further improvements up to 10 dB (transmitted pressure is reduced by a factor of 3) for particular performance indices; however, in many cases this was accompanied by poor performance in other regions. In the infinite panel frequency range acoustic treatments are more mass-efficient than additional panel mass at improving transmission loss, which limits the advantages of the simultaneous approach to regions of strong structural/acoustical interaction (i.e. coincidence.) Due to the efficiency of the treatment, there is a strong incentive to minimize panel mass in order to maximize treatment mass. Since the first step of the sequential design process is to design a minimum-mass panel, the sequential and simultaneous approaches often yield similar designs. Only for very pronounced structural/acoustical interactions does the simultaneous approach produce significant modifications to the sequential approach, balancing between the effects of the treatment and structural/acoustical interactions.

The largest differences occur when considering specific incidence  $TL$  at a given frequency, significant for tonal noise incident from a specific source location. The simultaneous approach alters panel rigidities in order to shift the coincidence region away from the tonal frequency, even though extra mass (which could be used in the treatment) must be added to the panel for structural purposes. Shifting coincidence up or down in this manner improves target frequency  $TL$  by as much as 9 dB for the panels studied. However, such improvements are usually obtained at the cost of poor performance in other directions and/or frequencies: for a highly anisotropic panel, a high coincidence frequency in one direction is accompanied by a low coincidence frequency in a different direction. (This directional tradeoff is accounted for by azimuthal averaging as with grazing incidence or field incidence.)

In some situations, the payoff of raising the coincidence frequency in one direction may override the desire to avoid low coincidence frequencies in other directions. Consider an advanced turboprop engine with a large number of blades creating high-frequency tonals. A sequentially designed panel could have a low coincidence frequency in the direction of the engine, coupling a direction of low transmission loss with a direction of high intensity noise. This could cause high cabin noise levels or require heavy acoustic treatments. A simultaneous approach would attempt to reduce transmission of the engine tonal by increasing the coincidence frequency in that direction. Optimizing the specific incidence transmission loss for the direction and frequency of the tonal might be a cost-effective way to study such a problem. A tradeoff would occur : balancing mass between the treatment and panel (done automatically during optimization) would address coincidence transmission of the tonal, although reducing coincidence frequencies in other directions might allow more noise to be transmitted from other sources (as deemed appropriate by the designer.)

When diffuse noise sources are considered, the structural/acoustical interaction is weakened by spatial averaging. All azimuthal directions must be accounted for; the designer does not have the luxury of being able to ignore poor performance in some directions. Improvements at low frequencies can be accomplished by raising the critical frequency since coincidence does not occur in any direction until above  $f_{crit}$ . The structural panel used for sequential designs has the highest critical frequency of any layup, so that the sequential and simultaneous approaches give similar results for low target frequencies. (Coincidence cannot be raised any further by altering the structural panel.)

For grazing incidence (azimuthally averaged transmission at  $\theta_c = 78^\circ$ ) the trans-coincidence region (where the most severe degradation occurs) extends from the critical frequency through  $f_{c_{max}}$ , the maximum grazing coincidence frequency. The width of this region,  $\Delta f_{coinc}$ , ranges from zero for the isotropic aluminum panel to over 14500 Hz for the shear-critical  $0^\circ$  panel. In the super-coincidence region, a moderate rigidity recovery occurs; high frequencies benefit most from lowering  $f_{c_{max}}$  to provide early super-coincidence. The  $90^\circ$  layup has the lowest critical frequency (3940 Hz) of the panels studied, but has a grazing coincidence

bandwidth of nearly 11000 Hz so that coincidence occurs as high as 14845 Hz. The narrow (2784 Hz) trans-coincidence region of the mass-critical 45° panel gives it the lowest  $f_{c_{max}}$  (7461 Hz) even though its critical frequency is slightly higher than the 90° panel. However, since mass-critical designs allow no treatment mass, the simultaneous approach chooses the shear-critical 45° panel as a compromise between the conflicting desires for early super-coincidence and maximum treatment mass. This design does not become super-coincident until 11847 Hz, but a moderate treatment mass of approximately 25% gives it good transmission loss at most frequencies.

With field incidence (excitation from all directions to  $\theta_i = 78^\circ$ ) all frequencies above  $f_{crit}$  are degraded to some extent by coincidence, although the trans-coincidence region ends at  $f_{c_{max}}$ . In super-coincidence the rigidity recovery occurs but is weaker than with grazing incidence; the incentive to shift treatment mass to the panel for a 45° design is weaker. In comparison with the sequential designs, the simultaneous designs are slightly different but not significantly better. Also, the computation time required for spatial integration becomes relatively large during optimization; compared to the specific incidence criterion, computation time increases by two to three orders of magnitude even with the approximate integration used for field incidence. Therefore, the simultaneous approach may be of limited utility with the field incidence acoustic criterion.

One issue revealed by the optimization results is the existence of multiple local optima. In several cases the mass-objective and loss-objective formulations give different designs, sometimes with large differences in acoustic performance. As an example, for grazing incidence at 12800 Hz both formulations choose 45° panels. The mass-objective formulation chooses a thick blanket and eliminates the septum for a target-frequency  $TL$  of 61.5 dB. The loss-objective formulation improves that performance index 12.7 dB by balancing mass between the blanket and septum. In most cases of multiple optima the mass-objective designs are better than the loss-objective designs not only at the target frequency but in other regions as well, i.e. the mass-objective formulation give superior results.

Another point to be made is that frequency-averaging schemes for representing performance over a wide frequency range require further investigation. The transmission loss level *TLL*, which is dominated by the transmission loss at high frequencies, increases computation time to thirty to fifty times the cost of a discrete frequency optimization. Better results are obtained at a lower cost by using the 12800 Hz target frequency. In effect, optimizing *TLL* wastes effort on regions which already have good acoustic performance. In contrast, the transmission difference level *TDL*, which costs about fifteen times as much as a discrete-frequency optimization, was intended to address the coincidence region. Designs which perform nearly as well near coincidence can be found by a sequential design using a target frequency near the structural panel coincidence frequency. However, the *TDL* approach is more mechanical in that it requires no a priori knowledge of the structural panel and is more appropriate when the structural/acoustical interaction is stronger so that sequential and simultaneous designs are more unique. Other similar frequency averaging schemes should be investigated and compared to discrete-frequency results.

In terms of theoretical and computational error, this analysis could be improved in two ways. First, other studies will require an improved structural analysis. The structural criterion (or criteria) must accurately reflect design considerations but not use inappropriately large amounts of computation time. The error introduced by the approximate solution used here may have influenced the optimization results by suppressing large changes in the layup angle away from the structural panel layup angle of 33°. However, due to the repetitive nature of numerical optimization, the eigenvalue solution required too much computation time to be suitable for this preliminary study. Second, an investigation should be made of the effects of integration errors on spatially averaged transmission losses and on optimizations which use these criteria. In particular, the effect of the Simpson's Rule approximate integration on field incidence transmission loss should be studied.

As an extension of this work, an optimization code is currently being written which uses a finite panel analysis to investigate structural/acoustical interactions at very low frequencies where panel boundary conditions must be accounted for. Panel rigidities are very influential

in this region in terms of low frequency panel vibrations and resonances. Also, treatments are less effective at low frequencies. Therefore, it is expected that structural/acoustical interactions may be more important and may further enhance the feasibility of the simultaneous approach.



## References

1. Rennison, D.C., Wilby, J.F., Marsh, A.H., and Wilby, E.G., "Interior Noise Control Prediction Study for High-Speed Propeller Driven Aircraft," Bolt, Beranek and Newman Inc., NASA Contractor Report 159200 (September 1979)
2. Roussos, L.A. , McGary, M.C., and Powell, C.A., "Studies of Noise Transmission in Advanced Composite Material Structures," 1984 ACEE Composite Structures Conference, Seattle, Washington, August 13, 1984
3. Mixson, J.S. et al., "Interior Noise Considerations for Advanced High-Speed Turboprop Aircraft," J. Aircraft, Vol. 20, No. 9 (September 1983)
4. Hopkins, J.P., and Wharton, M.E., "Study of the Cost/Benefit Trade-offs for Reducing the Energy Consumption of the Commercial Air Transport System," NASA Contractor Report 137927 (August, 1976)
5. Hayden, R.E., Murray, B.S., and Theobald, M.A., "A Study of Interior Noise Levels, Noise Sources, and Transmission Paths in Light Aircraft," NASA Contractor Report 172152 (July 1983)
6. Roussos, L.A. and Powell, C.A., "Noise Transmission Characteristics of Advanced Composite Structural Materials," AIAA-83-0694
7. Grosveld, F.W., and Metcalf, V.L., "Modal Response and Noise Transmission of Composite Panels," AIAA-85-0789
8. Jones, R.M., *Mechanics of Composite Materials*, Scripta Book Company, Washington D.C., 1975
9. Koval, L.R., "Field Incidence Transmission of Treated Orthotropic and Laminated Panels," NASA Technical Memorandum 85680 (August 1983)
10. Beranek, L.L., and Work, G.A., "Sound Transmission Through Multiple Structures Containing Flexible Blankets," J. Acoustical Society of America, Vol. 21, No. 4, July 1949

11. Rennison, D.C., and Wilby, J.F., "A Review of Analytical Models for Sound Transmission Through Fuselage Sidewalls With Application to General Aviation Aircraft," Bolt Beranek and Newman Inc., Rep. No. 3851 (September 1981)
12. Beranek, L.L., *Noise and Vibration Control*, McGraw-Hill Book Co., New York (1971)
13. Beranek, L.L., "Acoustical Properties of Homogeneous, Isotropic Rigid Tiles and Flexible Blankets," J. Acoustical Society of America, Vol. 19, No. 4, July 1947
14. Ashton, J.E., and Whitney, J.M., *Theory of Laminated Plates*, Technomic Publishing Co., Stanford, Connecticut (1970)
15. Miura, H., and Schmit, L.A. Jr., "NEWSUMT - A Fortran Program for Inequality Constrained Function Minimization - User's Guide," University of California, Los Angeles
16. Thareja, R., and Haftka, R.T., "NEWSUMTA - A Modified Version of NEWSUMT for Inequality and Equality Constraints," Aerospace & Ocean Engineering Department, Virginia Polytechnic Institute and State University, Blacksburg, Virginia (March 1985)

## Appendix A. Optimization Program TLTROP

Program TLTROP uses NEWSUMTA, a general-purpose function minimization subroutine, to perform simultaneous structural/acoustical design of treated composite panels. Subroutines TAUSUB, TLSUB, and TLLSUB compute transmission losses and loss levels. Subroutine TAUSUB computes the transmission coefficient TAUPAN for a panel insulated with an arbitrary combination of up to nine acoustic treatments. Arrays are used to store the surface mass and thickness of each layer, as well as an integer denoting the type of treatment (septum, airgap, or acoustic blanket.) The transmission coefficient is calculated from the pressure ratios  $RP(i)$  and the entry impedance ZENTRY.

The algorithm for finding  $RP(i)$  and ZENTRY takes the form of a loop on the number of treatments NT. For each layer, beginning with the innermost layer and working outwards towards the panel, the procedure is to

1. Assign a characteristic impedance.
2. Compute the entry impedance ZNEXT(i) of the next medium into which the acoustic wave will pass after it leaves the current layer. For the innermost layer, the next medium is the air inside the cabin and its entry impedance is the characteristic impedance of air,  $Z_0$ . For successive layers, ZNEXT(i) is the entry impedance of the previous layer.

3. Compute the pressure ratio across the current layer,  $RP(i)$ , which depends on  $ZNEXT(i)$ .

```

C [[
C [[
C [[      MAIN PROGRAM :      TL TROP
C [[
C [[ TL TROP uses NEWSUMTA, a general-purpose function minimization
C [[ subroutine, to maximize the acoustic performance of an insulated
C [[ isotropic or anisotropic panel subject to shear buckling strength
C [[ and mass constraints. The panel is described by a thickness and
C [[ a layup angle; the layup sequence may be changed by altering sub-
C [[ routine REPLY. Three types of add-on acoustic treatments are
C [[ available: limp-mass septa (IMATL=2), air gaps (IMATL=3), and
C [[ porous acoustic blankets (IMATL=4). The configuration is then
C [[ described by the treatment thicknesses, panel thickness, and
C [[ panel layup angle.
C [[ For simultaneous designs (IDESGN=1), all design variables are
C [[ allowed to change. For sequential designs (IDESGN=2), the panel
C [[ thickness and layup angle remain constant.
C [[ The acoustic constraint may be computed for either specific
C [[ incidence (INTEG=0), grazing incidence (INTEG=1,4), or field
C [[ incidence (INTEG=2,3); TL may be computed at the nth center freq-
C [[ uency (ITLL=n), or may be averaged over all frequencies (ITLL=0).
C [[ TL should be computed using infinite panel theory (IFIN=0).
C [[ Subroutines for finite panel theory (IFIN=1) are included, but
C [[ the theory does not account for directivity at low frequencies
C [[ and may therefore be in error.
C [[ As a structural constraint, the shear buckling stress of a
C [[ panel of specified size is compared to a specified minimum value.
C [[ Shear strength is calculated using either infinite-strip-sum
C [[ theory (NORDER=0) or an eigen-value solution (NORDER=4,6,8). DO
C [[ NOT use NORDER=4,6 or 8 during optimization ... it requires too
C [[ much CPU time.
C [[ The loss objective optimization strategy (JOB=1) maximizes
C [[ TL such that the specified maximum surface mass is not exceeded
C [[ and the panel strength is greater than the specified minimum.
C [[ The mass objective optimization strategy (JOPT=2) minimizes the
C [[ surface mass such that both TL and the panel strength exceed
C [[ their respective specified minimum values.
C [[ The mass constraint may be specified as either an inequality
C [[ (JOPT=1) or an equality (JOPT=2) constraint. In some cases where
C [[ the shear constraint is passive, using an equality constraint may
C [[ decrease CPU time; however, it may result in convergence
C [[ problems.
C [[ A structural/acoustic analysis may be performed without
C [[ calling NEWSUMTA by setting JOPT=0. Subroutine TEST is bypassed
C [[ if ITEST=0, but may be used to call other subroutines and then
C [[ stop without calling NEWSUMTA by setting ITEST=1.
C [[ All data is read from a file <TL TROP DATA>. For details
C [[ concerning the NEWSUMTA parameters JPRINT, RACUT, GO, MFLAG, RA,
C [[ and ALPEQC, consult Appendix A.
C [[
C [[
C [[
C [[      VARIABLE NAMES AND DEFINITIONS
C [[
C [[
C [[ AI      Square root of negative one
C [[ AKA      Wave number (AKA=W/CA)
C [[ ALPEQC   equality constraint multiplier in NEWSUMTA total function
C [[ APANL    Panel dimension in x-direction (m)
C [[ B        Blanket propagation constant
C [[ BLBND    Array of design variable lower bounds
C [[ BOTFREQ  Value of lowest center frequency (Hz)
C [[ BPANL    Panel dimension in y-direction (m)

```

```

C [] BUBND      Array of design variable upper bounds      []
C [] CA        Acoustic velocity in air (m/sec)            []
C [] CPUTIM     Approximate total CPU time used by NEWSUMTA (sec) []
C [] D         Panel stiffness  $D_{ij}$  ( $N \times m$ )                []
C [] DF        Interval between adjacent sub-band frequencies (Hz) []
C [] DOBJ      Array containing first derivatives of objective function []
C [] DDOBJ     Array containing second derivatives of objective function []
C [] ETA       Damping factor                               []
C [] E1,E2     Ply strength in x-direction ( $N/m \times 2$ )      []
C [] E2        Ply strength in y-direction ( $N/m \times 2$ )      []
C [] F         Frequency (Hz)                               []
C [] FDCV      Finite difference step sizes used by NEWSUMTA []
C [] FREQ      Array of center frequencies (Hz)             []
C [] FREQSB    Array of sub-band frequencies (Hz)           []
C [] G         Array containing values of constraints        []
C [] G0        Inequality constraint transition parameter    []
C [] G12       Ply torsional strength ( $N/m \times 2$ )          []
C [] H         Array of treatment thicknesses (m)           []
C [] HP        Panel thickness (m)                           []
C [] IFIN      Flag equal to 0 ... infinite panel           []
C []           1 ... finite panel                           []
C [] IGRAPH    Flag equal to 0 ... create 'GRAPH' file with plotting []
C []           information                                   []
C []           1 ... do not create 'GRAPH' file              []
C [] ILIN      Array denoting constraints and objective function as []
C []           linear/nonlinear                             []
C [] INFO      Flag directing flow of execution in TLTRAN   []
C [] IOPT      Flag equal to 0 ... 80-character printer plot from PRPLOT []
C []           1 ... 129-character printer plot             []
C [] IORTHG    Flag equal to 0 ... angle-ply panel          []
C []           1 ... cross-ply panel                        []
C [] IPLTSB    Flag equal to 0 ... PRPLOT plots only at center []
C []           frequencies                                   []
C []           1 ... PRPLOT plots at all sub-band           []
C []           frequencies                                   []
C [] ISIDE     Array of side bound flags                     []
C [] ISYM      Flag equal to 0 ... panel layup is not symmetric []
C []           1 ... panel layup is symmetric               []
C [] ITEST     Flag equal to 0 ... do not execute subroutine TEST []
C []           1 ... execute subroutine TEST                 []
C [] IWRITE    Flag equal to 0 ... do not print integration timing info []
C []           1 ... print integration timing information    []
C [] JBCS      Flag equal to 1 ... clamped B.C.'s in subroutine MODALF []
C []           2 ... simply supported B.C.'s in MODALF      []
C [] JDESIGN   Flag equal to 1 ... simultaneous design      []
C []           2 ... sequential design                       []
C [] JOBJ      Flag equal to 1 ... loss objective function   []
C []           2 ... mass objective function                 []
C [] JOPT      Flag equal to 0 ... do not perform optimization []
C []           1 ... use inequality constraint on mass       []
C []           2 ... use equality constraint on mass         []
C [] JPRINT    Flag controlling NEWSUMTA output              []
C [] MATL      Array of treatment-type flags:                []
C []           MATL(i)=1 ... panel                           []
C []           MATL(i)=2 ... limp-mass septum                []
C []           MATL(i)=3 ... air space                        []
C []           MATL(i)=4 ... acoustic blanket                []
C [] MFLAG     Flag equal to 0 ... use default values of RA,ALPEQC []
C []           1 ... user provides RA,ALPEQC                 []
C [] N         Number of plies in panel                      []

```

C [ ]	NB	Number of bands (center frequencies)	[ ]
C [ ]	NCASE	ID number, incremented each time program is used	[ ]
C [ ]	NCFNO	Center frequency band number ( 0<NCFNO<=NB )	[ ]
C [ ]	NDV	Number of design variables	[ ]
C [ ]	NMODES	Number of finite panel vibrational modes	[ ]
C [ ]	NN	Equals N/2 if ISYM=1; otherwise, NN=N	[ ]
C [ ]	NORDER	Flag equal to 0 ... use infinite strip shear function	[ ]
C [ ]		i ... use eigen-value shear, order=4,6 or 8	[ ]
C [ ]	NSB	Number of sub-bands per center frequency ( NSB<=10 )	[ ]
C [ ]	NSBNO	Sub-band frequency band number ( 0<NSBNO<=NSB )	[ ]
C [ ]	NT	Number of treatments (including panel)	[ ]
C [ ]	NTCE	Total number of constraint equations	[ ]
C [ ]	OBJ	Objective function	[ ]
C [ ]	PHEE	Azimuthal incidence angle (in plane of panel) (deg)	[ ]
C [ ]	PHI	Azimuthal incidence angle (in plane of panel) (rad)	[ ]
C [ ]	PLY	Array containing panel information; for the ith ply,	[ ]
C [ ]		PLY(I,1) = E1	[ ]
C [ ]		PLY(i,2) = E2	[ ]
C [ ]		PLY(i,3) = E1	[ ]
C [ ]		PLY(i,4) = E1	[ ]
C [ ]		PLY(i,5) = layup angle	[ ]
C [ ]		PLY(i,6) = ply thickness	[ ]
C [ ]	RA	Penalty multiplier in NEWSUMTA inequality constraints	[ ]
C [ ]	RACUT	Penalty multiplier reduction ratio	[ ]
C [ ]	RHO	Array of treatment densities (kg/m**3)	[ ]
C [ ]	RHOA	Air density (kg/m**3)	[ ]
C [ ]	RHOB	Blanket density (kg/m**3)	[ ]
C [ ]	RP	Array containing treatment pressure ratios	[ ]
C [ ]	RPTR	Pressure ratio across treated panel	[ ]
C [ ]	RPUNTR	Pressure ratio across untreated panel	[ ]
C [ ]	R1B	Blanket flow resistivity	[ ]
C [ ]	SCALE	Array of scaling factors	[ ]
C [ ]	SM	Array of surface masses (kg/m**2)	[ ]
C [ ]	SMT	Total surface mass (kg/m**2)	[ ]
C [ ]	SMTMAX	Maximum allowable total surface mass (kg/m**2)	[ ]
C [ ]	SMT0	Total surface mass of initial design (kg/m**2)	[ ]
C [ ]	SPSTR	Mass-specific transmission loss level	[ ]
C [ ]	T	Total panel thickness (m)	[ ]
C [ ]	TAML	Array of A-weighted mass law transmission losses	[ ]
C [ ]	TAMLL	A-weighted mass law transmission loss level	[ ]
C [ ]	TAMLSB	Array of A-weighted mass law sub-band transmission losses	[ ]
C [ ]	TATR	Array of A-weighted treated panel transmission losses	[ ]
C [ ]	TATRL	A-weighted treated panel transmission loss level	[ ]
C [ ]	TATRSB	Array of A-weighted treated panel sub-band transmission	[ ]
C [ ]		losses	[ ]
C [ ]	TAUGR	panel shear strength (N/m**2)	[ ]
C [ ]	TAUMIN	Minimum allowable shear strength	[ ]
C [ ]	TAUPAN	Pressure-squared ratio for mass law	[ ]
C [ ]	TAUTR	Pressure-squared ratio for treated panel	[ ]
C [ ]	TAU0	Shear strength of initial design	[ ]
C [ ]	TCRF	Finite panel (eigen-value) shear strength	[ ]
C [ ]	TCRI	Infinite strip function shear strength	[ ]
C [ ]	THETA	Incidence angle measured from normal (rad)	[ ]
C [ ]	THL	Upper limit on integration in theta (THL=78 deg)	[ ]
C [ ]	THTA	Incidence angle measured from normal (deg)	[ ]
C [ ]	TLD	Array of transmission loss differences (TLD = TLTR-TLML)	[ ]
C [ ]	TLEVEL	Transmission loss level	[ ]
C [ ]	TLEVLO	Transmission loss level of initial design	[ ]
C [ ]	TLLMIN	Minimum allowable transmission loss level	[ ]
C [ ]	TLML	Array of mass law transmission losses	[ ]



I

```

      CALL UGETIO(3,NIN,10)
C
C  UPDATE CASE NUMBER (UNIT 8 = CASENO FILE)
      READ(8,*) NCASE
      NCASE=NCASE + 1
      REWIND 8
      WRITE(8,*)NCASE
C
C
C      : .....
C      :  DATA INPUT BEGINS HERE  :
C      : .....
C
C  READ PROBLEM PARAMETERS AND INPUT DATA
      READ(5,1005) TITLE
      READ(5,*) JOPT,ITEST,NT,IFIN,      JDESGN,JOBJ,NTLL
      IF(JOBY.EQ.1) READ(5,*) SMTMAX,TAUMIN
      IF(JOBY.EQ.2) READ(5,*) TLLMIN,TAUMIN
      READ(5,*) NMODES,NORDER,APANL,BPANL
      READ(5,*) NB,NSB,BOTFRQ,          ITYPE,THTA,PHEE
      READ(5,*) RHOA,CA,ETA,R1B,N,ISYM
      READ(5,*) E1,E2,V12,G12
C
C  INITIALIZE NEWSUMTA PARAMETERS
      READ(5,*) JPRINT,RACUT,G0,      MFLAG,RA,ALPEQC
      NDV=NT+2
      NDVM=NDV-1
      NTCE=3
      N1 = NDV
      N2 = 3
      N3 = N1*(N1+1)/2
      N4 = N1*N2
      LOBJ=1
      IFD=-2
      DO 10 KK=1,NDV
10  FDCV(KK)=0.010
      XSTAR=1.0
      SCALE(NDV)=0.1
      X0(NDV)=XSTAR*SCALE(NDV)
      ISIDE(NDV)=0
      IF(JOPT.EQ.2)ILIN(1)=-2
C
C  READ INITIAL DESIGN VECTOR X0; SCALE DESIGN VARIABLES AND SIDE BOUNDS
      DO 30 I=1,NDVM
      READ(5,*) X0U,IMAT,RO,SCALE(I),ISIDE(I),BLBNDU,BUBNDU
      IF(I.EQ.1)GOTO 20
      IMATL(I-1)=IMAT
      RHO(I-1)=RO
      H(I-1)=X0U
20  X0(I)=X0U*SCALE(I)
      BLBND(I)=BLBNDU*SCALE(I)
30  BUBND(I)=BUBNDU*SCALE(I)
C
C
C      : .....
C      :  DATA INPUT ENDS HERE  :
C      : .....
C
C  INITIALIZE ARRAY PLY
      ANGLE=X0(1)/SCALE(1)
      T=X0(2)/SCALE(2)

```

I



```

NN=N
IF(ISYM.EQ.1)NN=NN/2
JREPLY= 1
ASHIFT=00.
CALL REPLY(JREPLY,T,ANGLE,ASHIFT,N,NN,PLY)
DO 90 K=1,NN
PLY(K,1)=E1
PLY(K,2)=E2
PLY(K,3)=V12
90 PLY(K,4)=G12

C
C CALCULATE FREQUENCY BAND CENTERS, SUB-BAND FREQUENCIES, AND
C SUB-BAND BANDWIDTHS
ANSB=FLOAT(NSB)
BNDF=2.**(1./3.)
FO=BOTFRQ/BNDF
FNB1=FO*BNDF*(NB+1)
DO 110 KK=1,NB
110 FREQ(KK)=FO*BNDF**KK
DO 120 INB=1,NB
IF(INB.EQ.1) FMINUS=FO
IF(INB.NE.1) FMINUS=FREQ(INB-1)
IF(INB.EQ.NB) FPLUS=FNB1
IF(INB.NE.NB) FPLUS=FREQ(INB+1)
FLB=SQRT(FMINUS*FREQ(INB))
FUB=SQRT(FREQ(INB)*FPLUS)
DO 120 INSB=1,NSB
AINSB=FLOAT(INSB)
FREQSB(INB,INSB)=FLB**((2.*ANSB-2.*AINSB+1.)/2./ANSB)
$ *FUB**((2.*AINSB-1.)/2./ANSB)
FLSB=FLB**((ANSB-AINSB+1.)/ANSB)*FUB**((AINSB-1.)/ANSB)
FUSB=FLB**((ANSB-AINSB)/ANSB)*FUB**((AINSB)/ANSB)
DF(INB,INSB)=FUSB - FLSB
120 CONTINUE

C
C COMPUTE STRUCTURAL/ACOUSTIC PROPERTIES OF INITIAL DESIGN
SMT0=0.0
DO 130 KK=1,NT
SM(KK)=RHO(KK)*H(KK)
130 IF(IMATL(KK).NE.3)SMT0=SMT0 + SM(KK)
CALL DIJ(PLY,NN,T,D)
IF(IFIN.GT.0)CALL MODALF(JBCS)
IF(ITYPE.EQ.1)ITYPE=4
DO 140 KK=1,NB
IF(ITYPE.EQ.4.AND.KK.GT.17)ITYPE=1
140 CALL TLSUB(KK)
CALL TLLSUB(TLL,TLEVLO)
CALL SHEAR(D,H,NORDER,TAU0)
CALL SHEAR(D,H,0,TCRI)
CALL SHEAR(D,H,4,TCRF)

C
C .....
C : PRINT PROBLEM DATA :
C .....
C
C UNIT 7 IS GRAPH FILE, UNIT 13 IS SYMBOL FILE
400 IGRAPH=1
IF(IGRAPH.EQ.0)GOTO 500
DO 410 INB=1,NB

```

```

DO 410 JSB=1,NSB
NUM=NSB*(INB-1) + JSB
WRITE( 7,1075)          NUM,FREQSB(INB,JSB),TLMLSB(INB,JSB)
                        TLTRSB(INB,JSB),TLINSB(INB,JSB)
$ IF(INT(FREQSB(INB,JSB)).EQ.1599)
$ WRITE(13,1075)        NUM,FREQSB(INB,JSB),TLMLSB(INB,JSB)
$                        TLTRSB(INB,JSB),TLINSB(INB,JSB)
$ IF(INT(FREQSB(INB,JSB)).EQ.8063)
$ WRITE(13,1075)        NUM,FREQSB(INB,JSB),TLMLSB(INB,JSB)
$                        TLTRSB(INB,JSB),TLINSB(INB,JSB)
$ IF(INT(FREQSB(INB,JSB)).EQ.12799)
$ WRITE(13,1075)        NUM,FREQSB(INB,JSB),TLMLSB(INB,JSB)
$                        TLTRSB(INB,JSB),TLINSB(INB,JSB)
C IF(INT(FREQSB(INB,JSB)).EQ.1600)
C $ WRITE(13,1075)        NUM,FREQSB(INB,JSB),TLMLSB(INB,JSB)
C $                        TLTRSB(INB,JSB),TLINSB(INB,JSB)
C WRITE(7,*)
C WRITE(7,*)NCASE,NB,NSB
410 CONTINUE
C
C UNIT 6 IS PRT FILE
500 WRITE(6,1370)NCASE
    WRITE(6,1006)TITLE
C
C PRINT TRANSMISSION LOSSES AT CENTER FREQUENCIES
IF(JPRINT.EQ.0.AND.JOPT.NE.0)GOTO 505
WRITE(6,1060)
NB2=NB/2.
NSKIP=NB-2*NB2
NB2P=NB2+NSKIP
DO 504 INB=1,NB2
INBP=NB2P + INB
504 WRITE(6,1070)INB ,FREQ(INB ),TLML(INB ),TLTR(INB ),TLIN(INB ),
$      INBP,FREQ(INBP),TLML(INBP),TLTR(INBP),TLIN(INBP)
$ IF(NSKIP.NE.0)
$   WRITE(6,1070)NB2P,FREQ(NB2P),TLML(NB2P),TLTR(NB2P),TLIN(NB2P)
505 WRITE(6,1100)TLEVL0
C
C PRINT OTHER PROBLEM DATA
520 IF( JPRINT.GT.0) WRITE(6,1110)
$      (D(1,II),II=1,3),PLY(1,5),PLY(1,6),
$      D(2,2),D(2,3), PLY(2,5),PLY(2,6),
$      D(3,3),      PLY(3,5),PLY(3,6),
$      PLY(4,5),PLY(4,6)
$
$      WRITE(6,1120)
$      WRITE(6,1130) (I,I=1,NT)
$      WRITE(6,1140) (MATL(IMATL(I)),I=1,NT)
IF( JPRINT.GT.0) WRITE(6,1150) (RHO(I),I=1,NT)
$      WRITE(6,1160) (H(I),I=1,NT)
IF( JPRINT.GT.0) WRITE(6,1170) (SM(I),I=1,NT)
IF( JPRINT.EQ.0) WRITE(6,1180) PLY(1,5)
IF(JPRINT.GT.0.OR.JOPT.EQ.0) WRITE(6,1190) SMT0,TCRI,TCRF
IF( JOPT.EQ.0) GOTO 525
IF( JDESGN.EQ.1.AND.NT.GT.1) WRITE(6,1200)
IF( JDESGN.EQ.2.AND.NT.GT.1) WRITE(6,1210)
525 IF( JOBJ.EQ.1.AND.JOPT.GT.0) WRITE(6,1220) SMTMAX,TAUMIN
IF( JOBJ.EQ.2.AND.JOPT.GT.0) WRITE(6,1230) TLLMIN,TAUMIN
IF( JOPT.EQ.1) WRITE(6,1240)
IF( JOPT.EQ.2) WRITE(6,1250)
IF( JPRINT.GT.0) WRITE(6,1260) ETA,R1B,RHOA,CA,

```

```

$ IF( ITYPE.EQ.0) WRITE(6,1270) E1,E2,V12,G12
IF(ITYPE.EQ.1.OR.ITYPE.EQ.4) WRITE(6,1271) PHEE,THTA
IF(ITYPE.EQ.2.OR.ITYPE.EQ.3) WRITE(6,1272) THTA
IF( JOPT.GT.0) WRITE(6,1280) NTLL
IF(NORDER.EQ.0.AND.JOPT.GT.0)WRITE(6,1285)
IF(NORDER.GT.0.AND.JOPT.GT.0)WRITE(6,1286) NORDER
IF( IFIN.GT.0) WRITE(6,1287) APANL,BPANL

C
C PRINT NATURAL FREQUENCIES IN HZ
IF(IFIN.LE.0.OR.JOPT.LT.1) GOTO 550
WRITE(6,1350)JBCS
DO 540 IMN=1,NMODES
DO 530 JMN=1,NMODES
530 FMN(IMN,JMN)=WMN(IMN,JMN)/2.0/PI
540 WRITE(6,1360)(FMN(IMN,JMN),JMN=1,NMODES)

C
C PRINT TRANSMISSION LOSSES AT SUB-BAND FREQUEECIES
550 IF(JPRINT.EQ.0.OR.NSB.EQ.1.OR.JOPT.NE.0)GOTO 590
WRITE(6,1080)
NB2=NB/2
NSKIP=NB - 2*NB2
NB2P=NB2 + NSKIP
DO 560 INB=1,NB2
DO 560 INSB=1,NSB
INB1=INB
INB2=INB+NB2P
NUM1=NSB*(INB1-1)+INSB
NUM2=NSB*(INB2-1)+INSB
560 WRITE(6,1090) NUM1,INB1,INSB,FREQSB(INB1,INSB),DF(INB1,INSB),
$ TLMLSB(INB1,INSB),TLTRSB(INB1,INSB),
$ NUM2,INB2,INSB,FREQSB(INB2,INSB),DF(INB2,INSB),
$ TLMLSB(INB2,INSB),TLTRSB(INB2,INSB)
IF(NSKIP.EQ.0)GOTO 590
DO 570 INSB=1,NSB
NUM=(NB2P-1)*NSB+INSB
570 WRITE(6,1090) NUM ,NB2P,INSB,FREQSB(NB2P,INSB),DF(NB2P,INSB),
$ TLMLSB(NB2P,INSB),TLTRSB(NB2P,INSB)

C
C CALL TEST SUBROUTINE (RETURNS IF ITEST=0)
590 CALL TEST (X0,ITEST)

C
C IF NOT USING NEWSUMTA: CALL PLOTTER, THEN STOP
IF(JOPT.NE.0)GOTO 599
IOPT=1
CALL UGETIO(3,NIN,NOUT)
CALL PRPLOT(IOPT,IPLTSB,NCASE)
STOP

CCCCCCCCCCCCCCCCCCCCCCCCCCCCCCCCCCCCCCCCCCCCCCCCCCCCCCCCCCCC
: CALL OPTIMIZER SUBROUTINE :
:.....:

599 CALL SUMT1L (TLTRAN , X0 , X , OBJ , TFMIN ,
$ FDCV , ILIN , ISIDE ,
$ BLBND , BUBND , BLM , BUM ,
$ XSAVE , DELX , S , SN ,
$ BL , BU , IIK , DH , DOBJ ,
$ G , GSAVE , G1 , G2 , G3 ,

```



I

```

      BUBNDU=BUBND(I)/SCALE(I)
      IF(I.EQ.1) WRITE(6,1050)I,XOU,BLBNDU,BUBNDU,SCALE(I),ANG
      IF(I.EQ.1) GOTO 827
      IF(ISI.EQ.1)WRITE(6,1030)I,XOU,BLBNDU,SCALE(I),MATL(IMAT)
      IF(ISI.EQ.2)WRITE(6,1050)I,XOU,BUBNDU,SCALE(I),MATL(IMAT)
      IF(ISI.EQ.3)WRITE(6,1050)I,XOU,BLBNDU,BUBNDU,SCALE(I),MATL(IMAT)
827  CONTINUE
C
C PRINT TRANSMISSION LOSSES AT CENTER FREQUENCIES
830  WRITE(6,1290)
      NB2=NB/2.
      NSKIP=NB - 2*NB2
      NB2P=NB2 + NSKIP
      DO 835 INB=1,NB2
      INBP=NB2P + INB
835  WRITE(6,1070)INB ,FREQ(INB ),TLML(INB ),TLTR(INB ),TLIN(INB ),
      $          INBP,FREQ(INBP),TLML(INBP),TLTR(INBP),TLIN(INBP)
      IF(NSKIP.NE.0)
      $          WRITE(6,1070)NB2P,FREQ(NB2P),TLML(NB2P),TLTR(NB2P),TLIN(NB2)
C
C PRINT OTHER PROBLEM DATA
      WRITE(6,1310)TLEVEL
      WRITE(6,1110)(D(1,II),II=1,3),PLY(1,5),PLY(1,6),
      $          D(2,2),D(2,3), PLY(2,5),PLY(2,6),
      $          D(3,3), PLY(3,5),PLY(3,6),
      $          PLY(4,5),PLY(4,6)
      WRITE(6,1320)
      WRITE(6,1130) (I,I=1,NT)
      WRITE(6,1140) (MATL(IMATL(I)),I=1,NT)
      WRITE(6,1160) (H(I),I=1,NT)
      WRITE(6,1170) (SM(I),I=1,NT)
      WRITE(6,1330) SMT,TCRI,TCRF,SPSTR,CPUTIM
C
C PRINT NATURAL FREQUENCIES IN HZ
      IF(IFIN.LE.0)GOTO 870
      WRITE(6,1350)JBCS
      DO 860 IMN=1,NMODES
      DO 850 JMN=1,NMODES
850  FMN(IMN,JMN)=WMN(IMN,JMN)/2.0/PI
860  WRITE(6,1360)(FMN(IMN,JMN),JMN=1,NMODES)
C
C PRINT OPTIMIZATION PARAMETERS
870  IF( JDESGN.EQ.1.AND.NT.GT.1) WRITE(6,1200)
      IF( JDESGN.EQ.2.AND.NT.GT.1) WRITE(6,1210)
      IF(          JOBJ.EQ.1) WRITE(6,1220) SMTMAX,TAUMIN,
      $          SMterr,TAUERR
      IF(          JOBJ.EQ.2) WRITE(6,1230) TLLMIN,TAUMIN,
      $          TLLERR,TAUERR
      IF(          JOPT.EQ.1) WRITE(6,1240)
      IF(          JOPT.EQ.2) WRITE(6,1250)
      IF(          ITYPE.EQ.0) WRITE(6,1270) PHEE,THTA
      IF(ITYPE.EQ.1.OR.ITYPE.EQ.4) WRITE(6,1271) THTA
      IF(ITYPE.EQ.2.OR.ITYPE.EQ.3) WRITE(6,1272)
      $          WRITE(6,1280) NTLL
      IF(          NORDER.EQ.0) WRITE(6,1285)
      IF(          NORDER.GT.0) WRITE(6,1286) NORDER
C
998  WRITE(6,1370)NCASE
      WRITE(6,1340)
999  STOP

```

I

C  
C  
C  
C  
C

```

.....
:
:   F O R M A T   S T A T E M E N T S   :
:
.....

```

```

1005 FORMAT(20A4)
1006 FORMAT(1X,'***** ',20A4)
1010 FORMAT(/' NEWSUMTA PARAMETERS: '/
$      ' NDV=',I2,9X,'NTCE=',I2,8X,'JPRINT=',I2/
$      ' RACUT=',F6.4,3X,'G0=',F8.6,4X,'MFLAG=',I2/
$      ' RA=',F8.6,4X,'ALPEQC=',F7.5)
1020 FORMAT(/' INITIAL DESIGN AND SIDE BOUNDS (UNSCALED) : '/
$      8X,'X0',8X,'BLBND',8X,'BUBND',6X,'SCALE FACTOR')
1030 FORMAT(I3,2F12.7,12X,E14.7,3X,A4)
1040 FORMAT(I3,F12.7,12X,F12.7,E14.7,3X,A4)
1050 FORMAT(I3,3F12.7,E14.7,3X,A4)
1060 FORMAT(/' SUMMARY OF INITIAL DESIGN: '/
$      ' I F TLML TLTR TLIN ',
$      ' I F TLML TLTR TLIN')
1070 FORMAT(I4,F9.1,3F11.6,6X,I4,F9.1,3F11.6)
1075 FORMAT(I4,F9.1,4F11.6)
1080 FORMAT('1 N I J FREQSB DF TL TLTR ',
$      ' N I J FREQSB DF TL TLTR '/')
1090 FORMAT(10(2I3,I2,F9.2,F7.1,2F8.4,
$      3X,2I3,I2,F9.2,F7.1,2F8.4))
1100 FORMAT(' TLEVLO=',F10.5)
1110 FORMAT(/' DIJ:',3F9.6,' ANGLES:',F5.1,' THICKNESSES:',F10.8/
$      14X,2F9.6, 9X,F5.1, 14X,F10.8/
$      23X, F9.6, 9X,F5.1, 14X,F10.8/
$      41X,F5.1, 14X,F10.8)
1120 FORMAT(' INITIAL DESIGN: '/)
1130 FORMAT(' I:',5X,I2,9(7X,I2))
1140 FORMAT(' MATL:',3X,A4,9(5X,A4))
1150 FORMAT(' RHO:',10F9.3)
1160 FORMAT(' H:',10F9.6)
1170 FORMAT(' SM:',10F9.4)
1180 FORMAT(/' LAYUP ANGLE=',F4.1/)
1190 FORMAT(/' SMT:',F9.5,5X,'TCRI=',E11.5/20X,'TCRF=',E11.5)
1200 FORMAT(51X,' SIMULTANEOUS DESIGN')
1210 FORMAT(51X,' SEQUENTIAL DESIGN')
1220 FORMAT(' SMTMAX=',F8.5,' TAUMIN=',E14.7,14X,'LOSS OBJECTIVE' /
$      ' SMterr=',F6.3,5X,'TAUERR=',F6.3)
1230 FORMAT(' TLLMIN=',F8.5,' TAUMIN=',E14.7,14X,'MASS OBJECTIVE' /
$      ' SMterr=',F6.3,5X,'TAUERR=',F6.3)
1240 FORMAT(51X,' INEQUALITY CONSTRAINT')
1250 FORMAT(52X,' EQUALITY CONSTRAINT')
1260 FORMAT(' ETA,R1B,RHOA,CA:',1X,F5.3,F8.1,F5.2,F6.1/
$      ' E1,E2:',2E11.4/
$      ' V12,G12:',F5.2,E11.4)
1270 FORMAT(T53,'SPECIFIC INCIDENCE'/T50,'PHI,THETA=',F7.5,',',F7.5)
1271 FORMAT(T55,'LINE INTEGRAL'/T55,'THETA=',F7.5)
1272 FORMAT(53X,'FIELD INTEGRATION')
1280 FORMAT(' TRANSMISSION LOSS LEVEL:',T58,'NTLL=',I2)
1285 FORMAT(' INFINITE STRIP SHEAR (NORDER=0) ')
1286 FORMAT(' FINITE PANEL SHEAR (NORDER=',I1,')')
1287 FORMAT(' PANEL SIZE:',F7.4,' X ',F7.4)
1290 FORMAT('1SUMMARY OF FINAL DESIGN: '/
$      ' I F TLML TLTR TLIN ',
$      ' I F TLML TLTR TLIN')
1310 FORMAT(' TLEVEL=',F10.5/)

```



I

```

JREPLY=1
ASHIFT=0.
CALL REPLY(JREPLY,T,ANGLE,ASHIFT,N,NN,PLY)
DO 20 KK=2,NDVM
20 H(KK-1)=X(KK)/SCALE(KK)
CALL DIJ(PLY,NN,H(1),D)
IF(IFIN.GT.0)CALL MODALF(JBCS)
CALL SHEAR(D,H,NORDER,TAUCR)
GOTO 60
C
C SEQUENTIAL DESIGN (JDESGN=2)
40 IF(JDESGN.NE.2)STOP
DO 50 KK=3,NDVM
50 H(KK-1)=X(KK)/SCALE(KK)
C
C COMPUTE STRUCTURAL/ACOUSTIC PARAMETERS OF NEW DESIGN
60 SMT=0.0
DO 70 KK=1,NT
SM(KK)=RHO(KK)*H(KK)
70 IF(IMATL(KK).NE.3)SMT=SMT+SM(KK)
IF(ITYPE.EQ.1)ITYPE=4
DO 80 KK=1,NB
IF(ITYPE.EQ.4.AND.KK.GT.17)ITYPE=1
80 IF(NTLL.EQ.0)CALL TLSUB(KK)
IF(NTLL.EQ.0)CALL TLLSUB(TLL,TLTRL)
IF(NTLL.EQ.0)TLEVEL=TLTRL
IF(NTLL.NE.0)CALL TLSUB(NTLL)
IF(NTLL.NE.0)TLEVEL=TLTR(NTLL)
C
90 GO TO (100, 200, 300, 400, 500), INFO
C
C COMPUTE OBJECTIVE FUNCTION
C
100 OBJ=X(NDV)
199 RETURN
C
C COMPUTE CONSTRAINTS
C
C LOSS OBJECTIVE (JOB=1)
200 IF(JOB.NE.1)GOTO 210
G(1)= 1.0 - SMT/SMTMAX
G(2)=X(NDV)/SCALE(NDV) - TLEVLO/TLEVEL
G(3)=TAUCR/TAUMIN - 1.0
RETURN
C MASS OBJECTIVE (JOB=2)
210 IF(JOB.NE.2)STOP
G(1)=X(NDV)/SCALE(NDV) - SMT/SMT0
G(2)=TLEVEL/TLLMIN - 1.0
G(3)=TAUCR/TAUMIN - 1.0
- 299 RETURN
C
C COMPUTE THE FIRST AND SECOND DERIVATIVES OF OBJECTIVE FUNCTION
C
300 DO 310 KK=1,N1
IF(KK.NE.NDV)DOBJ(KK)=0.0
310 IF(KK.EQ.NDV)DOBJ(KK)=1.0
320 DO 330 KK=1,N3
- 330 DDOBJ(KK)=0.0
- 399 RETURN
C

```

I





```

      GOTO (50,100,200,300,400), INTEG1
C
C INTEG=0 (NO INTEGRATION, SPECIFIC PHI AND THETA)
  50 CALL TAUSUB(NCFNO,NSBNO,PHEE,THTA,TAUPAN,TAUTR)
    TAUPML=1.0/( 1.0+(FFM*COS(THTA))*2 )
    GOTO 500
C
C INTEG=1 (AZIMUTHAL INCIDENCE LINE INTEGRATION USING DCADRE)
  100 PHI1=0.0
    PHI2=PI
    AERR=0.1E-4
    RERR=0.0
    ITIME=0
    FLDIN=DCADRE(ARG1,PHI1,PHI2,AERR,RERR,ERROR,IER)
    IF(IWRITE.NE.0)WRITE(6,10)INTEG,NCFNO,NSBNO,ITIME
    CNST=PI
    TAUTR=FLDIN/CNST
    TAUPML=1.0/( 1.0+(FFM*COS(THTA))*2 )
    GOTO 500
C
C INTEG=2 (FIELD INCIDENCE DOUBLE INTEGRATION USING DBLIN)
  200 PH1=0.0
    PH2=1.0*PI
    AERR=0.1E-4
    ITIME=0
    FLDIN=DBLIN(ARG2,PH1,PH2,TH1,TH2,AERR,ERROR,IER)
    IF(IWRITE.NE.0)WRITE(6,10)INTEG,NCFNO,NSBNO,ITIME
    CNST=PI*(SIN(THL))*2
    TAUTR=FLDIN/CNST
    TAUPML=LOG((1.+FFM**2)/(1.+(COS(THL)*FFM)**2)) /
$      ((SIN(THL)*FFM)**2)
    GOTO 500
C
C INTEG=3 (FIELD INCIDENCE DOUBLE INTEGRATION USING DMLIN)
  300 A3(1)=0.0
    A3(2)=0.0
    B3(1)=PI
    B3(2)=THL
    NV=2
    MAXFCN=256**NV
    AERR=0.1E-4
    RERR=0.0
    ITIME=0
    FLDIN=DMLIN(ARG3,A3,B3,NV,MAXFCN,AERR,RERR,IER)
    IF(IWRITE.NE.0)WRITE(6,10)INTEG,NCFNO,NSBNO,ITIME
    CNST=PI*(SIN(THL))*2
    TAUTR=FLDIN/CNST
    TAUPML=LOG((1.+FFM**2)/(1.+(COS(THL)*FFM)**2)) /
$      ((SIN(THL)*FFM)**2)
    GOTO 500
C
C INTEG=4 (AZIMUTHAL INCIDENCE LINE INTEGRATION USING DMLIN)
  400 A4(1)=0.0
    B4(1)=PI
    NV=1
    MAXFCN=256**NV
    AERR=0.1E-2

```

[illegible]



```

      CK=CKI(1)
      GOTO 20
10  DO 15 KK=2,6
      IF(FR1.GT.FRI(KK)) GOTO 15
      CKDIFF=CKI(KK) - CKI(KK-1)
      FRDIFF=FRI(KK) - FRI(KK-1)
      CK=CKI(KK-1) + CKDIFF * (FRI-FRI(KK-1))/FRDIFF
      GOTO 20
15  CONTINUE
      CK=CKI(6)
C
20  B=AI*W*CSQRT( Y/CK*CMPLX(RHOA*SF*CF2/CF1,-1.2*R1B/W/CF1) )
      ALPHA=REAL(B)
      BETA=AIMAG(B)
      STB=AKA*ST/BETA
      CTB=SQRT(1.-STB**2)
      ZOB=-AI*CK*B/W/Y
25  CONTINUE
C
C CALCULATE ZOP
      INFINITE PANEL THEORY
      IF(IFIN.GT.0)GOTO 30
      DP=D(1,1)*CP**4 + 4.*D(1,3)*CP**3*SP+2.*(D(1,2)+2.*D(3,3))*
$ (CP*SP)**2 + 4.*D(2,3)*CP*SP**3 + D(2,2)*SP**4
      ZOP=CMPLX(ETA*DP*W**3*(ST/CA)**4 , W*SM(1)-DP*W**3*(ST/CA)**4 )
      GOTO 50
C
      FINITE PANEL THEORY
30  AKX=AKA*ST*CP
      AKY=AKA*ST*SP
      TOPSUM=0.0
      BOTSUM=0.0
      DO 40 M=1,NMODES
      DO 40 N=1,NMODES
      AM=FLOAT(M)
      AN=FLOAT(N)
      TERM1=AM*AN*(-1.)*(M+N) / (AKX**2-(AM*PI/APANL)**2)
$ / (AKY**2-(AN*PI/BPANL)**2)
      TERM2=COS(AKX*APANL) - (-1.)*M + AI*SIN(AKX*APANL)
      TERM3=COS(AKY*BPANL) - (-1.)*N + AI*SIN(AKY*BPANL)
      TOPSUM=TOPSUM + TERM1*TERM2*TERM3
40  BOTSUM=BOTSUM + TERM1*TERM2*TERM3 / (WMN(M,N)**2 - W**2)
      ZOP=-AI*SM(1)*TOPSUM/W/BOTSUM
C
C DO LOOP ON NUMBER OF TREATMENTS BEGINS HERE
50  DO 200 II=1,NT
      I=NT+1-II
      IMI=IMATL(I)
      IMP=IMATL(I+1)
C
C ASSIGN VALUE OF ZO(I)
60  IF(IMI.EQ.1)ZO(I)=ZOP
      IF(IMI.EQ.2)ZOS=AI*W*SM(I)
      IF(IMI.EQ.2)ZO(I)=ZOS
      IF(IMI.EQ.3)ZO(I)=ZOA
      IF(IMI.EQ.4)ZO(I)=ZOB
C
C COMPUTE ZNEXT(I) (IMPEDANCE OF NEXT MEDIUM INTO WHICH WAVE WILL PASS)
      IF(I.EQ.NT)ZNEXT(I)= ZOA
      IF(I.EQ.NT)GOTO 100
      IF(IMP.EQ.2)ZNEXT(I)=ZNEXT(I+1) + AI*W*SM(I+1)

```





[illegible]











```

C []
C []      DIJ calculates panel directional stiffnesses D(3,3).      []
C []
C [][][][][][][][][][][][][][][][][][][][][][][][][][][][]
C []      SUBROUTINE DIJ(PLY,NN,T,D)
C
C      DIMENSION D(3,3),PLY(16,6),QB(3,3)
C
C      DO 30 KI=1,3
C      DO 30 KJ=1,3
30 D(KI,KJ)=0.0
C
C      DO 50 K=1,NN
C      DENOM=1.0 - PLY(K,3)**2*PLY(K,2)/PLY(K,1)
C      Q11=PLY(K,1)/DENOM
C      Q22=PLY(K,2)/DENOM
C      Q12=PLY(K,3)*Q22
C      Q66=PLY(K,4)
C      THTAP=PLY(K,5)*ARCOS(-1.)/180.
C      C=COS(THTAP)
C      S=SIN(THTAP)
C
C      QB(1,1)=Q11*C**4 + 2.0*(Q12+2.0*Q66)*S*S*C*C + Q22*S**4
C      QB(1,2)=(Q11+Q22-4.0*Q66)*S*S*C*C + Q12*(S**4+C**4)
C      QB(2,1)=QB(1,2)
C      QB(1,3)=(Q11-Q12-2.0*Q66)*S*C**3 + (Q12-Q22+2.0*Q66)*S**3*C
C      QB(3,1)=QB(1,3)
C      QB(2,2)=Q11*S**4 + 2.0*(Q12+2.0*Q66)*S*S*C*C + Q22*C**4
C      QB(2,3)=(Q11-Q12-2.0*Q66)*S**3*C + (Q12-Q22+2.0*Q66)*S*C**3
C      QB(3,2)=QB(2,3)
C      QB(3,3)=(Q11+Q22-2.0*Q12-2.0*Q66)*S*S*C*C + Q66*(S**4+C**4)
C
C      TK=PLY(K,6)
C      TSUM=0.0
C      DO 35 KK=1,K
35 TSUM=TSUM + PLY(KK,6)
C      ZKB=TSUM - (T+TK)/2.0
C      DO 40 KI=1,3
C      DO 40 KJ=1,3
C      DDD=QB(KI,KJ)*(TK*ZKB**2+TK**3/12.0)
C ASSUME PANEL LAYUP IS SYMMETRIC (ISYM=1)
40 D(KI,KJ)=D(KI,KJ)+2.0*DDD
50 CONTINUE
RETURN
END

C
C
C      INPUT DATA FILE
C
C
C      TITLE ... 72 CHAR OR LESS
C      0 0 4 1 1 1 1
C      2.828 0.831E7
C      1 0 .241 .406
C      28 3 25.0 0 1.361365 0.00
C      1.21 343. 0.0 43000. 8 1
C      13.7E10 9.65E9 0.30 4.80E9
C      1 0.100 0.1000 0 0.00500 01.000
C      33.600000 0 0. 0.010 3 -5.0 95.00000 ANGLE
C      0.0011088 1 1550. 100.000 1 0.0 0.05000 PANEL
C      JOPT,ITEST,NT,IFIN JDESGN,JOBJ,NTLL
C      (SMTMAX OR TLLMIN),TAUMIN
C      NMODES,NORDER,APANL,BPANL
C      NB,NSB,BOTFRQ INTEG,THTA,PHEE
C      RHOA,CA,ETA,R1B,N,ISYM
C      E1,E2,V12,G12
C      JPRINT,RACUT,G0 MFLAG,RA,ALPEQC

```

```

0.010000 3 1.21 10.000 3 0.0 0.50000 AIRSPACE
0.010000 4 9.60 10.000 1 0.0 0.50000 BLANKET
0.000100 2 1000. 1000.000 1 0.0 0.05000 SEPTUM
***** FORMAT *****
JOPT=0 FOR NO, =1 FOR INEQ, =2 FOR EQ || NORDER=0 FOR SHEARI, =4 FOR SHEARF
IFIN=0 FOR INFINITE, >0 FOR FINITE || DEFAULT NEWSUMTA PARAMETERS:
JDESGN=1 FOR SIMUL., =2 FOR SEQ. || RACUT,G0,RA,ALPEQC=.1,.1,1.0
JOBJ=1 FOR LOSS, =2 FOR MASS || IF MFLAG=1, SPECIFY RA & ALPEQC
NTLL=0 FOR TLEVEL, =J FOR TLTR(J) || IPRLT=1 PLOTS ALL SUB-BANDS

```

..... TYPICAL VALUES .....

```

TITLE ... 72 CHAR OR LESS
0 0 4 1 1 1 1 JOPT,ITEST,NT,IFIN JDESGN,JOBJ,NTLL
2.828 0.831E7 (SMTMAX OR TLLMIN),TAUMIN
1 0 .241 .406 NMODES,NORDER,APANL,BPANL
28 3 25.0 0 1.361365 0.00 NB,NSB,BOTFRQ INTEG,THTA,PHEE
1.21 343. 0.0 43000. 8 1 RHOA,CA,ETA,R1B,N,ISYM
13.7E10 9.65E9 0.30 4.80E9 E1,E2,V12,G12
1 0.100 0.1000 0 0.00500 01.000 JPRINT,RACUT,G0 MFLAG,RA,ALPEQC
33.600000 0 0. 0.010 3 -5.0 95.00000 ANGLE
0.0011088 1 1550. 100.000 1 0.0 0.05000 PANEL
0.010000 3 1.21 10.000 3 0.0 0.50000 AIRSPACE
0.010000 4 9.60 10.000 1 0.0 0.50000 BLANKET
0.000100 2 1000. 1000.000 1 0.0 0.05000 SEPTUM

```



## Appendix B. Shear Buckling Strength of Finite Panels and Infinite Strips

**Eigenvalue Solution:** As in Ref [14], the equation of motion for a simply supported midplane symmetric rectangular plate is

$$D_{11}\frac{\partial^4 w}{\partial x^4} + 4D_{16}\frac{\partial^4 w}{\partial x^3\partial y} + 2(D_{12} + 2D_{66})\frac{\partial^4 w}{\partial x^2\partial y^2} + 4D_{26}\frac{\partial^4 w}{\partial x\partial y^3} + D_{22}\frac{\partial^4 w}{\partial y^4} + \rho\frac{\partial^2 w}{\partial t^2} = q + N_x\frac{\partial^2 w}{\partial x^2} + 2N_{xy}\frac{\partial^2 w}{\partial x\partial y} - N_y\frac{\partial^2 w}{\partial y^2} \quad [B.1]$$

with the boundary conditions that at  $x = 0$  and  $x = a$ ,

$$w = 0$$

$$M_x = -D_{11}\frac{\partial^2 w}{\partial x^2} - D_{12}\frac{\partial^2 w}{\partial y^2} - 2D_{16}\frac{\partial^2 w}{\partial x\partial y} = 0 \quad [B.2]$$

and at  $y = 0$  and  $y = b$ ,

$$w = 0$$

$$M_y = -D_{12}\frac{\partial^2 w}{\partial x^2} - D_{22}\frac{\partial^2 w}{\partial y^2} - 2D_{26}\frac{\partial^2 w}{\partial x\partial y} = 0 \quad [B.3]$$



Using the method of Galerkin, the out-of-plane deflection is assumed to be of the form

$$w(x, y) = \sum_{m=1}^M \sum_{n=1}^N w_{mn} \phi_m(x) \psi_n(y) \quad [B.4]$$

Then the coefficients  $w_{mn}$  are determined by using orthogonality conditions of the form

$$\begin{aligned} \int_0^a \int_0^b & \left[ D_{11} \frac{\partial^4 w}{\partial x^4} + 4D_{16} \frac{\partial^4 w}{\partial x^3 \partial y} + 2(D_{12} + 2D_{66}) \frac{\partial^4 w}{\partial x^2 \partial y^2} \right. \\ & \left. + 4D_{26} \frac{\partial^4 w}{\partial x \partial y^3} + D_{22} \frac{\partial^4 w}{\partial y^4} \right] \phi_m(x) \psi_n(y) dx dy \\ & = \int_0^a \int_0^b \left[ N_x \frac{\partial^2 w}{\partial x^2} + 2N_{xy} \frac{\partial^2 w}{\partial x \partial y} \right] \phi_m(x) \psi_n(y) dx dy \end{aligned} \quad [B.5]$$

Here,  $w(x, y)$  is taken as a double sine series:

$$w(x, y) = \sum_{m=1}^M \sum_{n=1}^N w_{mn} \sin \frac{m\pi x}{a} \sin \frac{n\pi y}{b} \quad [B.6]$$

This satisfies the deflection boundary conditions, but not the moment boundary conditions; therefore, the following additional terms must be added to the orthogonality conditions to account for the deficiency (Ref. [14]):

$$\begin{aligned} - \int_0^a 2D_{26} \left[ \frac{\partial^2 w}{\partial x \partial y} \right]_{y=b} - \frac{\partial^2 w}{\partial x \partial y} \Big|_{y=0} \Big] \frac{l\pi}{b} \sin \frac{k\pi x}{a} dx \\ - \int_0^b 2D_{16} \left[ \frac{\partial^2 w}{\partial x \partial y} \right]_{x=a} - \frac{\partial^2 w}{\partial x \partial y} \Big|_{x=0} \Big] \frac{k\pi}{a} \sin \frac{l\pi y}{b} dy \end{aligned} \quad [B.7]$$

Then, the orthogonality conditions become

$$\begin{aligned}
& [D_{11}\kappa^4 + 2(D_{12} + 2D_{66})\kappa^2\lambda^2 + D_{22}\lambda^4] \frac{ab\pi^4}{4} w_{kl} - \sum_m \sum_{\substack{n \\ n \neq l}} D_{16} 2mn\pi^2 \kappa^2 \alpha_{ln} \beta_{ln} w_{mn} \\
& - \sum_{\substack{m \\ m \neq k}} \sum_{\substack{n \\ n \neq l}} [D_{16}\mu^2 + D_{26}v^2] mn\pi \alpha_{km} \alpha_{ln} \beta_{km} \beta_{ln} w_{mn} - \sum_m \sum_{\substack{n \\ m \neq k}} D_{26} 2mn\pi^2 \lambda^2 \alpha_{km} \beta_{km} w_{mn} \quad [B.8] \\
& = \sum_m \sum_{\substack{n \\ m \neq k, n \neq l}} N_{xy} \alpha_{km} \alpha_{ln} \beta_{km} \beta_{ln} w_{mn}
\end{aligned}$$

where

$$\begin{aligned}
\alpha_{km} &= 1 - (-1)^{k+m} \\
\alpha_{ln} &= 1 - (-1)^{l+n} \\
\beta_{km} &= \left[ \frac{1}{k-m} + \frac{1}{k+m} \right] \\
\beta_{ln} &= \left[ \frac{1}{l-n} + \frac{1}{l+n} \right]
\end{aligned} \quad [B.9]$$

and

$$\begin{aligned}
\mu &= m/a \\
v &= n/b \\
\kappa &= k/a \\
\lambda &= l/b
\end{aligned} \quad [B.10]$$

Equation (B.3) can be rewritten as a matrix equation and solved as an eigenvalue problem of the form

$$A \vec{w} = N_{xy} B \vec{w} \quad [B.11]$$

Program TLROP uses the IMSL subroutine EIGZF to find the minimum value of the shear buckling strength  $N_{xy}$ .

**Approximate Solution:** The critical shear stress of an infinite strip (thin plate of finite width and infinite length) is presented by Ashton and Whitney in Ref. [14]. The critical shear stress for a specially orthotropic simply supported infinite strip is found as follows:

A value of the shear buckling coefficient  $K$  is interpolated from Table 6 depending on the value of  $\theta_\infty$  given by

$$\theta_\infty = \frac{1}{D_3} \sqrt{D_{11}D_{22}} \quad [B.12]$$

where  $D_3 = D_{12} + D_{66}$ . Then, if  $K < 1$ ,

$$\tau_{cr} \Big|_{a \rightarrow \infty} = 4K \frac{(D_{22}D_3)^{1/2}}{b^2 t_p} \quad [B.13]$$

$$\tau_{cr} \Big|_{b \rightarrow \infty} = 4K \frac{(D_{11}D_3)^{1/2}}{a^2 t_p} \quad [B.14]$$

Or, if  $K \geq 1$ ,

$$\tau_{cr} \Big|_{a \rightarrow \infty} = 4K \frac{(D_{11}D_{22}^3)^{1/4}}{b^2 t_p} \quad [B.15]$$

$$\tau_{cr} \Big|_{b \rightarrow \infty} = 4K \frac{(D_{11}^3 D_{22})^{1/4}}{a^2 t_p} \quad [B.16]$$

Then, the approximate critical shear stress ( used during optimization for its relatively low computation time) is given by

$$\tilde{\tau} = \tau_{cr} \Big|_{a \rightarrow \infty} + \tau_{cr} \Big|_{b \rightarrow \infty} \quad [B.17]$$

**Table 1. Infinite Strip Shear Buckling Coefficients**

$\theta_\infty$	0.0	0.2	0.5	1.0	2.0	3.0	5.0	10.	20.	40.
K	11.71	11.80	12.20	13.17	10.80	9.95	9.25	8.70	8.40	8.25

## Appendix C. Acoustic Properties of Fibrous Blankets

In order to describe the transmission of an acoustic wave through a fibrous blanket, one must find the material's characteristic impedance  $Z_b$  and propagation constant  $b_b$ . Expressions for these are developed in Ref. [12] and Ref. [13] and are summarized here for convenience.

Beranek<sup>[12]</sup> proposes a fictional gas with complex effective compressibility  $K$  and complex effective density  $\rho'$  to replace the gas contained within the acoustic blanket. This fictional gas system accounts for both inertial and viscous effects.

The complex compressibility depends on frequency and on the flow resistivity  $R_f$  of the porous material. According to Beranek, at atmospheric pressure the phase angle is small enough to be neglected for the range of frequencies considered here. Therefore, the present program interpolates between real values taken from Figure 10.6 on page 254 of Ref. [12].

For a porous material of bulk density  $\rho_m$  and fiber density  $\rho_f$ , the porosity is

$$Y = 1 - \frac{\rho_f}{\rho_m} \quad [C.1]$$

and then the effective complex density is approximated as

$$\rho' = \frac{\rho s}{f_1} \left( f_2 - \frac{1.2 j R_1}{\rho s \omega} \right) \quad [C.2]$$

where, for “soft” acoustic blankets,

$$f_1 = 1 + \left( \frac{1.2 R_1}{\rho_m \omega} \right)^2 \quad [C.3]$$

$$f_2 = 1 + \left( Y + \frac{\rho_m}{\rho s} \right) \left( \frac{1.2 R_1}{\rho_m \omega} \right)^2 \quad [C.4]$$

and where  $\rho$  is the air density,  $\omega$  is the excitation frequency in rad/sec, and  $s$  is a dimensionless structure factor which accounts for the physical characteristics of the blanket material. The structure factor is estimated from Figure 10.5 on page 253 of Ref. [12].

Finally, the blanket propagation constant and characteristic impedance are given by the following forms:

$$b_b = j\omega \sqrt{Y \rho' / K} \quad [C.5]$$

$$Z_{0_b} = \sqrt{\rho' K / Y} \quad [C.6]$$

## **Appendix D. Figures**

# Figures



**NOISE TRANSMISSION IN  
ADVANCED COMPOSITE MATERIAL STRUCTURES  
RESEARCH PROGRAM**

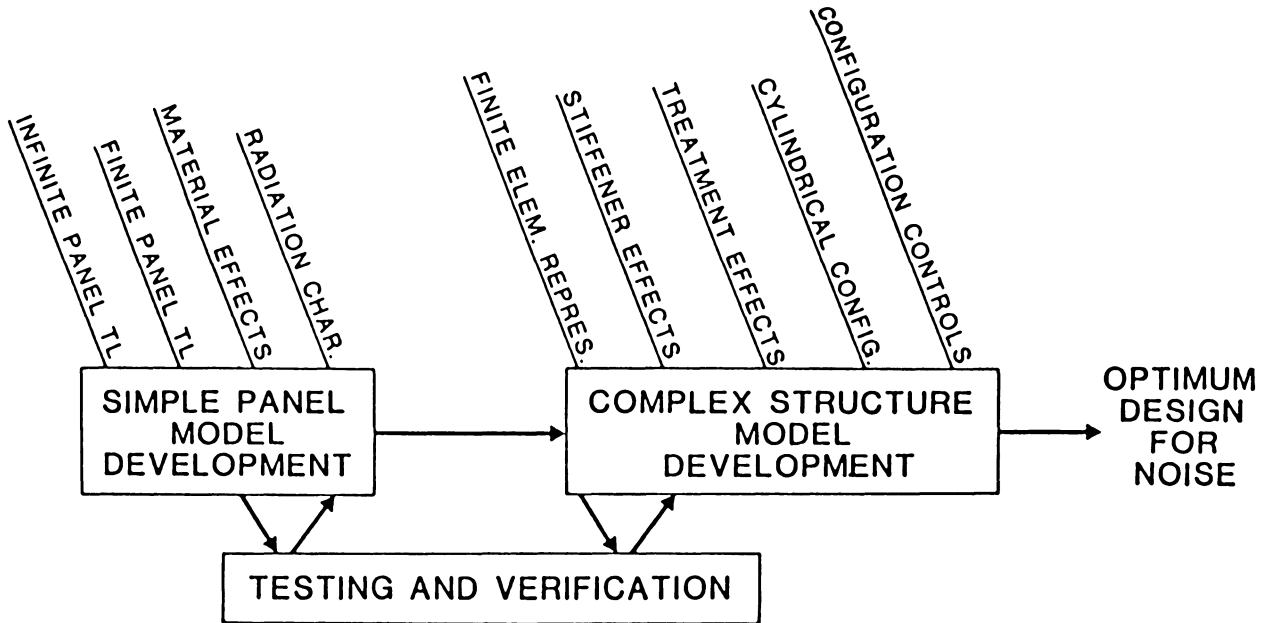


Figure 1. Basic Elements of NASA Research Program

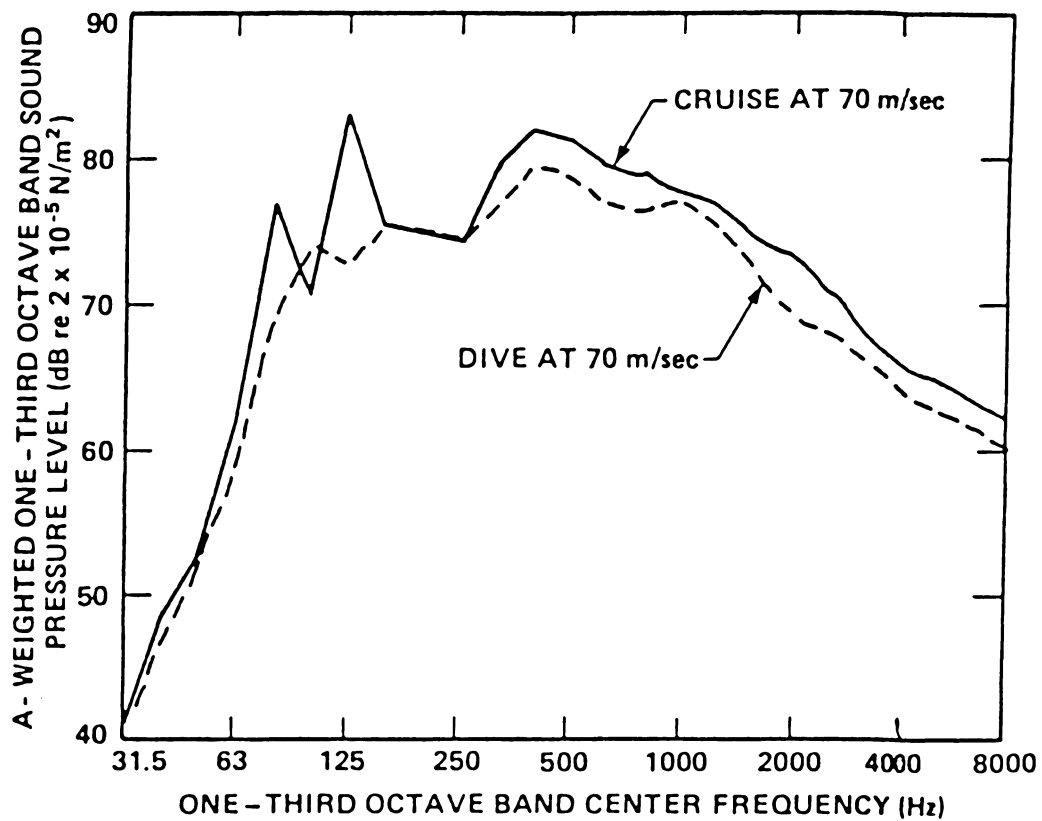
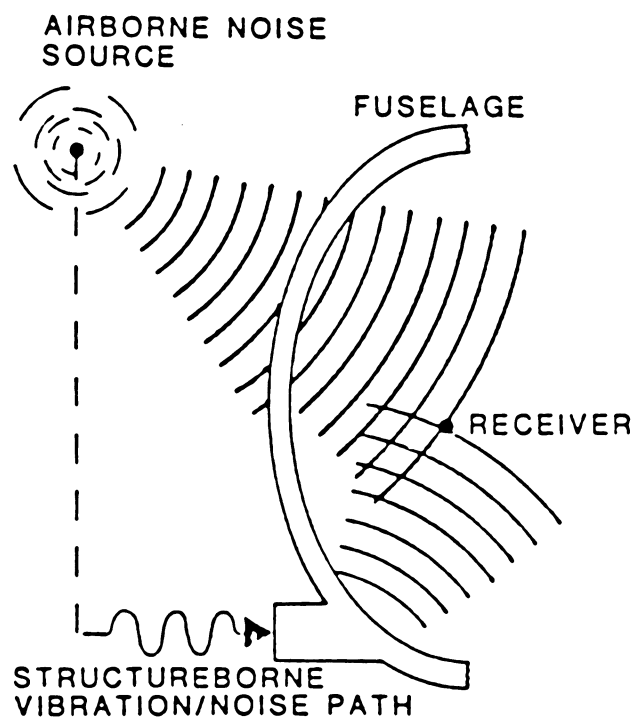


Figure 2. Cabin Noise Levels With And Without Propulsor-Generated Noise



**Figure 3. Airborne vs. Structureborne Transmission Paths**

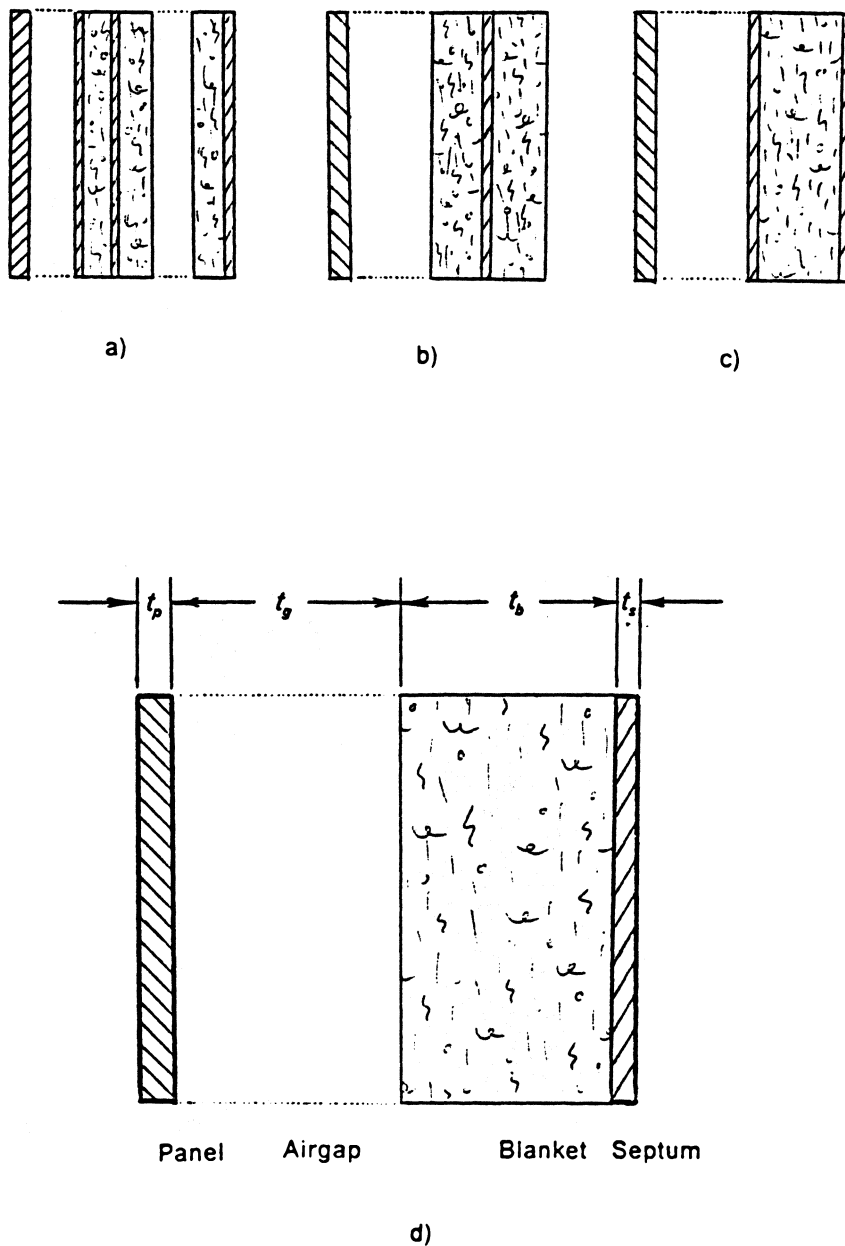
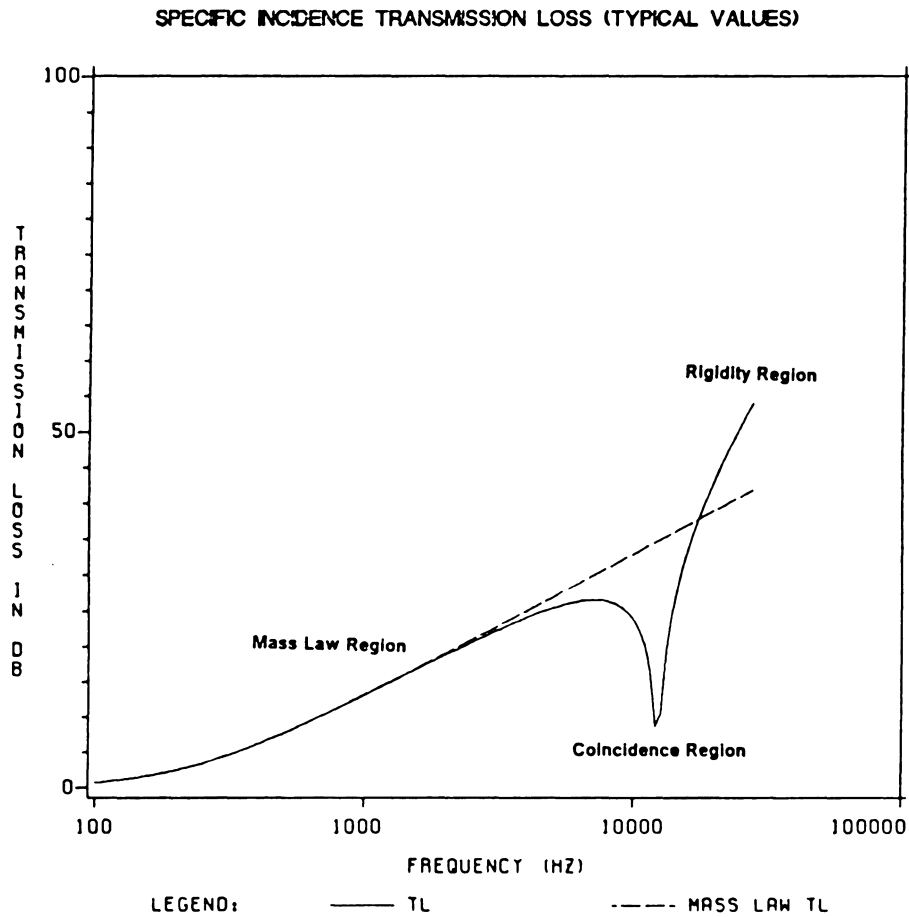
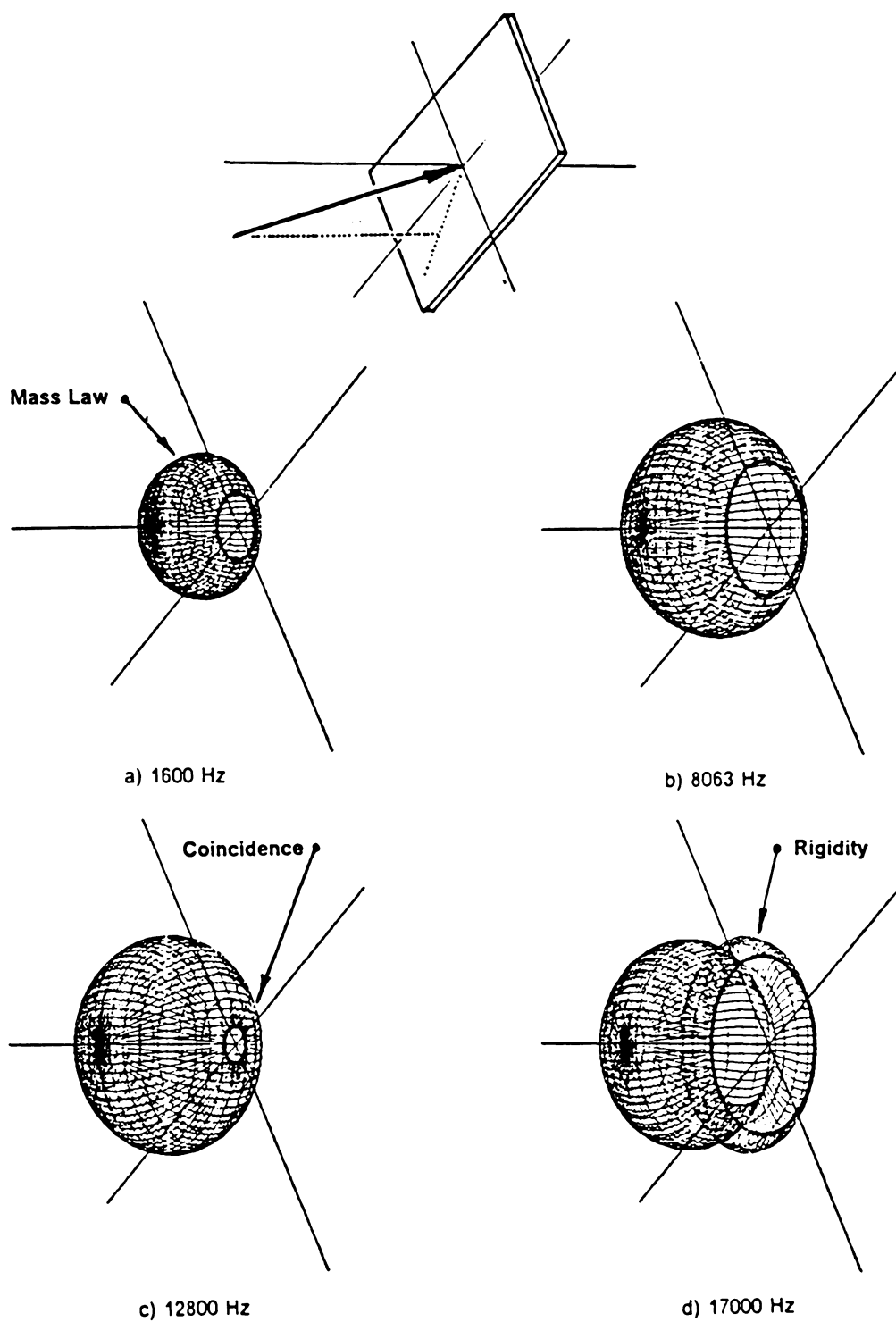


Figure 4. Typical Treatment Configurations



**Figure 5. Typical Specific Incidence Transmission Loss vs. Frequency**



**Figure 6. Transmission Loss vs. Incidence Direction (Aluminum Panel)**

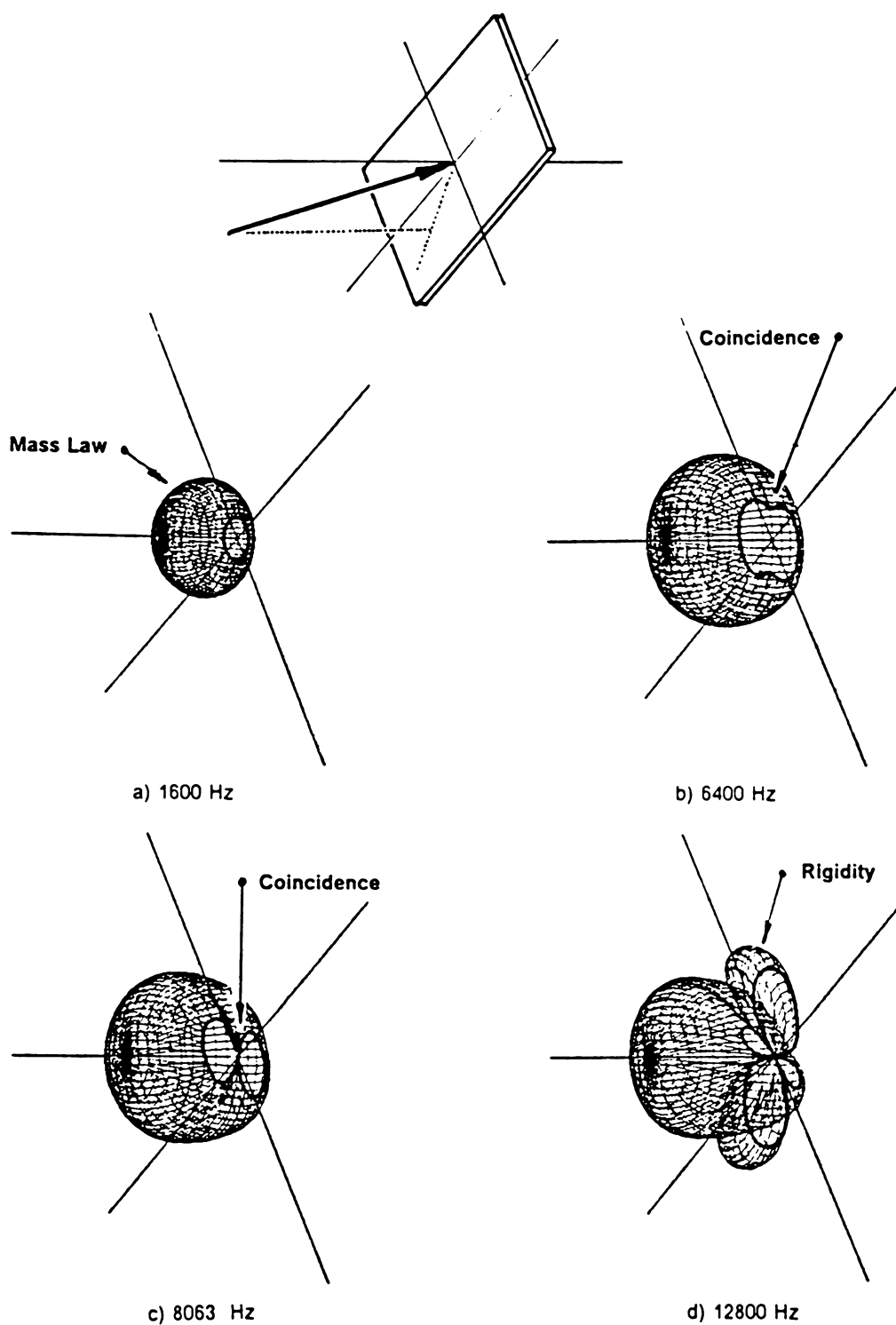


**Figure 7. Transmission Loss vs. Incidence Direction (Graphite/Epoxy Panel)**

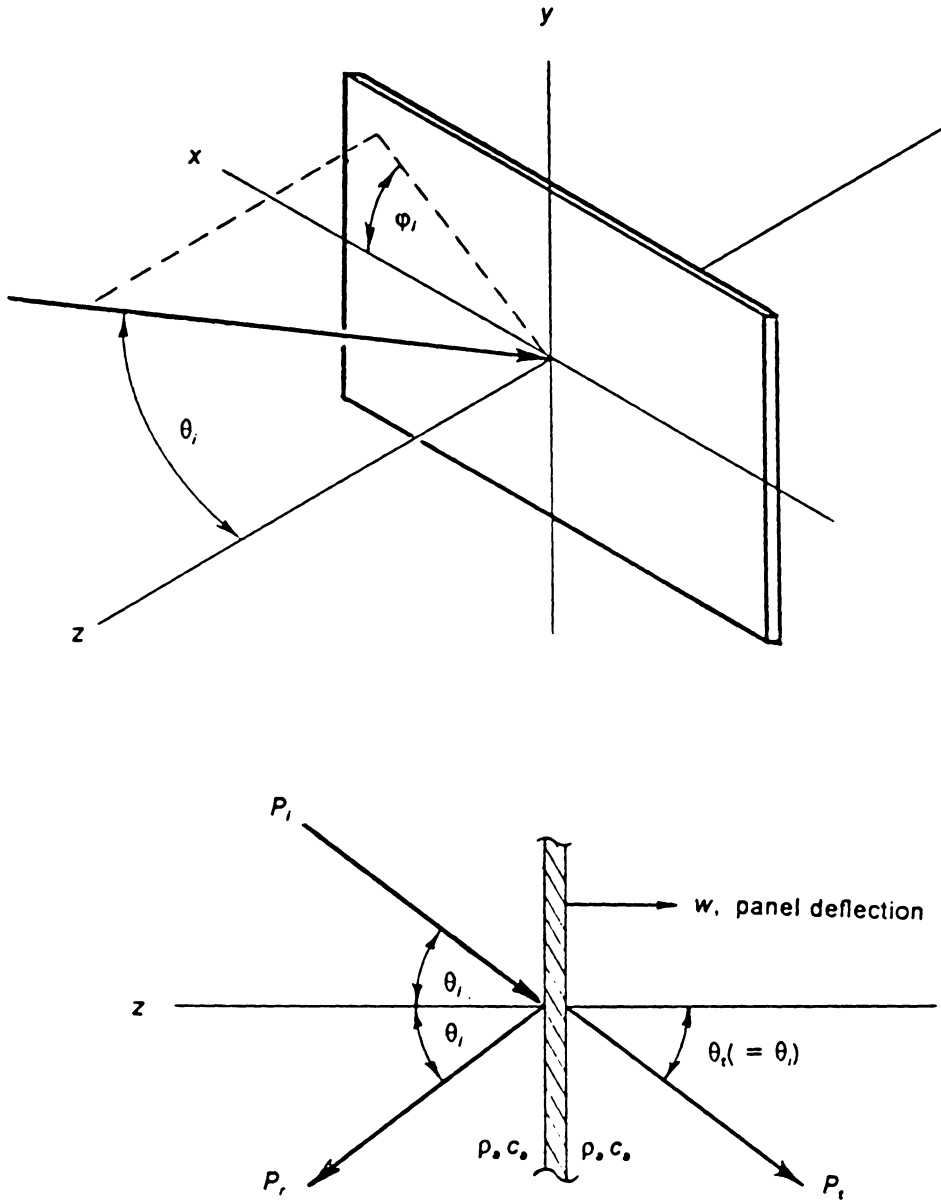


Figure 8. Geometry of Infinite Panel Transmission



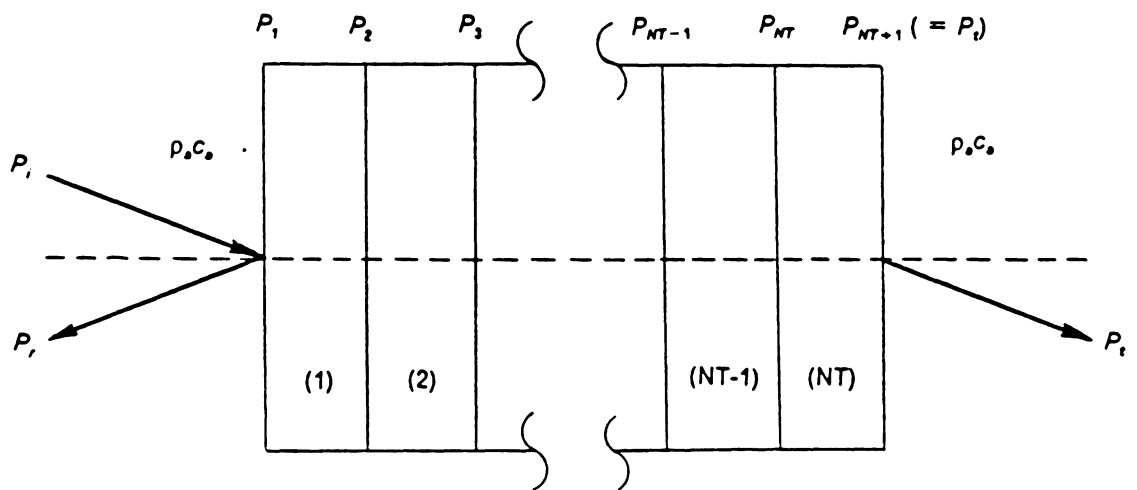
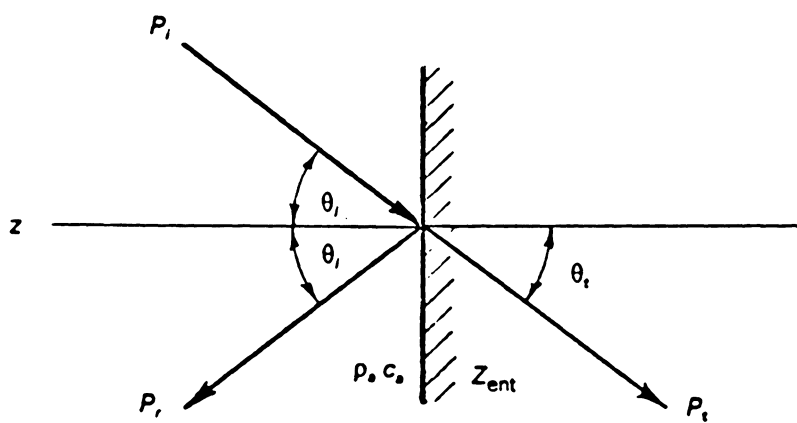


Figure 9. Blocked Pressures For Multi-Layered System



**Figure 10. Plane Interface Between Two Semi-Infinite Media**

TRANSMISSION LOSS TL AND TRANSMISSION DIFFERENCE TD VS. FREQUENCY

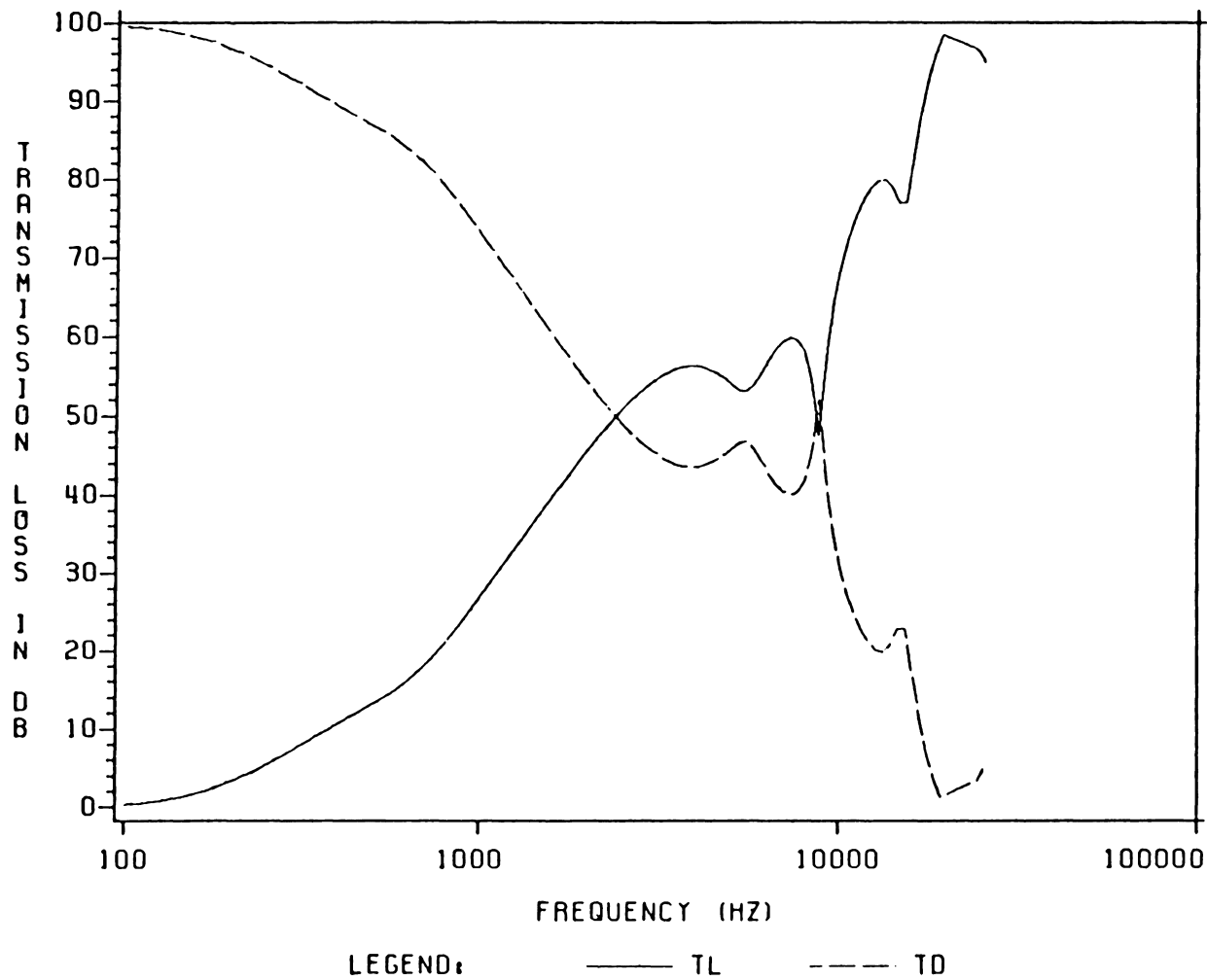
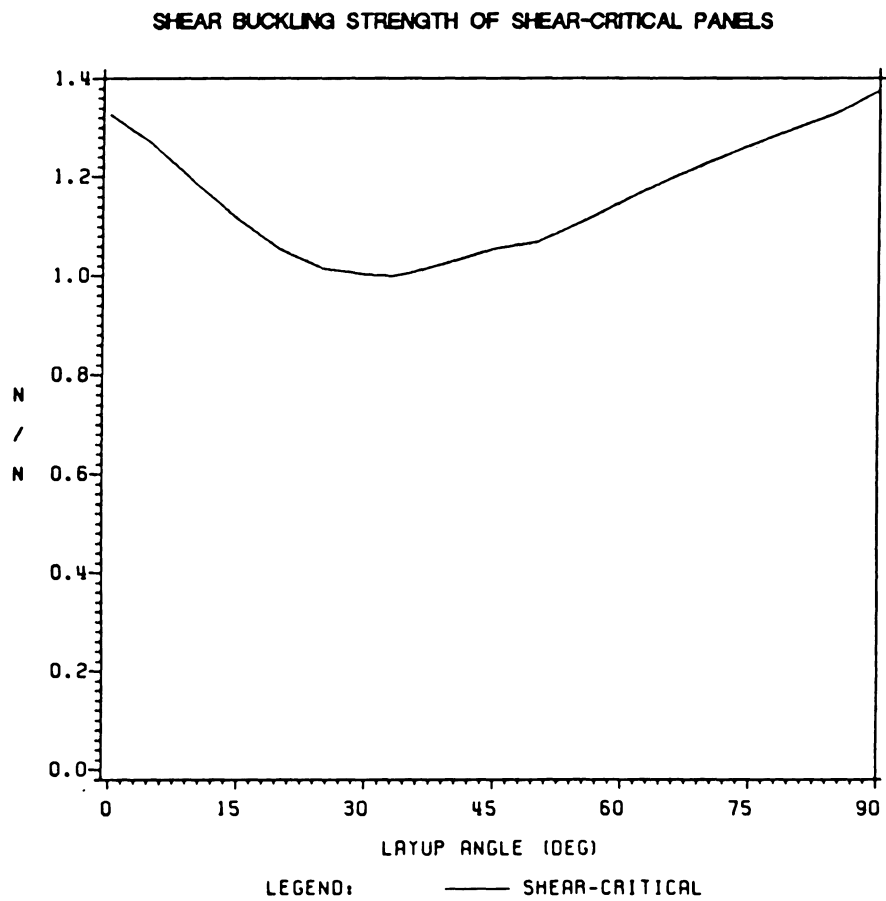


Figure 11. Comparison of Transmission Loss TL and Transmission Difference TD



**Figure 12. Eigenvalue Shear Buckling Strength of Shear-Critical Panels**

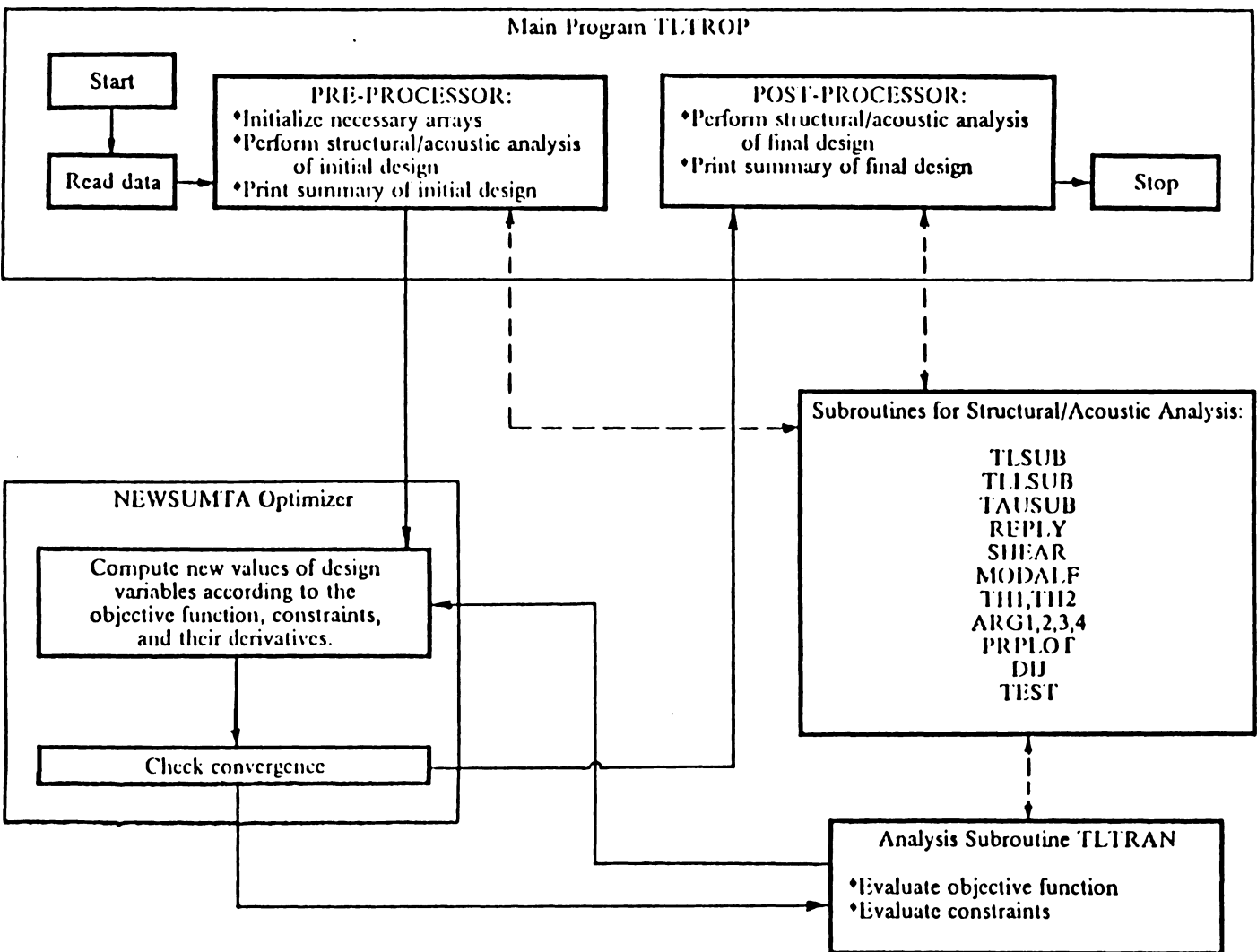
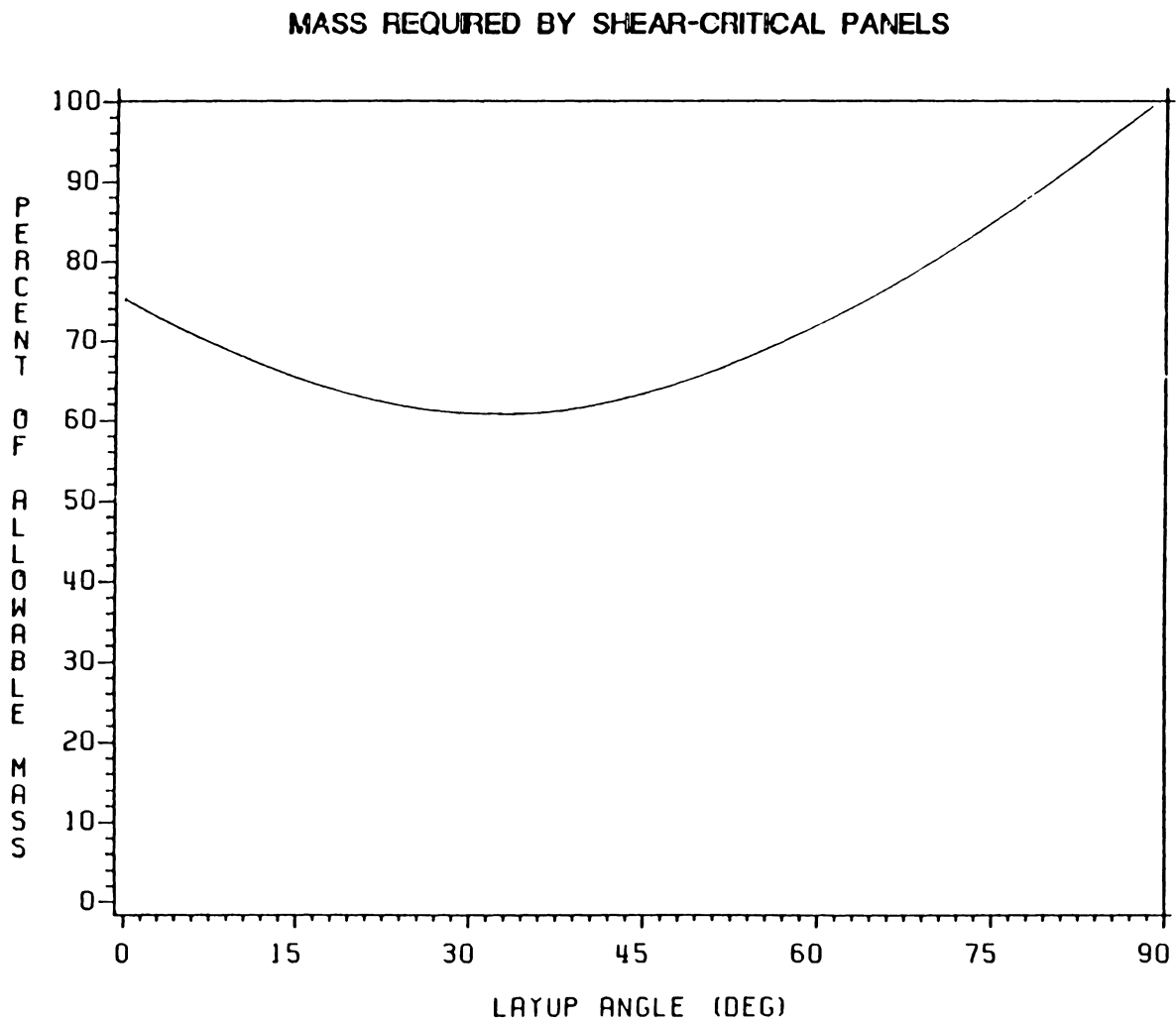
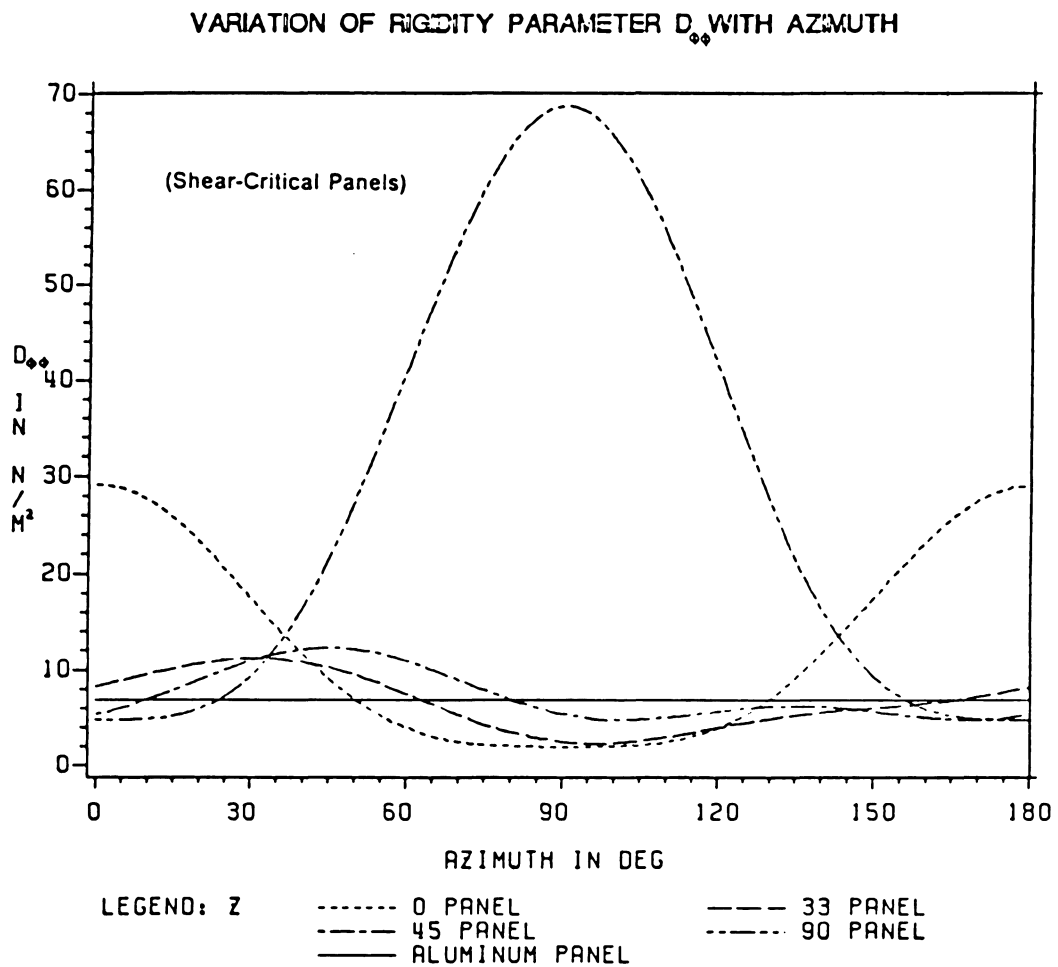


Figure 13. Flowchart of Program TLTRAP



**Figure 14. Mass Required By Shear-Critical Panels**



**Figure 15. Variation of Rigidity Parameter With Azimuth**

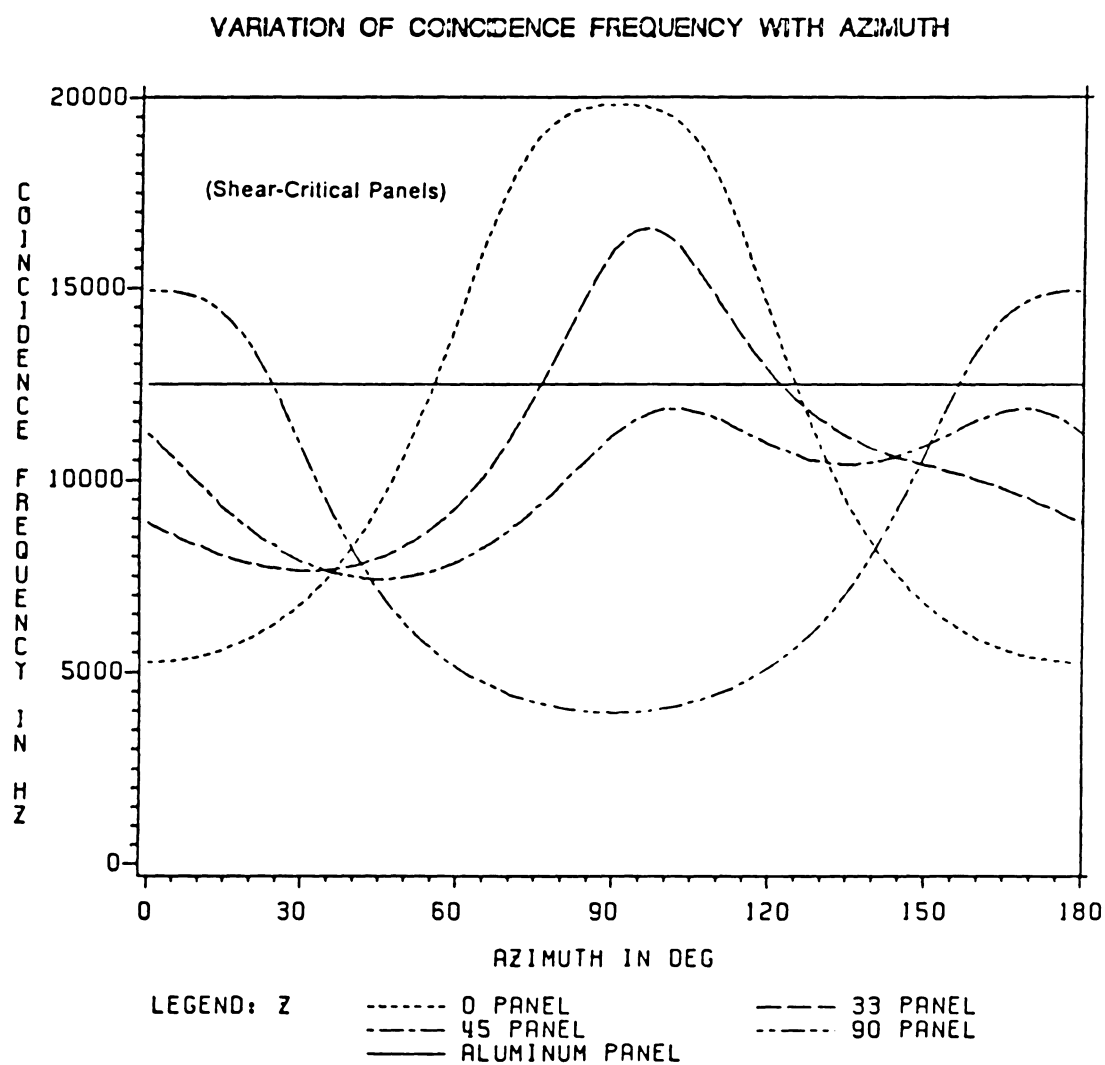
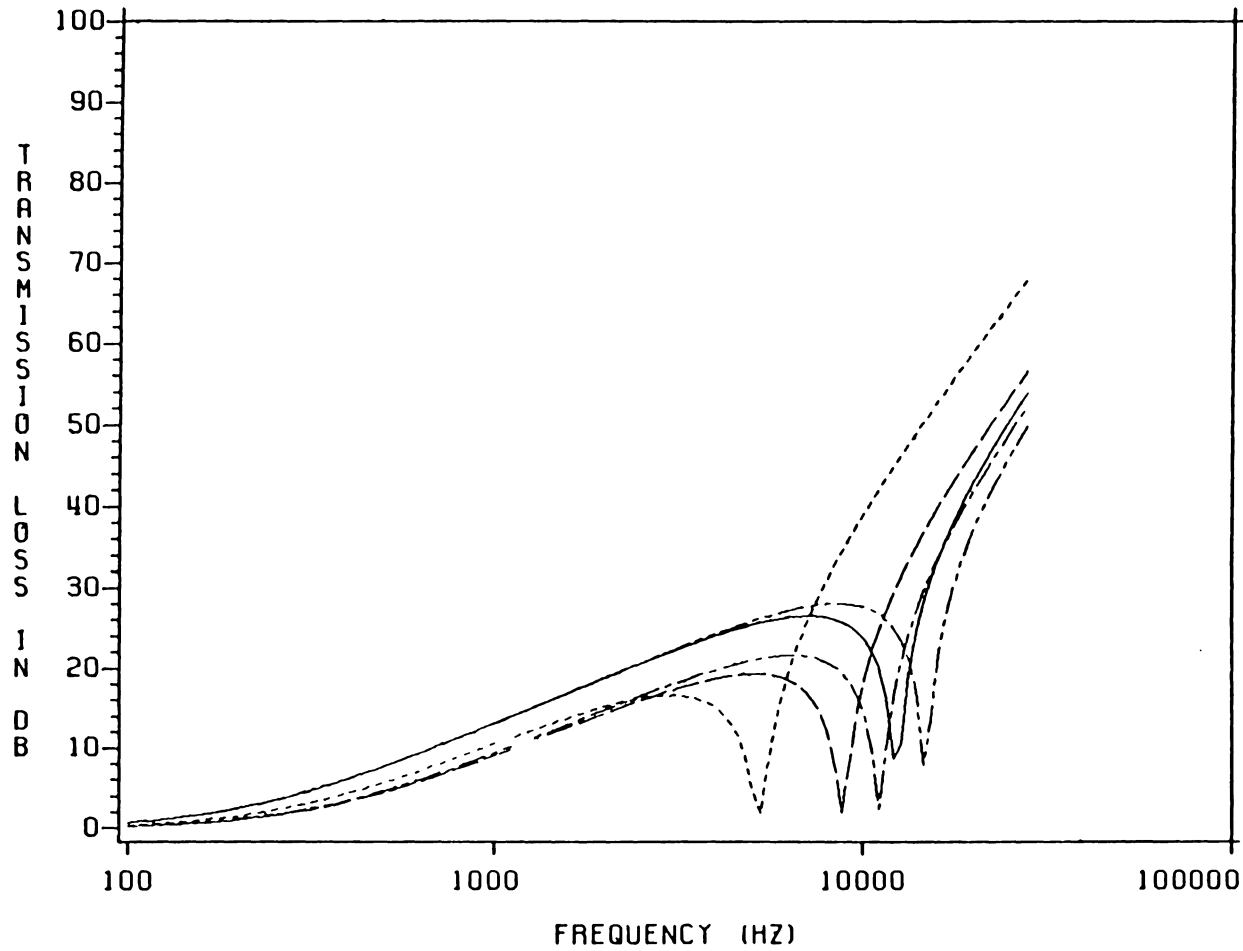


**Figure 16. Variation of Coincidence Frequency With Azimuth**



# SPECIFIC INCIDENCE TRANSMISSION LOSS OF SHEAR-CRITICAL PANELS



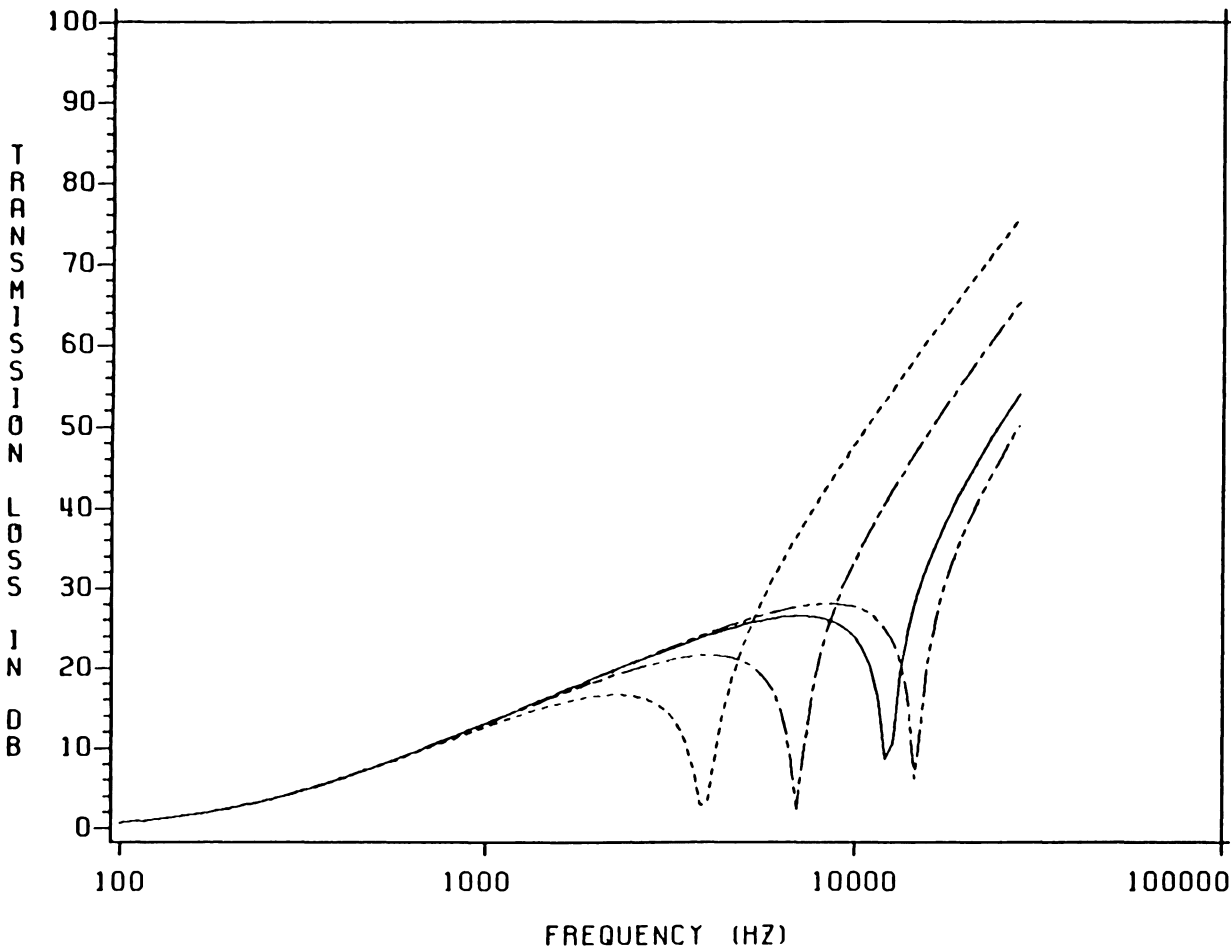
LEGEND:

----- 0-DEG PANEL  
 -.-.-.- 45-DEG PANEL  
 \_\_\_\_\_ ALUMINUM PANEL

----- 33-DEG PANEL  
 -.-.-.- 90-DEG PANEL

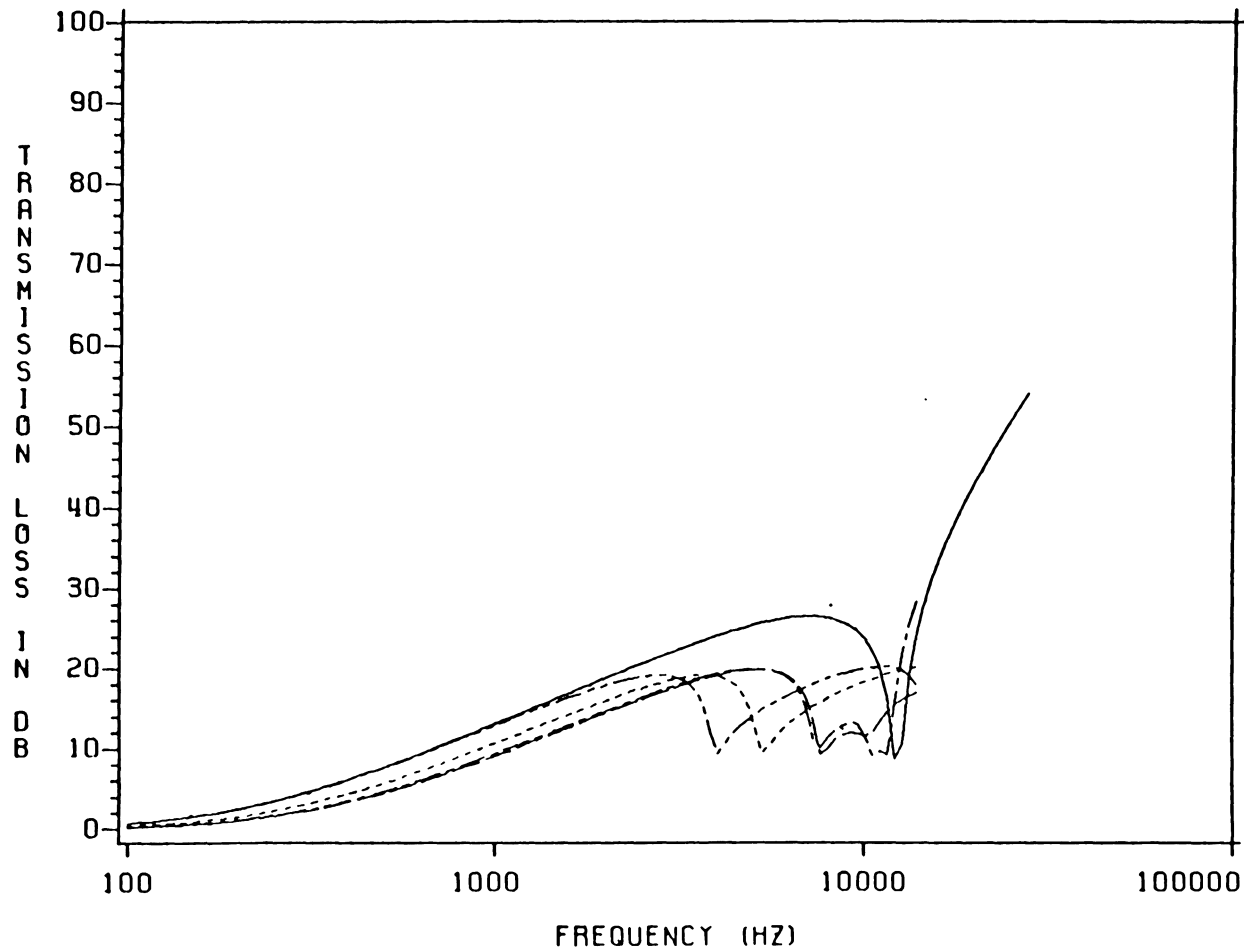
Figure 17. Specific Incidence Transmission Loss of Shear-Critical Panels

SPECIFIC INCIDENCE TRANSMISSION LOSS OF MASS-CRITICAL PANELS



LEGEND:      - - - - - 0-DEG PANEL      - . - . - 45-DEG PANEL  
                 - . . . . 90-DEG PANEL      - - - - - ALUMINUM PANEL

# GRAZING INCIDENCE TRANSMISSION LOSS OF SHEAR-CRITICAL PANELS



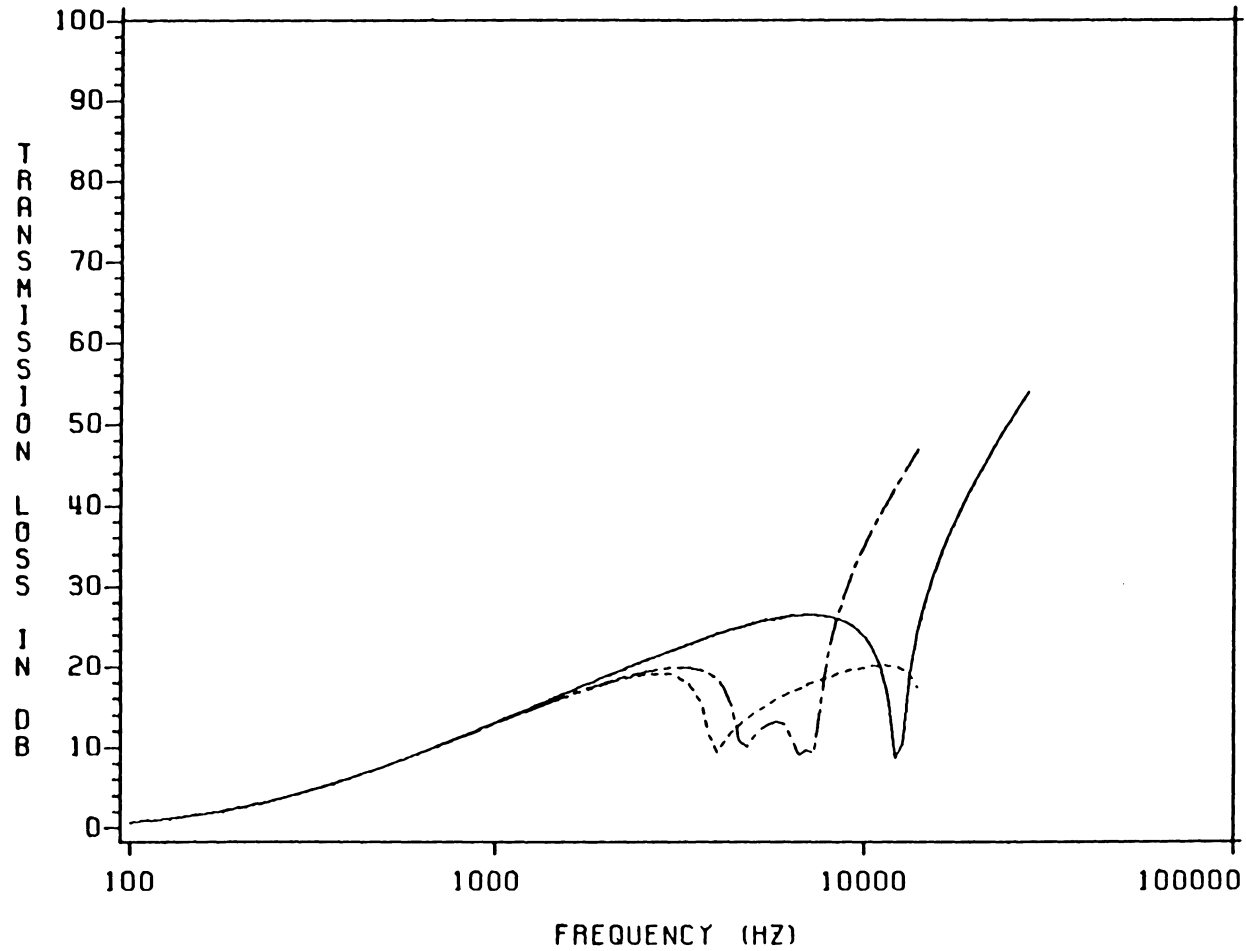
LEGEND:

..... 0-DEG PANEL  
 ----- 45-DEG PANEL  
 ————— ALUMINUM PANEL

----- 33-DEG PANEL  
 - . - . - 90-DEG PANEL

Figure 19. Grazing Incidence Transmission Loss of Shear-Critical Panels

# GRAZING INCIDENCE TRANSMISSION LOSS OF MASS-CRITICAL PANELS



LEGEND:

----- 0-DEG, 90-DEG  
 ——— ALUMINUM PANEL

----- 45-DEG PANEL

Figure 20. Grazing Incidence Transmission Loss of Mass-Critical Panels

# FIELD INCIDENCE TRANSMISSION LOSS OF SHEAR-CRITICAL PANELS

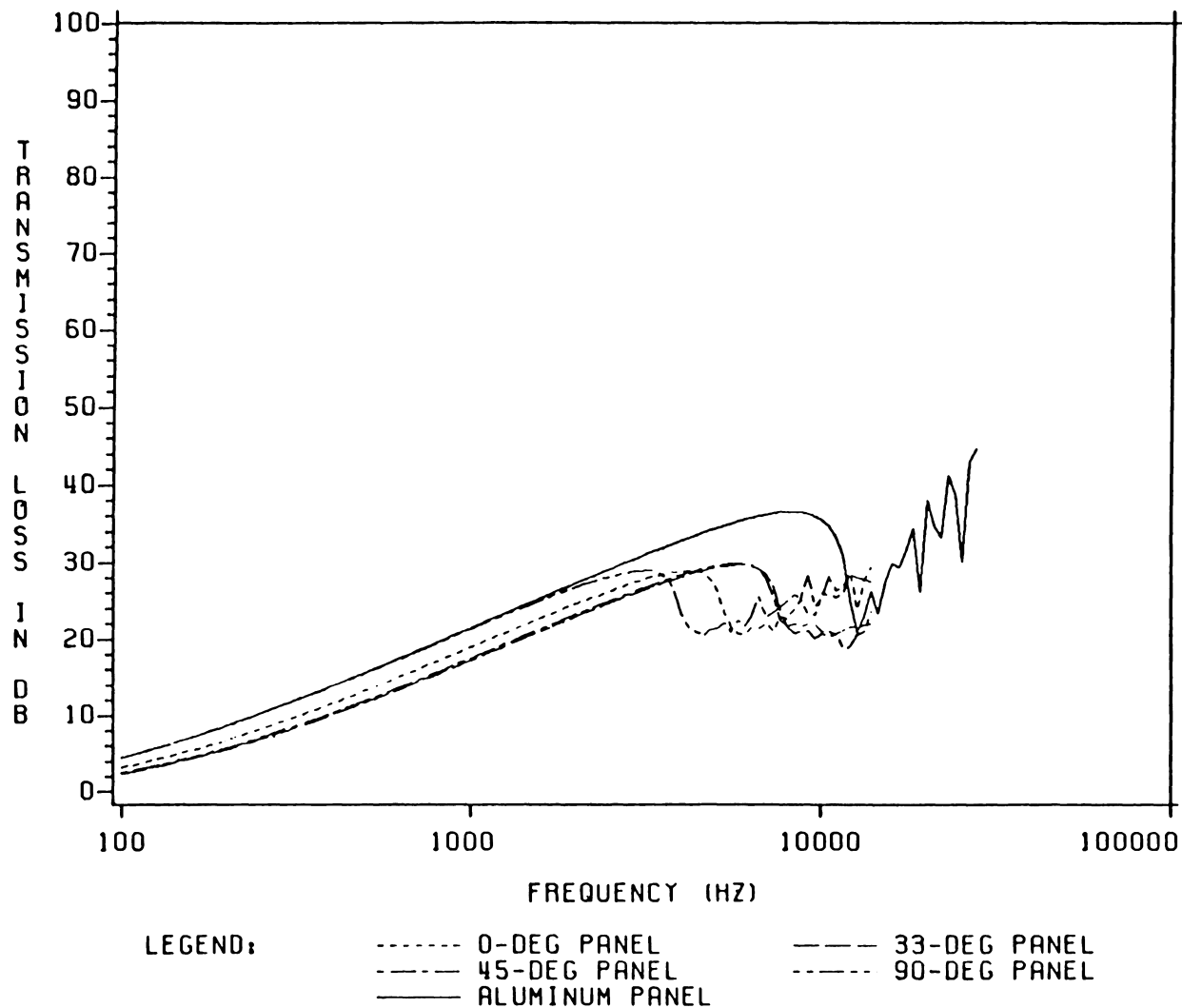
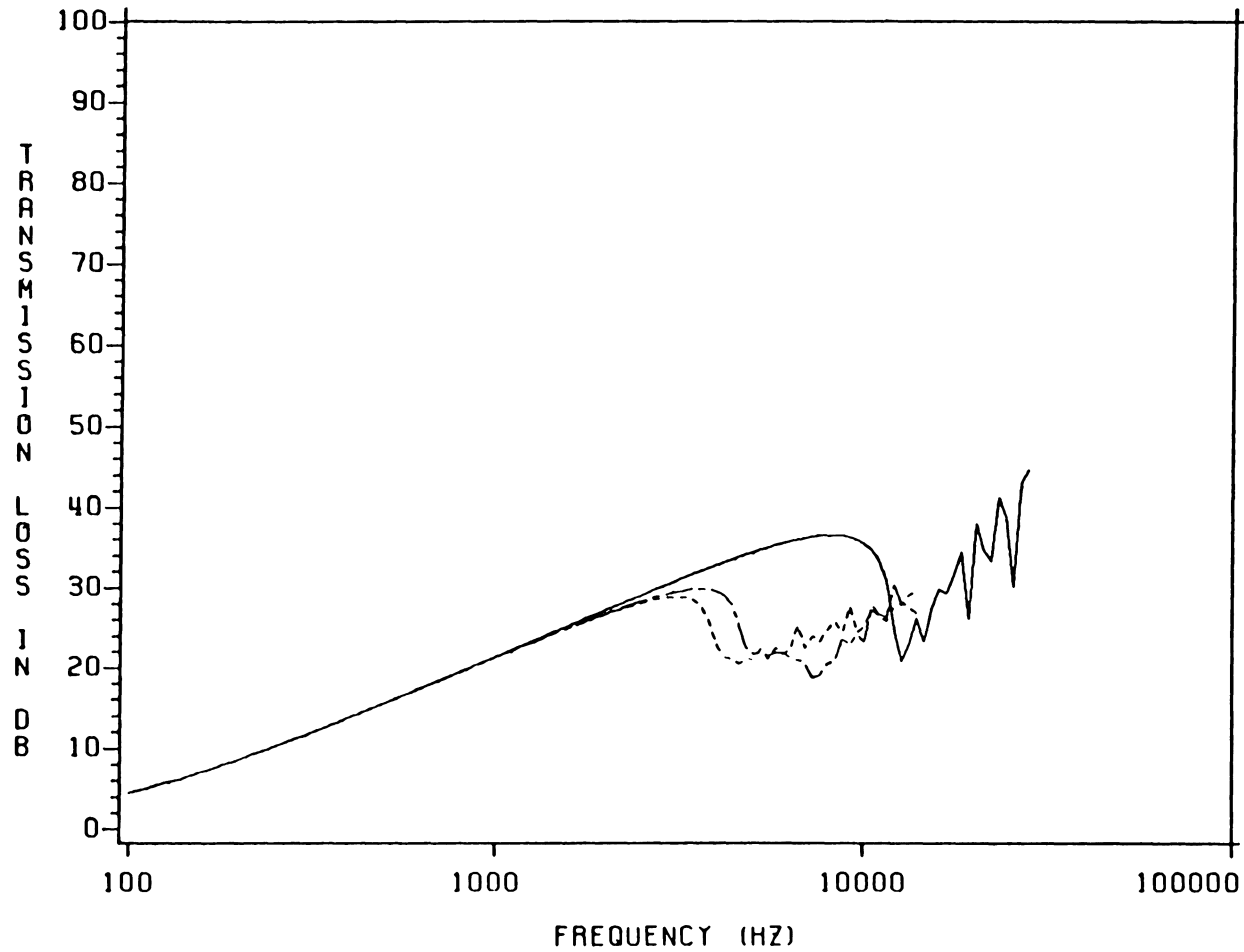


Figure 21. Field Incidence Transmission Loss of Shear-Critical Panels

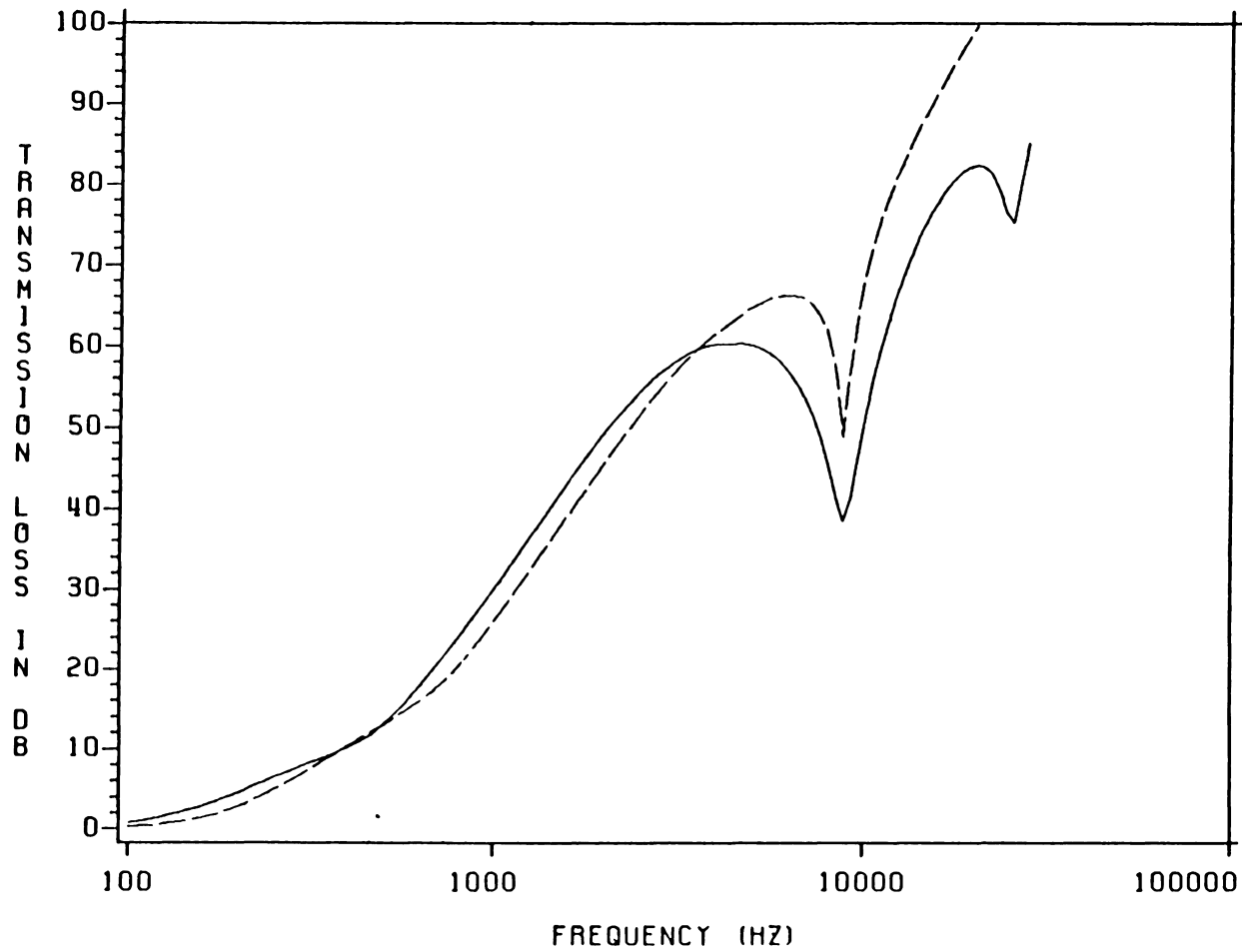
# FIELD INCIDENCE TRANSMISSION LOSS OF MASS-CRITICAL PANELS



LEGEND:      - - - - - 0-DEG, 90-DEG      - . - . - 45-DEG PANEL  
                  - - - - - ALUMINUM PANEL

Figure 22. Field Incidence Transmission Loss of Mass-Critical Panels

# LOW AND MID FREQUENCY TREATMENTS (SPECIFIC INCIDENCE)



LEGEND: ——— LOW FREQUENCY      - - - - HIGH FREQUENCY

Figure 23. TL of Typical Mid and Low Frequency Treatments

# TRANSMISSION LOSS OF ALUMINUM PANEL

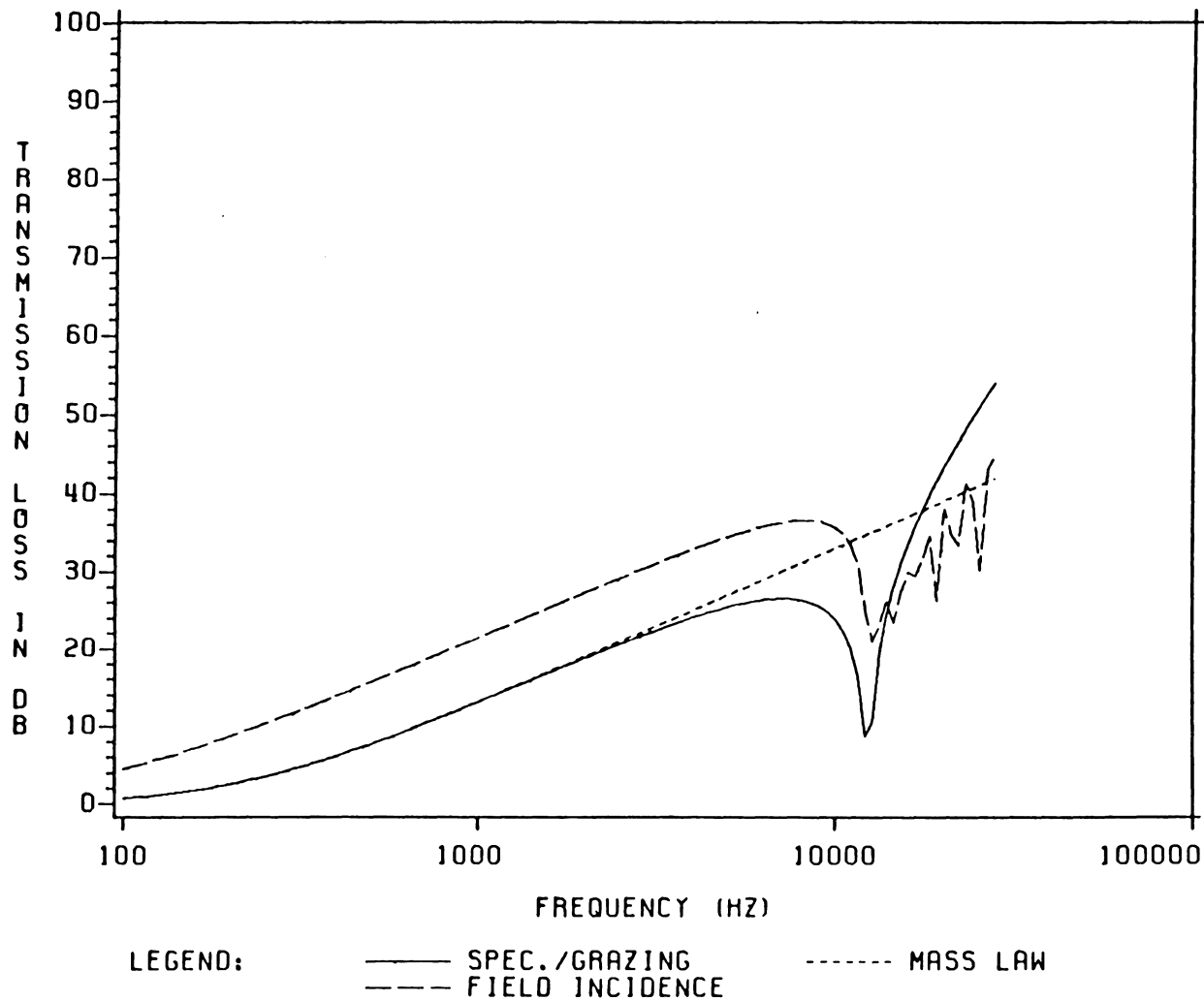


Figure 24. TL of Untreated Aluminum Panel



# SPECIFIC INCIDENCE / 1600 HZ

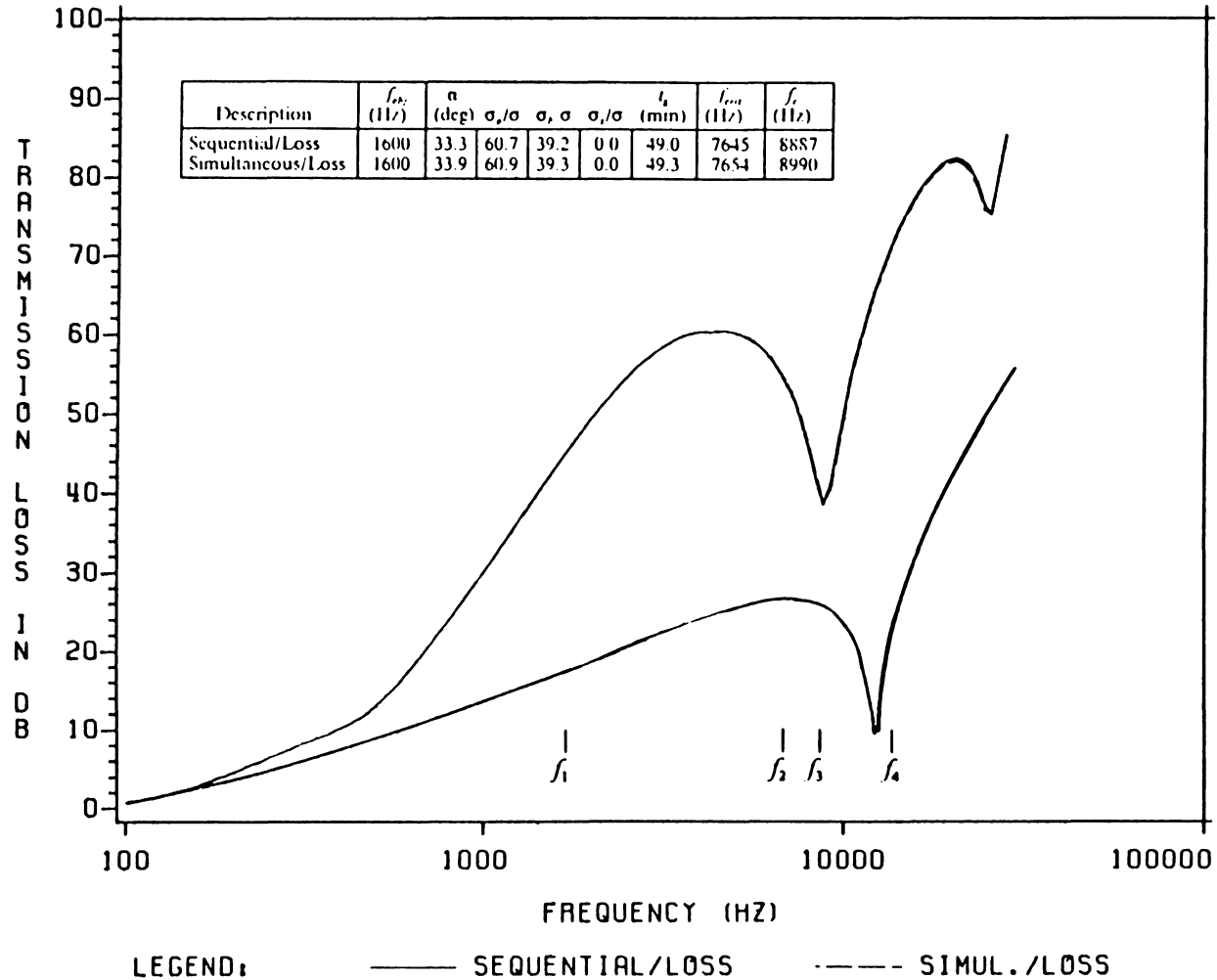


Figure 25. TL of Optimal Designs: Specific Incidence / 1600 Hz

# SPECIFIC INCIDENCE / 6400 HZ

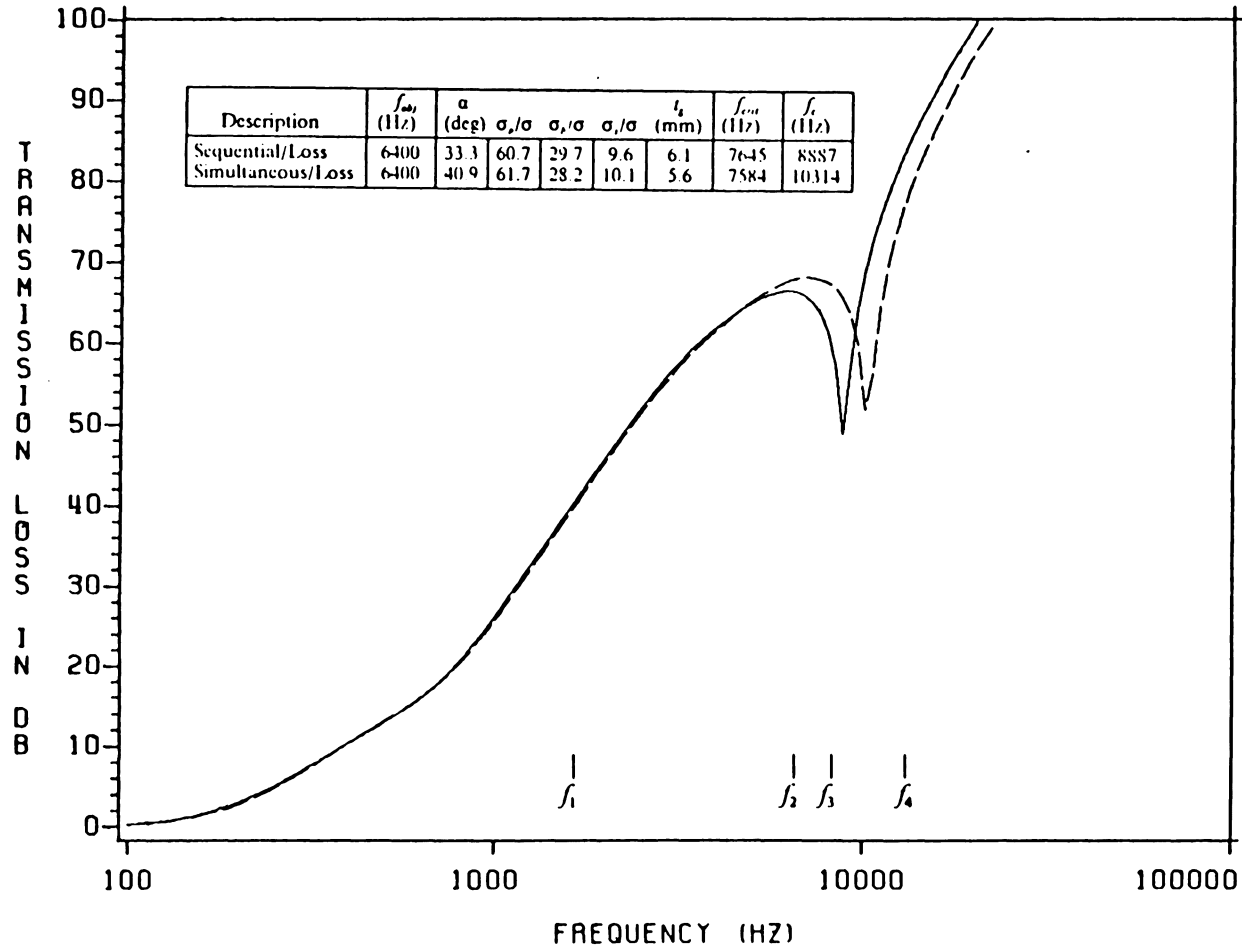
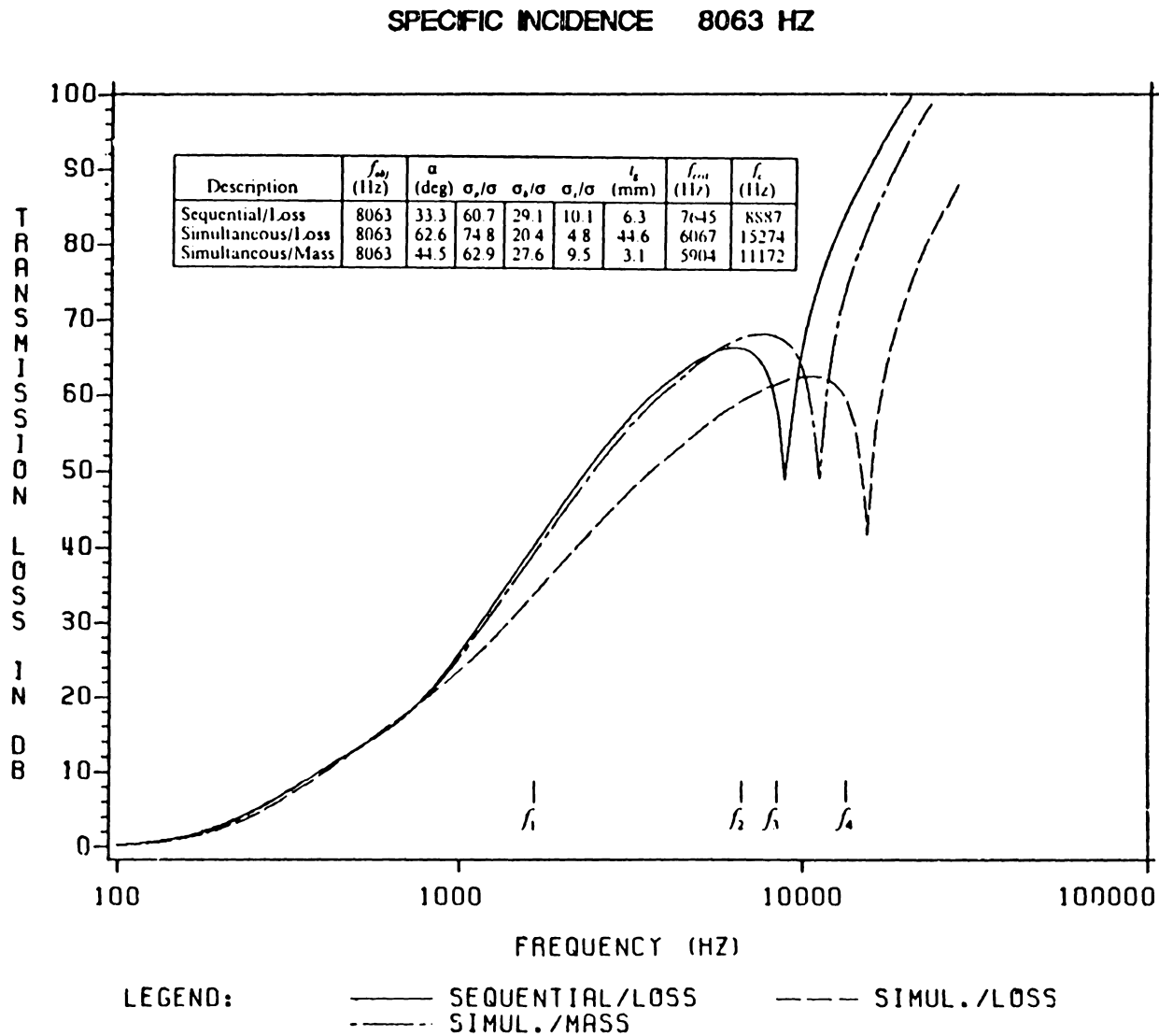
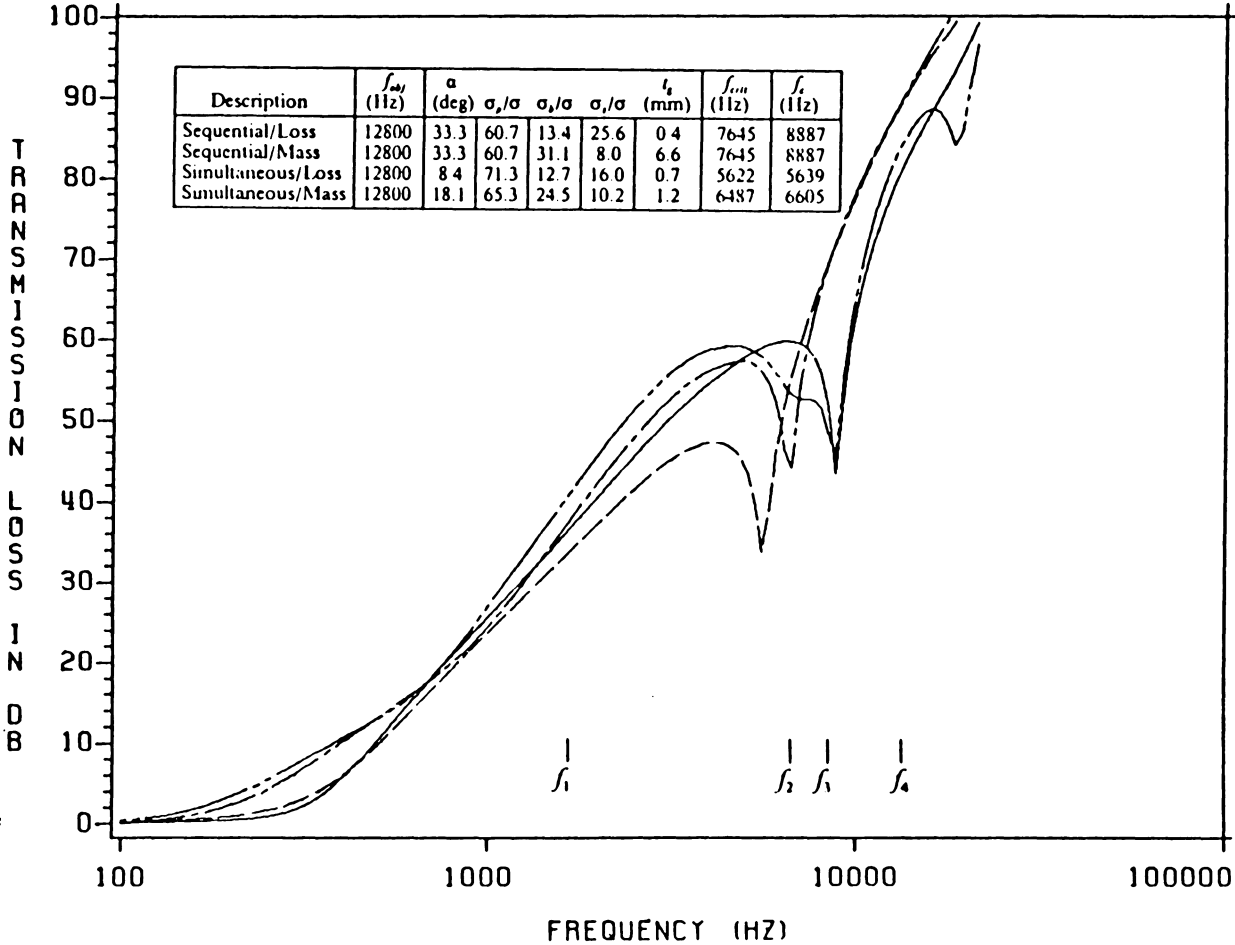


Figure 26. TL of Optimal Designs: Specific Incidence / 6400 Hz

Figure 27. TL of Optimal Designs: Specific Incidence / 8063 Hz



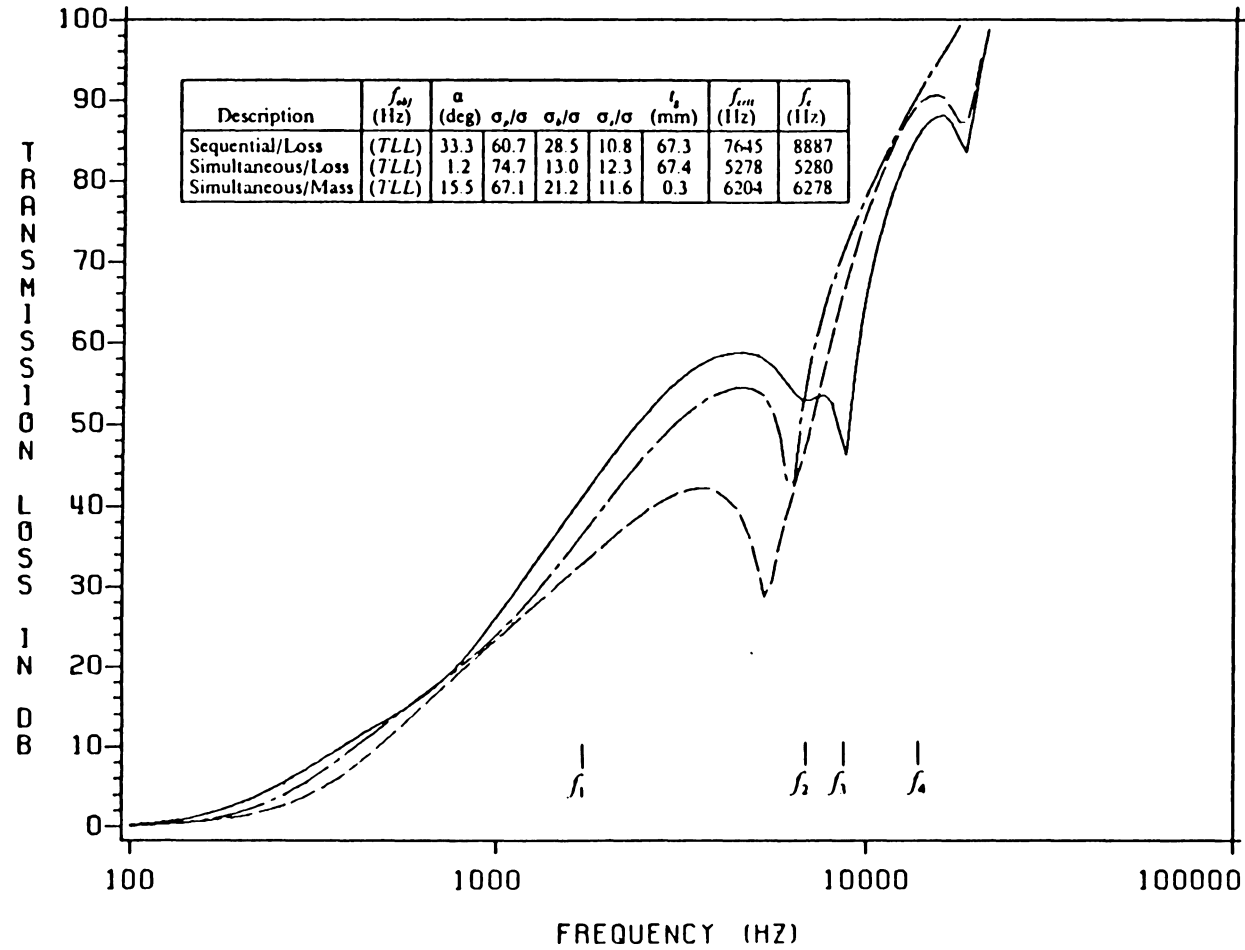
SPECIFIC INCIDENCE / 12800 HZ



LEGEND:      — SEQUENTIAL/LOSS      - - - SEQUENTIAL/MASS  
                 - - - SIMUL./LOSS      - · - SIMUL./MASS

Figure 28. TL of Optimal Designs: Specific Incidence / 12800 Hz

# SPECIFIC INCIDENCE / TLL



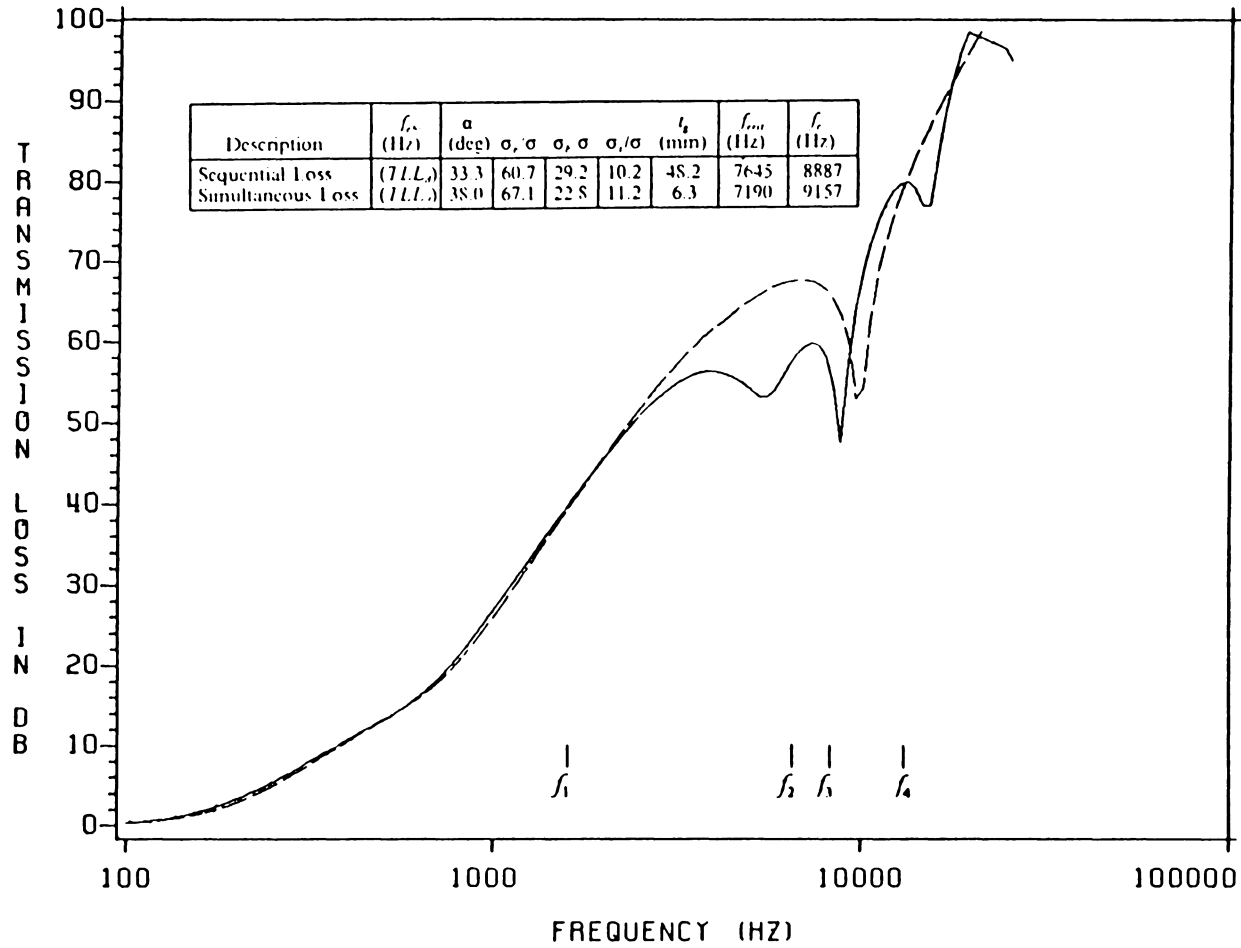
LEGEND:

— SEQUENTIAL/LOSS  
 - - - SIMUL./LOSS  
 - . - SIMUL./MASS

— SIMUL./LOSS

Figure 29. TL of Optimal Designs: Specific Incidence / TLL

# SPECIFIC INCIDENCE / TDL



LEGEND: — SEQUENTIAL/LOSS      --- SIMUL./LOSS

Figure 30. TL of Optimal Designs: Specific Incidence / TDL

# GRAZING INCIDENCE / 1600 HZ

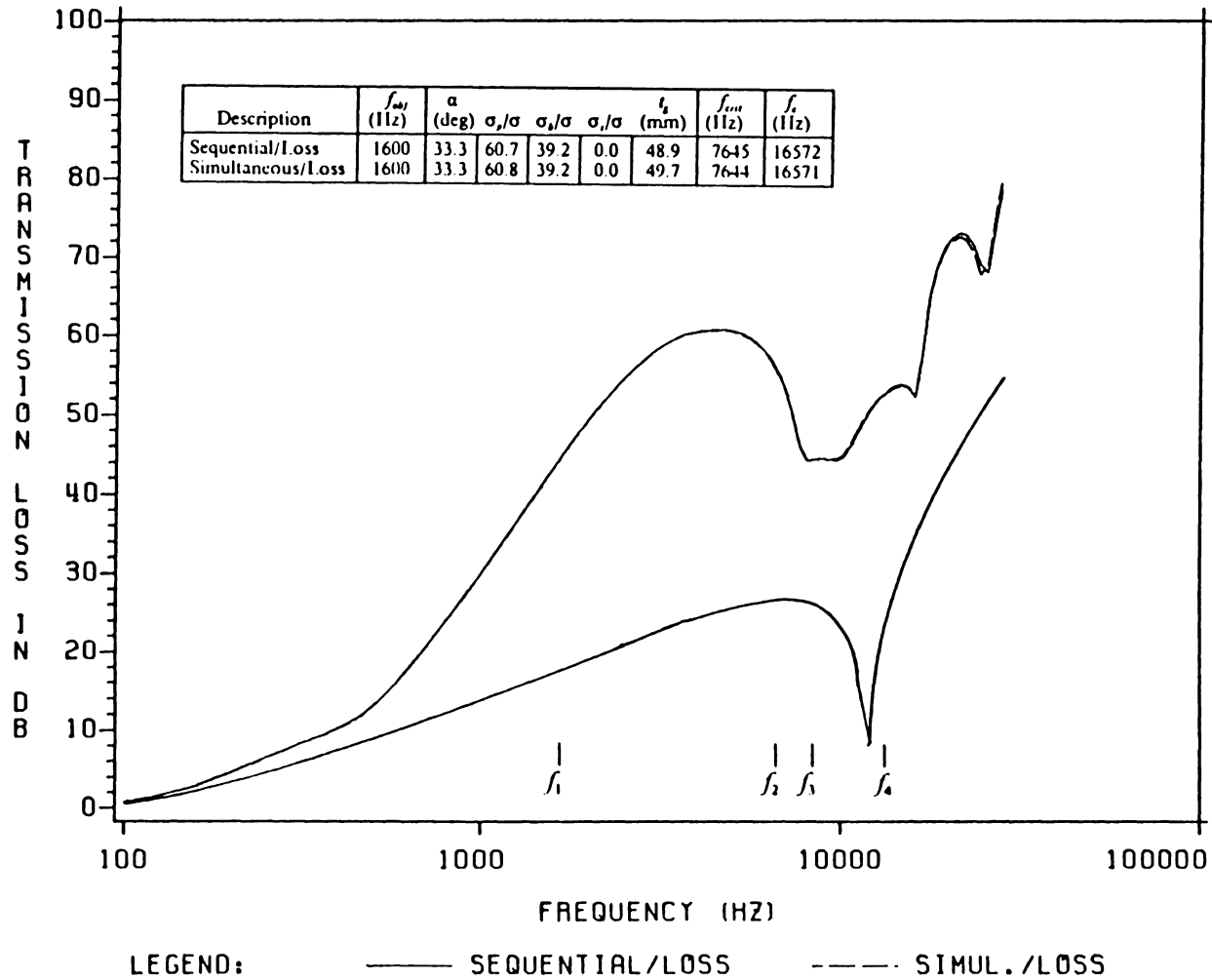
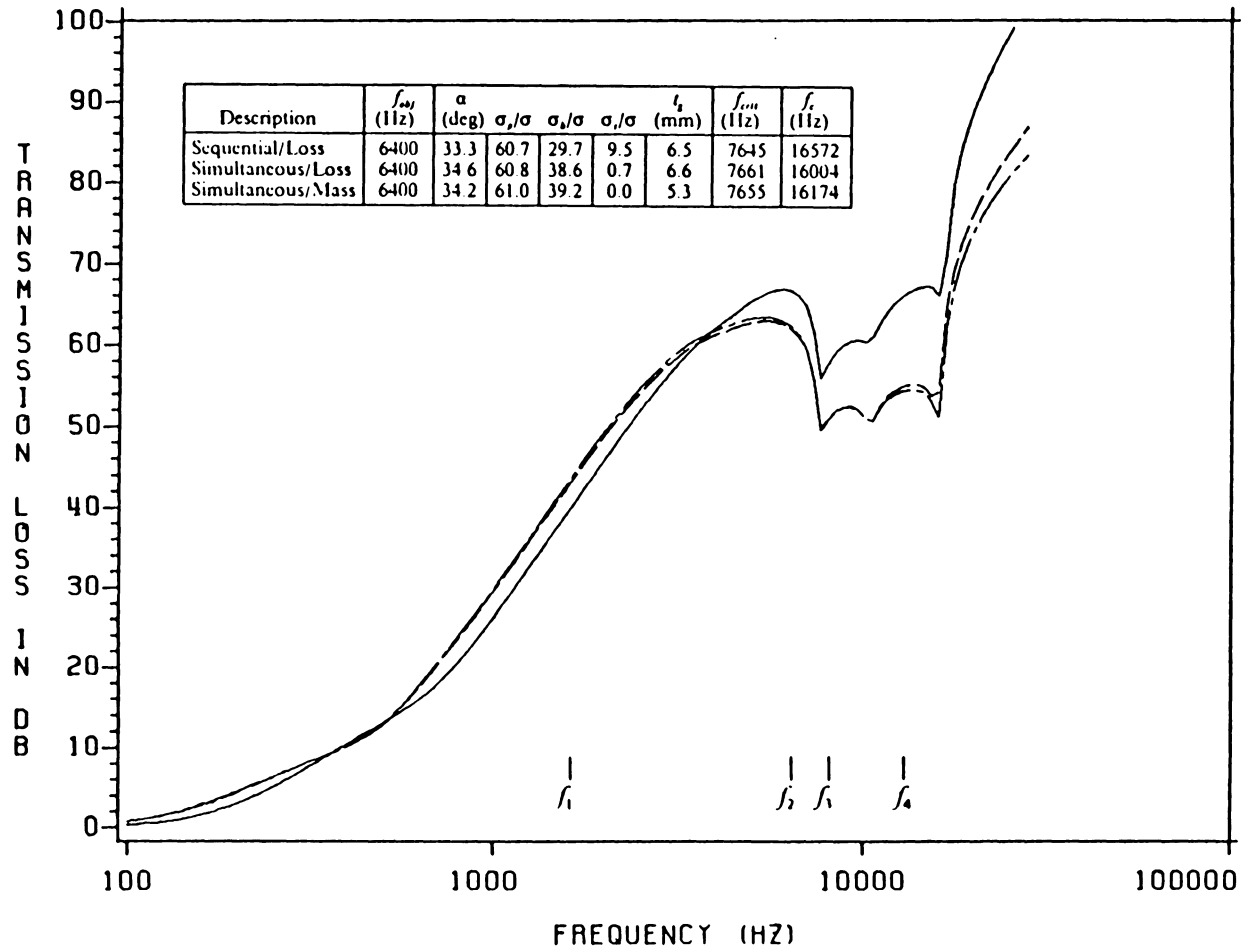


Figure 31. TL of Optimal Designs: Grazing Incidence / 1600 Hz

# GRAZING INCIDENCE / 6400 HZ

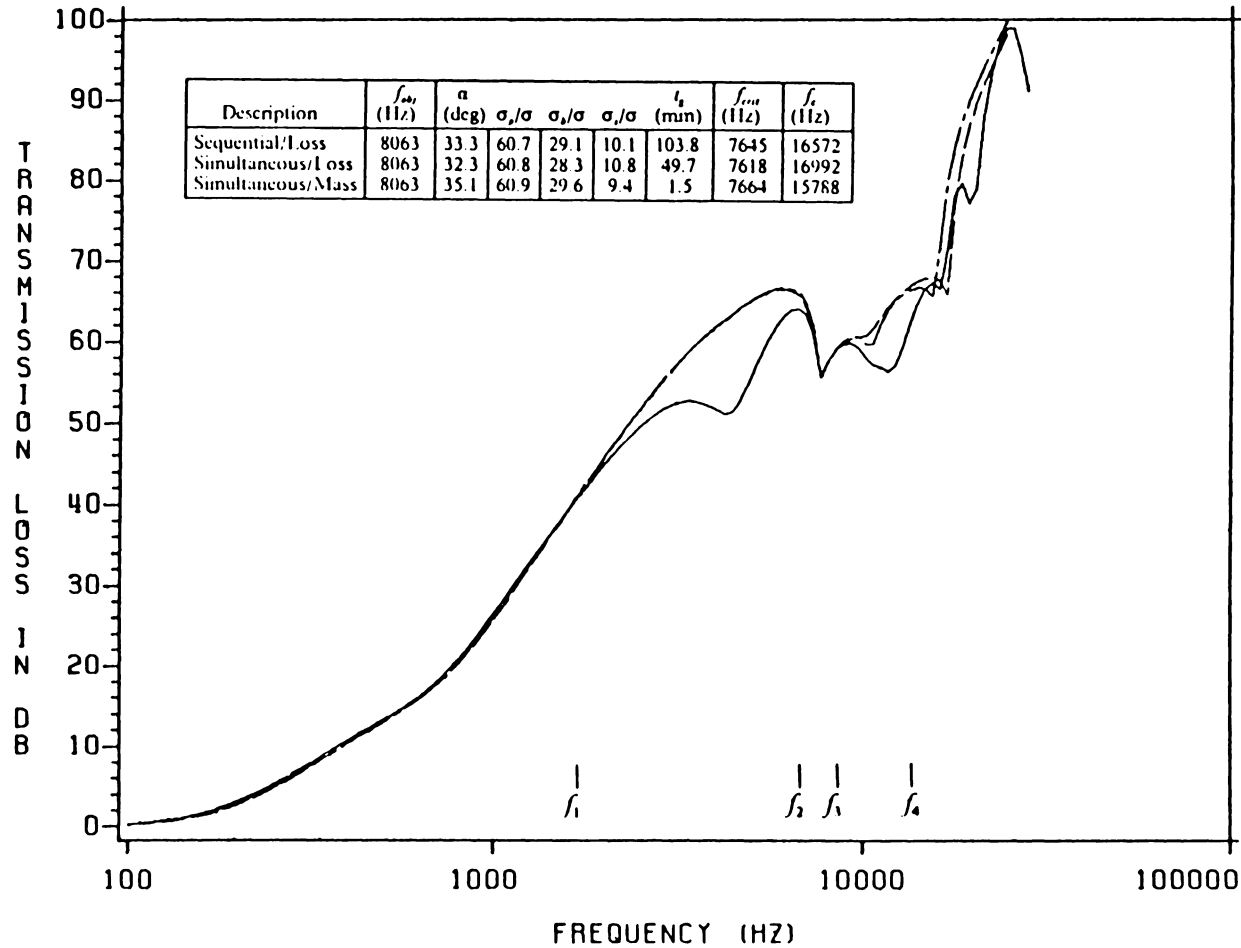


LEGEND: — SEQUENTIAL/LOSS      - - - SIMUL./LOSS  
 - . - . SIMUL./MASS

Figure 32. TL of Optimal Designs: Grazing Incidence / 6400 Hz



# GRAZING INCIDENCE / 8063 HZ



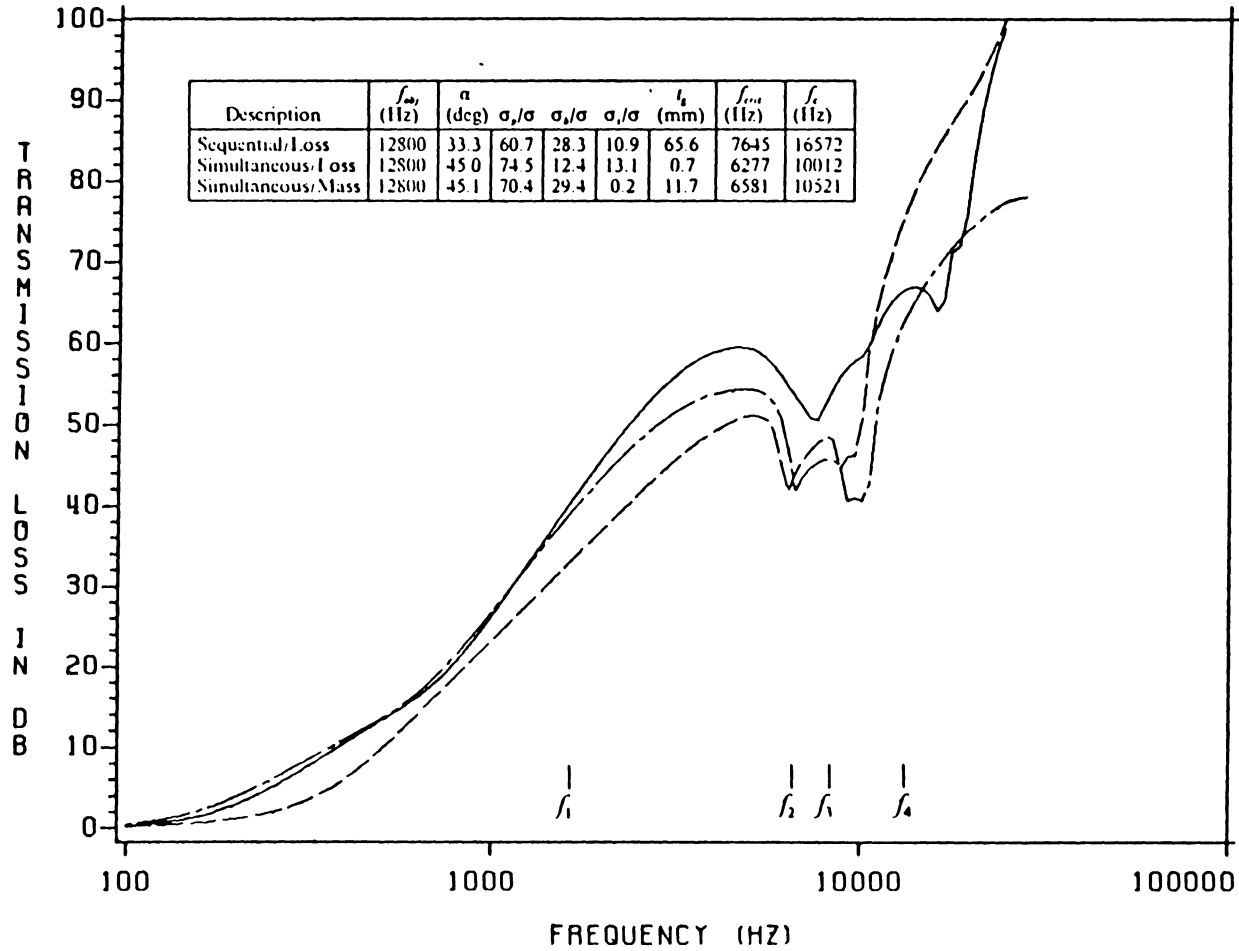
LEGEND:

— SEQUENTIAL/LOSS  
 - - - SIMUL./LOSS  
 - . - SIMUL./MASS

— SIMUL./LOSS

Figure 33. TL of Optimal Designs: Grazing Incidence / 8063 Hz

# GRAZING INCIDENCE / 12800 HZ



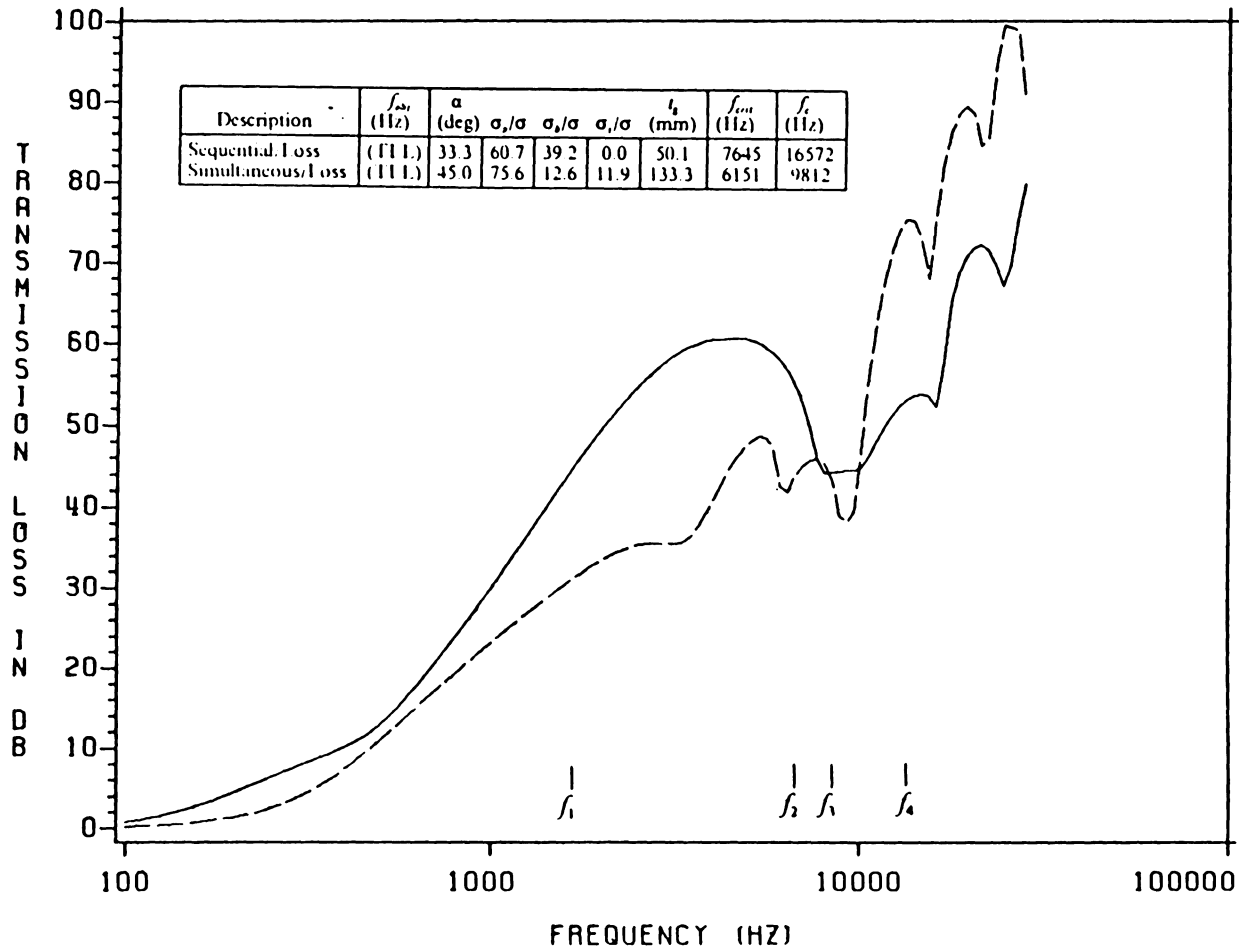
LEGEND:

— SEQUENTIAL/LOSS  
 - - - SIMUL./LOSS  
 - . - SIMUL./MASS

— SIMUL./LOSS

Figure 34. TL of Optimal Designs: Grazing Incidence / 12800 Hz

# GRAZING INCIDENCE / TLL



LEGEND: — SEQUENTIAL/LOSS      - - - SIMUL./LOSS

Figure 35. TL of Optimal Designs: Grazing Incidence / TLL

# FIELD INCIDENCE / 1600 HZ

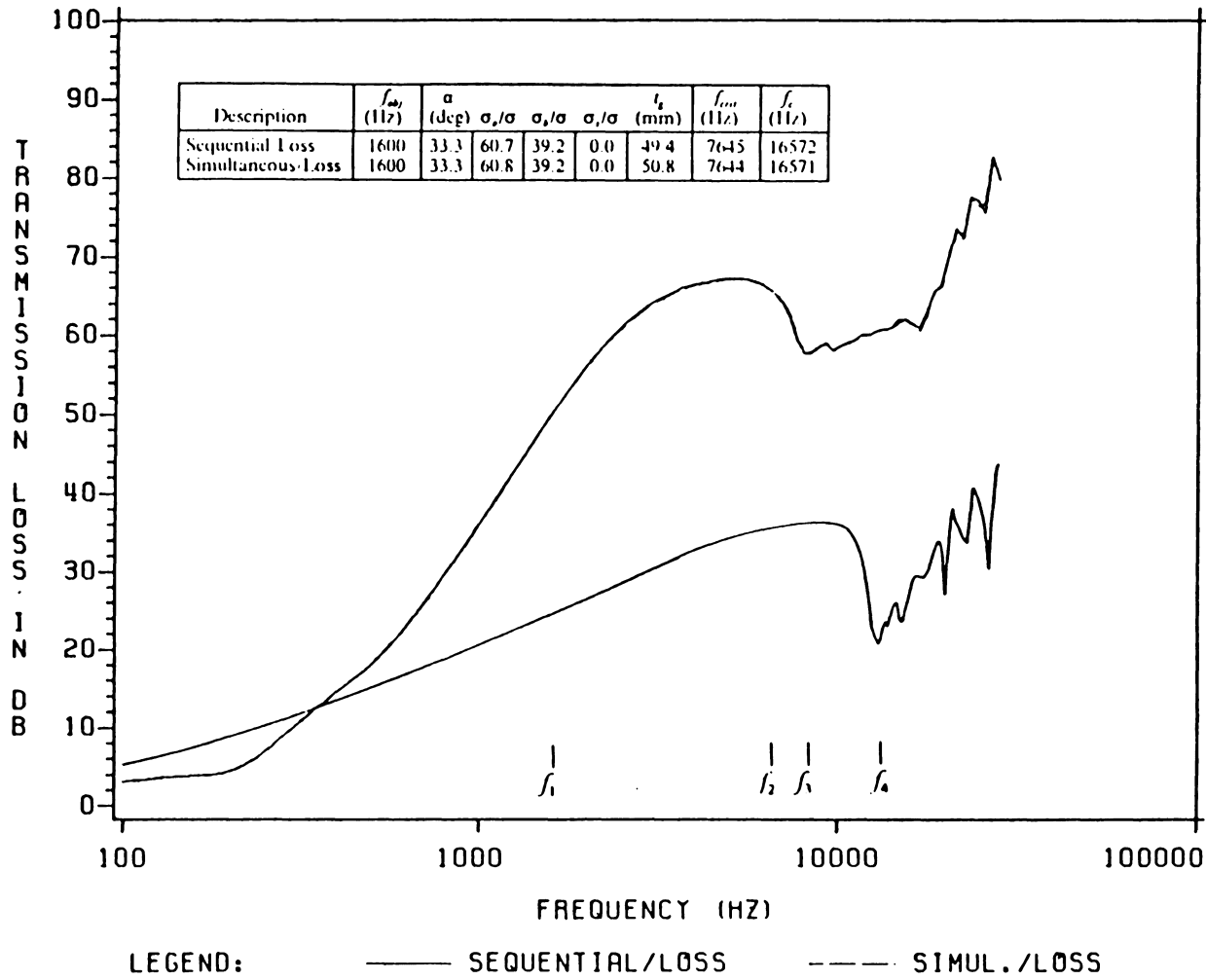
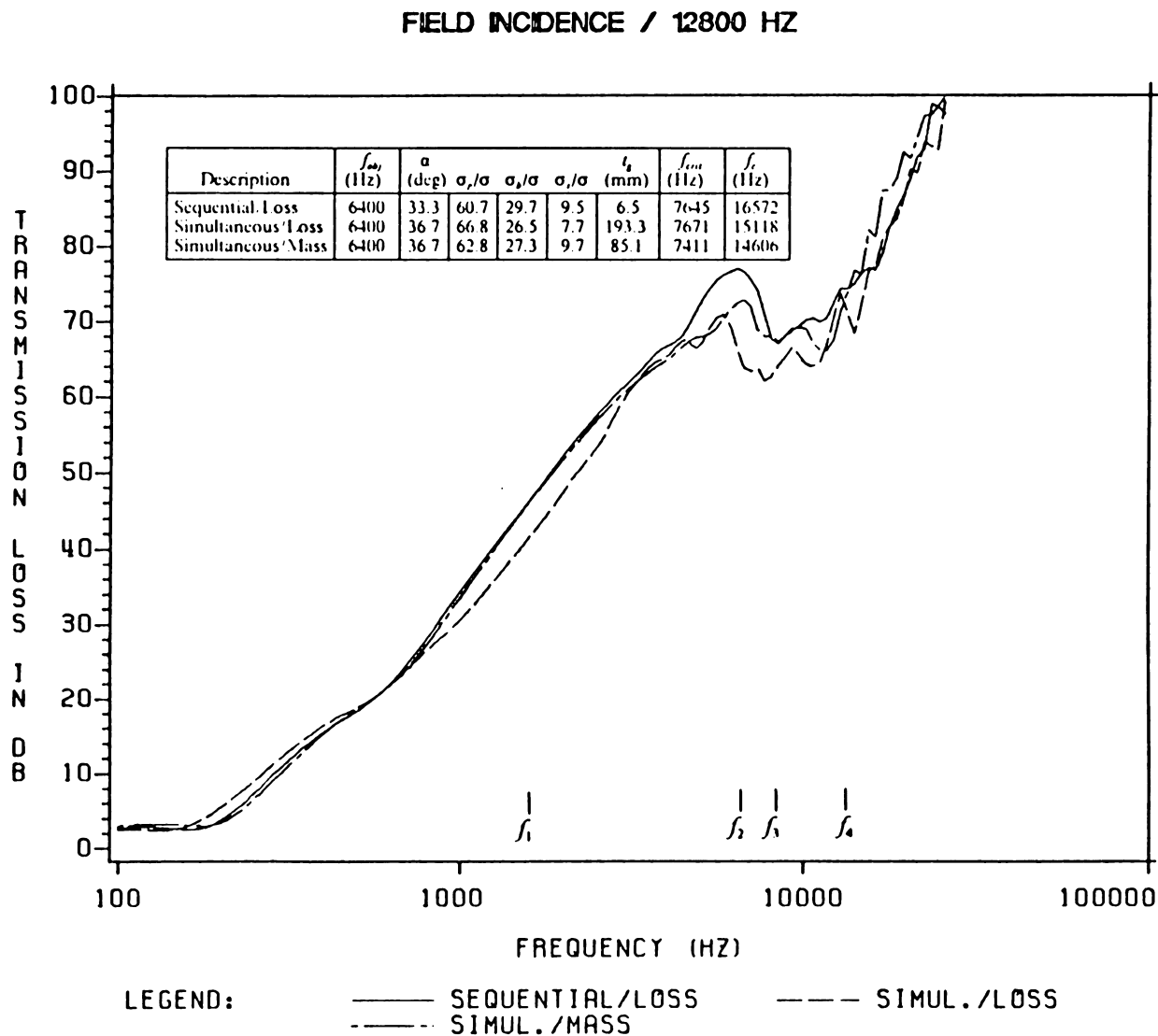


Figure 36. TL of Optimal Designs: Field Incidence / 1600 Hz



The vita has been removed  
from the scanned document